Carcinogenic liver fluke secretes extracellular vesicles that promote cholangiocytes to adopt a tumorigenic phenotype

Sujittra Chaiyadet[1,2*], Javier Sotillo[2*], Michael Smout[2], Cinzia Cantacessi[2,3], Malcolm K. Jones[4,5], Michael S. Johnson[6], Lynne Turnbull[6], Cynthia B. Whitchurch[6], Jeremy Potriquet[4], Marut Laohaviroj[7], Jason Mulvenna[4], Paul J. Brindley[8], Jeffrey M. Bethony[8], Thewarach Laha[9], Banchob Sripa[7], Alex Loukas[2 #]

[1]Biomedical Sciences, Graduate School, Khon Kaen University, Khon Kaen, Thailand

[2]Centre for Biodiscovery and Molecular Development of Therapeutics, Australian Institute of Tropical Health and Medicine, James Cook University, Cairns, QLD, Australia

[3]Department of Veterinary Medicine, University of Cambridge, Cambridge, UK

[4]QIMR Berghofer Medical Research Institute, Brisbane, QLD, Australia

[5]School of Veterinary Sciences, The University of Queensland, Gatton, QLD, Australia

[6]The iThree Institute, University of Technology Sydney, Sydney, NSW, Australia

[7]Department of Pathology, Faculty of Medicine, Khon Kaen University, Khon Kaen, Thailand

[8]Department of Microbiology, Immunology and Tropical Medicine, and Research Center for Neglected Diseases of Poverty, George Washington University, Washington DC, USA

[9]Department of Parasitology, Faculty of Medicine, Khon Kaen University, Khon Kaen, Thailand

[*] Both authors equally contributed to the manuscript

[#] Corresponding Author: Alex Loukas. Email: alex.loukas@jcu.edu.au

Running title: Liver-fluke extracellular vesicles

Abstract: 245 words

Text: 6,311 words

ABSTRACT (200 words)

Background

Throughout Asia there is an unprecedented link between cholangiocarcinoma and infection with the liver fluke *Opisthorchis viverrini*. Multiple processes including chronic inflammation and secretion of parasite proteins into the biliary epithelium drive infection towards cancer. Until now, the mechanism and effects of parasite protein entry into cholangiocytes was unknown.

Methods

Various microscopy techniques were used to identify *O. viverrini* extracellular vesicles (EVs) and their internalization by human cholangiocytes. Using mass spectrometry we characterised the EV proteome and associated changes in cholangiocytes after EV uptake, and detected EV proteins in bile of infected hamsters and humans. Cholangiocyte proliferation and IL-6 secretion was measured to assess the impact of EV internalization.

Results

EVs were identified in fluke culture medium and bile of infected hosts. EVs internalized by cholangiocytes drove cell proliferation and IL-6 secretion and induced changes in protein expression associated with endocytosis, wound repair and cancer. Antibodies to an *O. viverrini* tetraspanin blocked EV uptake and IL-6 secretion by cholangiocytes.

Conclusions

This is the first time that EVs from a multicellular pathogen have been identified in host tissues. Our findings imply a role for *O. viverrini* EVs in pathogenesis and highlight an approach to vaccine development for this infectious cancer.

Keywords: extracellular vesicles; *Opisthorchis viverrini*; cholangiocarcinoma; liver fluke; cancer

FOOTNOTES

Conflict of interest

All authors: No reported conflicts.

Funding statement

This work was supported by a Project Grant (APP1085309) from the National Health and Medical Research Council of Australia (NHMRC). AL is supported by a NHMRC principal research fellowship. SC was supported by the Thailand Research Fund (TRF)-the Royal Golden Jubilee PhD scholarship (RGJ) through Dr. Banchob Sripa. The funders had no role in study design, data collection and analysis, decision to publish, or preparation of the manuscript.

Correspondence should be addressed to:

Professor Alex Loukas

Centre for Biodiscovery and Molecular Development of Therapeutics

Australian Institute of Tropical Health & Medicine

James Cook University

McGregor Rd, Smithfield

Cairns, QLD 4878

Australia

Ph. +61 7 4232 1608

Email. Alex.Loukas@jcu.edu.au

Introduction (3487 words)

The liver fluke, *Opisthorchis viverrini*, is classified as a group 1 carcinogen by the International Agency for Research on Cancer, and is a major public health problem in many parts of Southeast Asia. In Northeast Thailand alone, more than 8 million people harbour the parasite [1] due to traditional dietary preferences for eating uncooked fish that harbour the infective stage of the fluke [2]. Upon ingestion of infected fish, the metacercariae excyst in the duodenum and migrate to the bile ducts of the definitive host where they feed on the biliary epithelia. Infection is associated with a spectrum of hepatobiliary abnormalities including bile duct cancer or cholangiocarcinoma (CCA) [2, 3]. The incidence of CCA in Northeast Thailand is substantially higher than elsewhere in the world, and associates strongly with the prevalence of *O. viverrini* infection [4].

The mechanisms involved in liver fluke-driven tumorigenesis are multi-factorial, with apparent roles for (i) mechanical damage caused by parasites grazing on the biliary epithelium; (ii) chronic immunopathologic processes that are dominated by pro-inflammatory cytokines such as IL-6 [1]; (iii) the active release of parasite-derived excretory/secretory (ES) products into the bile ducts that drive unchecked cell proliferation [2, 5-7]. Intriguingly, some of these ES products have been identified inside cholangiocytes of experimentally infected hamsters [6, 8, 9], akin to the intracellular presence of the CagA protein from another carcinogenic pathogen, *Helicobacter pylori* [10]. Until now, the mechanisms by which liver fluke ES proteins are internalized by cholangiocytes, and the ramifications of this process for the host cell, have remained unknown.

Recent reports have highlighted the presence of secreted extracellular vesicles (EVs) from parasites of both unicellular [11, 12] and multicellular (helminths) [13-15] origin, and provide a plausible explanation for the abundance in helminth ES products of apparently "intracellular" proteins [16]. EVs are small membrane-enclosed structures that are released by many different cell types [17, 18]. EVs from unicellular parasites have been shown to

influence host physiological processes, including immunomodulation, and adherence and communication between host and parasite [12, 19, 20]. A recent report described the uptake of parasitic platyhelminth EVs by host cell lines *in vitro* using low resolution fluorescence microscopy [13], but the molecular impact of EV uptake on the recipient cell, and detection of helminth EVs *in vivo* has until now, not been reported.

Here we show that *O. viverrini* secretes EVs that induce a pro-inflammatory/tumorigenic phenotype in human cholangiocytes. We also show that cellular uptake of *O. viverrini* EVs can be blocked by antibodies to an EV recombinant tetraspanin, highlighting the potential utility of EV proteins as vaccines to prevent fluke infection and associated cholangiocarcinogenesis.

Materials and Methods

Ethics statement

Hamsters were maintained at Khon Kaen University (KKU), Thailand. The study was approved by the KKU Animal Ethics Committee (AEKKU 55/2554). Human bile was collected under an approved protocol (HE 521209) from the KKU Institutional Review Board.

Parasite material, isolation of ES products and EV purification

Parasites were obtained from experimentally infected hamsters and ES products were isolated as described [8]. EVs were purified from ES products using differential ultracentrifugation following a modified protocol [21]. Briefly, parasite culture media was centrifuged at 2,000 *g* for 30 min at 4°C to remove larger debris; supernatant was further centrifuged at 15,000 *g* for 30 min at 4°C. ES supernatants were filtered using a 0.2 μm membrane (Schleicher and Schuell Bioscience) then ultracentrifuged at 110,000 *g* for 2 h at 4°C. The pellet was washed in PBS containing protease inhibitor cocktail (Roche) and

ultracentrifuged for 1 h. Crude pellet was resuspended in 200 µl PBS/ protease inhibitor cocktail and stored at 4°C.

Preparation of EVs for Transmission Electron Microscopy

Five µl of purified EVs was applied to a carbon-formvar coated grid and air dried. Grids were negatively stained in 2% uranyl acetate for 15 secs. Stained grids were viewed in a JEM1011 transmission electron microscope (JEOL) equipped with a Morada side-mounted digital camera (Olympus).

Fluorescence labelling of EVs membranes

EVs were labelled with Alexa Fluor 488 5-SDP Ester (AF488) (Life Technologies) following the manufacturer's protocol. EV pellets were resuspended in 400 µl of PBS and mixed with 50 µg of AF488 for 1 h at 4°C. The samples were collected by ultracentrifugation at 110,000 *g* for 2 h to remove excess dye, washed twice and resuspended in 400 µl of PBS.

Cell co-cultures and fluorescence microscopy

To investigate internalization of EVs by mammalian cells, normal immortalized human cholangiocytes (H69) were grown to 80% confluence as described [22]. Cells were starved of FCS overnight, incubated with AF488-EVs for 6 h, and analysed by fluorescence microscopy. Cell nuclei were stained with Hoechst dye and visualized using an AxioImager M2 ApoTome fluorescence microscope (Zeiss). Two technical and 2 biological replicates were performed and at least 5 fields were analysed in each replicate. Fluorescence was quantified using ImageJ.

Ultra-resolution microscopy

To convincingly demonstrate internalization of *O. viverrini* EVs by cholangiocytes, we used 3D-Structured Illumination microscopy (3D-SIM). H69 cholangiocytes were grown to 50% confluence and co-cultured with AF488-EVs or an equivalent amount (based on fluorescence) of ES products (10 µg/ml) for up to 6 h. Treated cells were fixed in 4% paraformaldehyde, permeabilised in 0.1% Triton X-100 in PBS and stained with Alexa Fluor 568 Phalloidin (Life Technologies). Specimens were mounted in 5% N-propyl-Gallate (Sigma) and 3D-SIM was performed on isolated single cells using a DeltaVision OMX 3D-SIM system (Applied Precision Inc, GE Healthcare). Solid state lasers (405, 488, 593 nm) provided wide-field illumination and multi-channel images were captured simultaneously using three 512× 512 pixel size PCO edge scientific CMOS cameras. All data capture used a 60× 1.4 NA oil objective and standard excitation and emission filter sets (in nm, 405 EX / 419-465 EM, 488 EX / 500-550 EM and 592.5 EX / 608-648 EM). 3D-SIM images were sectioned using a 125 nm Z-step size. Raw 3-phase images were reconstructed as previously described [23]. Reconstructed images were rendered in 3D using IMARIS version 7.X (Bitplane Scientific).

Proteomic analysis of EVs

Sample preparation for proteomic analysis was performed as described [13]. Peptides were resuspended in 5% formic acid and analysed by LC-MS/MS. Ten microliters was injected onto a C18 trap column (Thermo Scientific Acclaim) and flushed into an analytical column (Agilent) and eluted via a mobile phase gradient: 5–80% solvent B over 120 min. The eluted material was directly applied to the nanospray source of a QSTAR Elite instrument (Applied Biosystems), and data analysis was conducted with Analyst 2.0 (Applied Biosystems).

iTRAQ analysis

H69 cells were co-cultured with the quantity of EVs that corresponded to 1.2 µg/ml of ES protein in PBS for 30 min, 3 h and 16 h. Cells were washed using PBS containing protease inhibitor cocktail and lysed in 5 M urea, 2 M thiourea, 0.1% SDS, 1% triton X-100 and 40 mM Tris (pH 7.4). Each sample was ground with a TissueLyser II (QIAGEN) and centrifuged at 12,000 *g* for 20 min. The protein supernatant was precipitated with cold methanol, centrifuged at 8,000 *g* and air dried pellets re-dissolved in 0.5 M triethylammonium bicarbonate (TEAB)/0.05% SDS, then centrifuged at 12,000 *g*. Samples were resuspended in 0.5 M TEAB prior to reduction, alkylation, digestion and iTRAQ labelling (AB Sciex) then analysed on a 5600 TripleTOF mass spectrometer as described [24].

Bioinformatic analysis of protein expression data

For proteomic characterization of *O. viverrini* EV proteins, the *O. viverrini* genome database [25] was interrogated using MASCOT (Matrix-Science) allowing two missed cleavages and mass tolerance of 1.2 Da in MS mode and 0.8 Da on MS/MS product ions. Probability ($P < 0.05$) of FDR was calculated for every search using the MASCOT decoy database facility. For iTRAQ, two biological and two technical replicates were conducted. Database searches were performed against NCBInr using MASCOT allowing two missed cleavages and a mass tolerance of 0.1 Da on MS and MS/MS modes, and results were validated using Scaffold v.4.2.1 (Proteome Software). Differentially expressed (dysregulated) proteins were determined using a Kruskal-Wallis test and results expressed in log2 ratios. Only proteins whose expression level underwent a significant ($P < 0.05$) log2 fold-change of >0.6 or <-0.6 for upregulated and downregulated proteins respectively were further considered. KEGG and Reactome functional enrichment analyses for dysregulated proteins were performed using KEGGMapper and DAVID [26]. Protein-protein interaction analysis was performed using String [27].

Detection of EV proteins in bile of O. viverrini-infected humans and hamsters

Bile was collected from *O. viverrini*-infected humans by aspiration of resected gallbladders, and experimentally infected and uninfected hamsters (controls) by puncture of the gallbladder from euthanized animals, and EVs isolated as described above. Selected Reaction monitoring (SRM) was performed on a 5600 TripleTOF to identify *O. viverrini* EV proteins in bile. All analyses were performed using SRM-initiated IDA experiments in which a SRM survey scan triggered the acquisition of MS/MS spectra. Skyline 3.1 was used to generate SRM transitions and for data analysis.

Cell proliferation

H69 cholangiocytes were cultured as described above until 80% confluent. Cells were starved of FCS overnight and cultured with the amount of EVs that corresponded to 1.2 µg/ml of ES protein over 72 h at 37°C. Control cells were incubated with 1.2 µg/ml of ES products (not ultra-centrifuged) or 1.2 µg/ml BSA for the negative control group. Cell proliferation was assessed by measuring cell index (CI) values in real time using an xCELLigence SP system and E plates (Acea). Three biological replicates were analysed and a 2-way ANOVA was performed.

Blocking internalization of EVs with a□□□□□□□□□□□□recombinant Ov-TSP-1

AF488-EVs were incubated with mouse a□□□-*Ov*-TSP-1 serum [28] or normal mouse serum (NMS) at different dilutions (1:2.5, 1:5, 1:20) at RT for 1 h. EV:antibody complexes were added to H69 cells and co-cultured for 6 h. Images were obtained using an ECLIPSE Ni-u confocal microscope (Nikon) at 60× magnification. Thirty fields from 2 biological replicates were analysed and a 1-way ANOVA was performed. Cell fluorescence was quantified using ImageJ.

IL-6 detection

H69 cholangiocytes were cultured as above to monitor cell proliferation over 24 h. Culture media were collected and centrifuged at 2000 *g* for 10 min to remove cell debris. IL-6 levels were quantified using an IL6-ELISA kit (R&D System) following the manufacturer's instructions. Three biological replicates were analysed and statistical analysis was performed using a 2-way ANOVA.

Results

Excretory/secretory products from O. viverrini contain EV-like vesicles

After filtration and ultracentrifugation of ES products from adult *O. viverrini* we identified microvesicular structures using negative staining in transmission electron microscopy (Figure 1). These spherical vesicles had an external diameter of 40-180 nm, resembling EVs recently reported from other trematodes [13, 14].

Proteomic analysis of O. viverrini *EVs reveals conserved and novel proteins*

O. viverrini EVs were digested with trypsin and submitted to LC-MS/MS. We identified 108 different proteins (Supplementary Table 1), 42 of which were homologous to mammalian EV proteins in Exocarta [29], including proteins that are diagnostic of mammalian exosomes such as tetraspanins, HSP-70, cytoskeletal, regulatory and trafficking proteins. Gene Ontology (GO) analysis of the proteins (Supplementary Figure 1) returned 212 biological process terms. Pfam analysis identified proteins with an EF hand domain as the most frequently represented (Supplementary Figure 1).

O. viverrini exosome proteins are identified in bile of infected hosts

SRM analysis confirmed the presence of specific EV proteins in the bile of *O. viverrini* infected humans and hamsters. Seven of the top 15 proteins identified in the EV proteomic

analysis (based on number of peptides identified) were successfully quantified (Supplementary Figure 2).

O. viverrini EVs are internalized by human cholangiocytes

We monitored the uptake of AF488-EVs by human cholangiocytes *in vitro*. Within 60 min punctate fluorescent structures were detected, the number of which increased markedly over 6 h (Figure 2A). Cell fluorescence of all fields from the two biological replicates revealed fluorescence coverage of 62.44 ±9.52% and 90.57±4.58% at 0.5 h and 6 h respectively. 3D-SIM analysis confirmed the intracellular presence of AF488-EVs within the cytoskeletal network of well-separated individual cells as evidenced by their position between the basal and apical membranes outlined with phalloidin (Figure 2B, C, Supplementary Movie). We attempted to co-localize EVs to defined organelles using specific fluorescent markers but did not observe co-localization (not shown), suggestive of a cytoplasmic location.

O. viverrini EVs promote cell proliferation and stimulate wound healing and tumorigenic pathways in cholangiocytes

H69 cholangiocytes were incubated for 72 h with (i) crude ES products, (ii) EVs purified from crude ES products, or (iii) an irrelevant protein control, Bovine Serum Albumin (BSA). We chose BSA as a control rather than EVs from another source because H69 cholangiocytes produce (and uptake) their own exosomes in culture [30]. ES and EVs both induced significant ($P < 0.05$) cell proliferation compared to BSA-treated control cells (Figure 3). A total of 705 proteins containing at least 2 peptides were identified and quantified with a 99.9% protein threshold and 1.2% false discovery rate (FDR) from 6,863 unique peptides (peptide threshold = 95% and 0.82% FDR) from H69 cholangiocytes that were co-cultured with EVs (Supplementary Table 2); a total of 396 proteins from

cholangiocytes co-cultured with EVs were differentially expressed ($P < 0.05$ as determined using a Kruskal-Wallis test) and presented a fold-difference ≥ 1.5 ($\log_2 \geq 0.6$) at ≥1 time point (Supplementary Table 2). The greatest changes in protein expression in EV-co-cultured cells compared to control cells occurred after 3 h, where 238 (60.1%) proteins were differentially expressed (fold-difference ≥ 1.5 ($\log_2 \geq 0.6$)) in cells incubated with EVs (Figure 4A).

A total of 274 proteins from EV-treated cells matched homologous proteins in the KEGG database associated with 186 distinct biological pathways; 171 of these proteins were assigned to 14 Reactome pathways (Supplementary Table 3). The 25 KEGG and Reactome pathways associated with the largest numbers of proteins differentially expressed after incubation with EVs are shown in Figure 4B and C respectively. The expression of proteins linked to four pathways implicated in cancer and wound healing was significantly modified by EVs (Figure 4B). Supplementary Table 4 highlights all cholangiocyte proteins and KEGG pathways related to cancer and wound healing and their expression following co-culture with EVs. A total of 7 proteins involved in the Phagosome pathway were differentially expressed following exposure of human cholangiocytes to EVs (Supplementary Figure 3, Supplementary Table 5).

When differentially expressed proteins were assigned to Reactome pathways, those associated with Apoptosis, Regulation of activated PAK-2p34 by proteasome, and Cdh1-mediated degradation of Skp2 pathways were differentially regulated in cholangiocytes co-cultured with EVs (Figure 4C). Expression of 17 proteins associated with Apoptosis was regulated by EVs, and protein-protein interactions revealed that the majority of dysregulated cholangiocyte proteins formed a cluster belonging to the proteasome complex (Supplementary Figure 4).

Uptake of EVs and pro-inflammatory cytokine production by cholangiocytes can be blocked with antibodies to an O. viverrini *EV tetraspanin*

Due to the roles of tetraspanins in the formation of EVs by mammalian cells and their subsequent uptake by recipient cells [31], and the recent identification of the *Ov*-TSP-1 tetraspanin on the surface of *O. viverrini* [28], we explored the role of *Ov*-TSP-1 in the uptake of EVs by cholangiocytes. Antiserum to recombinant *Ov*-TSP-1 blocked the uptake of EVs by cholangiocytes compared to normal mouse serum ($P < 0.001 - P < 0.0001$) (Figure 5). ES and EVs both stimulated the secretion of significantly more IL-6 from cholangiocytes than did control cells incubated with media alone ($P < 0.01 - P < 0.001$; Figure 7), and IL-6 secretion was significantly reduced when EV internalisation was blocked by antiserum to *Ov*-TSP-1 ($P < 0.05$; Figure 6).

Discussion

While the mechanisms that drive chronic liver fluke infection towards cancer are multi-factorial, a pivotal role for fluke ES products in promoting a tumorigenic phenotype has been demonstrated [7]. The intracellular localization of *O. viverrini* ES proteins in cholangiocytes of infected hosts has prompted speculation on the mechanisms underlying this process of parasite protein internalization and its potential pathologic and carcinogenic consequences [6, 7]. Herein we show that *O. viverrini* secretes EVs that are internalized by human cholangiocytes *in vitro* and trigger a cascade of inflammatory and pro-tumorigenic changes within the cell, thereby providing a plausible mechanism by which ES proteins are taken up by biliary cells of infected hosts and contribute to the development of CCA in infected individuals.

Investigations on the interactions between EVs derived from single celled parasites and the cells that they encounter in an infected host have shed light on a novel means of host-parasite cellular communication [11, 12]. Protozoan parasite EVs are also capable of

modulating pro-inflammatory immune responses and inducing production of regulatory cytokines in recipient cells [19]. EV production by helminth parasites however has received considerably less attention. A seminal study recently showed that the parasitic nematode *Heligmosomoides polygyrus* secretes exosomes that contain microRNAs which suppress type 2 innate responses [15]. However, little is known about the production and particularly the biological effects of EVs from parasitic flatworms (platyhelminths). EVs were reported in the ES products from the flatworms *Fasciola hepatica* and *Echinostoma caproni* [13], and more recently *Dicrocoelium dendriticum* [14], and while the authors showed binding of fluke EVs to cell lines, neither the functional implications nor *in vivo* evidence of EV uptake by tissues of infected hosts were addressed. We show here for the first time that helminth EVs are unequivocally internalized by host cells, and major EV proteins can be detected in the bile of naturally infected humans and experimentally infected hamsters. From proteomic analyses, we identified 108 proteins from *O. viverrini* EVs, and only a handful (13) of these had been previously identified in a proteomic analysis of the ES products of the fluke [32].

Cholangiocytes line the bile ducts and provide the first line of defence against pathogens in the biliary system. We show here that *O. viverrini* EVs drive production of IL-6 from recipient human cholangiocytes, implicating these EVs in the hepatic disease process. IL-6 has been associated with chronic periductal fibrosis and CCA in opisthorchiasis patients [33], and IL-6 has been implicated in the maintenance of a chronic inflammatory milieu that could lead to tumorigenesis [34]. *O. viverrini* EVs were also capable of driving proliferation of cholangiocytes, a phenomenon that has been convincingly documented in the hamster infection model [35]. This relentless cell proliferation, coupled with other carcinogenic insults such as chronic immunopathology and elevated intake of dietary nitrosamines [2] culminates in the establishment of an environment that is conducive to malignant changes.

Uptake of EVs by cholangiocytes resulted in dysregulated expression of proteins with documented roles in wound healing and cancer. Indeed, wound repair has long been

implicated in tumorigenesis, and there are striking histological and moelcular similarities between tumor stroma and wounded tissues [36]. Nineteen KEGG pathways related to cancer and wound healing were affected by EVs in human cholangiocytes. Among the proteins significantly regulated we found different tropomyosin isoforms, PAK-2 and the tight junction protein ZO-2. PAK-2 is an important kinase that mediates tumor cell invasion [37]. We also noted that PAK-2 could play an important role in tumour progression by interacting with different components of the proteasome and with vimentin, a protein involved in maintaining cellular integrity and providing resistance against stress in several epithelial cancers [37]. Moreover, tight junction proteins play important roles in cell-cell junction assembly and organization, and are up-regulated during cell proliferation and wound healing [38].

Other important cholangiocyte proteins underwent dysregulated expression after co-culture with EVs, notably proteins involved in the proteasome complex. Most of the proteins involved in this complex were upregulated in cholangiocytes exposed to EVs and are known to interact with other proteins involved in cancer and wound healing processes. The proteasome complex regulates directly or indirectly many important cellular processes, and has been suggested as a therapeutic target for cancer [39, 40].

EV uptake by dendritic cells can be blocked with antibodies to EV tetraspanins [41]. Tetraspanins are thought to be involved in the regulation of protein assembly and microRNA recruitment in mammalian exosomes [31] and influence cell selectivity [42]. Our findings highlight an important role for *Ov*-TSP-1 in *O. viverrini* EV uptake by cholangiocytes. Although tetraspanins are found on the surface membranes of all exosomes, their discovery here is particularly pertinent due to their abundance on the surface membranes of parasitic helminths [43] and their importance in the development of the *O. viverrini* tegument [28]. Tetraspanins are efficacious helminth vaccine antigens [44-46], and our findings here suggest that the mechanism of vaccine efficacy is linked to interruption of parasite EV uptake by

recipient host cells *in vivo* and subsequent disruption of key physiological (and pathological) processes.

Our study describes for the first time the release of EVs in the secreted products of the carcinogenic liver fluke, *O. viverrini*, and highlights the role of fluke EVs in promoting an inflammatory yet simultaneously modulatory (wound healing) environment that ultimately facilitates the development of biliary cancer. Our findings do however offer hope for the eventual control of this debilitating neglected tropical disease by highlighting a key physiological process that can be potentially interrupted via subunit vaccines targeting key EV surface molecules.

FUNDING

This work was supported by a Project Grant (APP1085309) from the National Health and Medical Research Council of Australia (NHMRC). AL is supported by a NHMRC principal research fellowship. SC was supported by the Thailand Research Fund (TRF)-the Royal Golden Jubilee PhD scholarship (RGJ) through Dr. Banchob Sripa. The funders had no role in study design, data collection and analysis, decision to publish, or preparation of the manuscript.

ACKNOWLEDGMENTS

We thank Drs Antonio Marcilla and Rafael Toledo for helpful discussions and Mr Alun Jones for assistance with proteomics.

CONFLICT OF INTEREST

The authors have no conflicts of interest to declare.

REFERENCES

1. Sripa B, Bethony JM, Sithithaworn P, et al. Opisthorchiasis and Opisthorchis-associated cholangiocarcinoma in Thailand and Laos. Acta Trop **2011**; 120 Suppl 1:S158-68.

2. Sripa B, Kaewkes S, Sithithaworn P, et al. Liver fluke induces cholangiocarcinoma. PLoS Med **2007**; 4:e201.

3. Vatanasapt V, Uttaravichien T, Mairiang EO, Pairojkul C, Chartbanchachai W, Haswell-Elkins M. Cholangiocarcinoma in north-east Thailand. Lancet **1990**; 335:116-7.

4. Srivatanakul P, Ohshima H, Khlat M, et al. *Opisthorchis viverrini* infestation and endogenous nitrosamines as risk factors for cholangiocarcinoma in Thailand. Int J Cancer **1991**; 48:821-5.

5. Thuwajit C, Thuwajit P, Kaewkes S, et al. Increased cell proliferation of mouse fibroblast NIH-3T3 in vitro induced by excretory/secretory product(s) from *Opisthorchis viverrini*. Parasitology **2004**; 129:455-64.

6. Smout MJ, Laha T, Mulvenna J, et al. A granulin-like growth factor secreted by the carcinogenic liver fluke, *Opisthorchis viverrini*, promotes proliferation of host cells. PLoS Pathog **2009**; 5:e1000611.

7. Smout MJ, Sripa B, Laha T, et al. Infection with the carcinogenic human liver fluke, *Opisthorchis viverrini*. Mol Biosyst **2011**; 7:1367-75.

8. Sripa B, Kaewkes S. Relationship between parasite-specific antibody responses and intensity of *Opisthorchis viverrini* infection in hamsters. Parasite Immunol **2000**; 22:139-45.

9. Pinlaor P, Kaewpitoon N, Laha T, et al. Cathepsin F cysteine protease of the human liver fluke, *Opisthorchis viverrini*. PLoS Negl Trop Dis **2009**; 3:e398.

10. Hatakeyama M. *Helicobacter pylori* CagA and gastric cancer: a paradigm for hit-and-run carcinogenesis. Cell Host Microbe **2014**; 15:306-16.

11. Regev-Rudzki N, Wilson DW, Carvalho TG, et al. Cell-cell communication between malaria-infected red blood cells via exosome-like vesicles. Cell **2013**; 153:1120-33.

435 12. Twu O, de Miguel N, Lustig G, et al. *Trichomonas vaginalis* exosomes deliver cargo to
436 host cells and mediate hostratioparasite interactions. PLoS Pathog **2013**; 9:e1003482.
437 13. Marcilla A, Trelis M, Cortes A, et al. Extracellular vesicles from parasitic helminths
438 contain specific excretory/secretory proteins and are internalized in intestinal host cells. PLoS
439 One **2012**; 7:e45974.
440 14. Bernal D, Trelis M, Montaner S, et al. Surface analysis of *Dicrocoelium dendriticum*. The
441 molecular characterization of exosomes reveals the presence of miRNAs. J Proteomics **2014**;
442 105:232-41.
443 15. Buck AH, Coakley G, Simbari F, et al. Exosomes secreted by nematode parasites transfer
444 small RNAs to mammalian cells and modulate innate immunity. Nat Commun **2014**; 5:5488.
445 16. Curwen RS, Ashton PD, Sundaralingam S, Wilson RA. Identification of novel proteases
446 and immunomodulators in the secretions of schistosome cercariae that facilitate host entry.
447 Mol Cell Proteomics **2006**; 5:835-44.
448 17. Schorey JS, Bhatnagar S. Exosome function: from tumor immunology to pathogen
449 biology. Traffic **2008**; 9:871-81.
450 18. Mathivanan S, Ji H, Simpson RJ. Exosomes: extracellular organelles important in
451 intercellular communication. J Proteomics **2010**; 73:1907-20.
452 19. Silverman JM, Clos J, Horakova E, et al. Leishmania exosomes modulate innate and
453 adaptive immune responses through effects on monocytes and dendritic cells. J Immunol
454 **2010**; 185:5011-22.
455 20. Silverman JM, Reiner NE. Exosomes and other microvesicles in infection biology:
456 organelles with unanticipated phenotypes. Cell Microbiol **2011**; 13:1-9.
457 21. Thery C, Amigorena S, Raposo G, Clayton A. Isolation and characterization of exosomes
458 from cell culture supernatants and biological fluids. Curr Protoc Cell Biol **2006**; Chapter
459 3:Unit 3 22.

460 22. Smout MJ, Mulvenna JP, Jones MK, Loukas A. Expression, refolding and purification of
461 Ov-GRN-1, a granulin-like growth factor from the carcinogenic liver fluke, that causes
462 proliferation of mammalian host cells. Protein Express Purif **2011**; 79:263-70.
463 23. Gustafsson MG, Shao L, Carlton PM, et al. Three-dimensional resolution doubling in
464 wide-field fluorescence microscopy by structured illumination. Biophys J **2008**; 94:4957-70.
465 24. Prasopdee S, Tesana S, Cantacessi C, et al. Proteomic profile of *Bithynia siamensis*
466 *goniomphalos* snails upon infection with the carcinogenic liver fluke *Opisthorchis viverrini*. J
467 Proteomics **2015**; 113:281-91.
468 25. Young ND, Nagarajan N, Lin SJ, et al. The *Opisthorchis viverrini* genome provides
469 insights into life in the bile duct. Nat Commun **2014**; 5:4378.
470 26. Huang da W, Sherman BT, Lempicki RA. Systematic and integrative analysis of large
471 gene lists using DAVID bioinformatics resources. Nat Protoc **2009**; 4:44-57.
472 27. Franceschini A, Szklarczyk D, Frankild S, et al. STRING v9.1: protein-protein interaction
473 networks, with increased coverage and integration. Nucleic Acids Res **2013**; 41:D808-15.
474 28. Kalra H, Simpson RJ, Ji H, et al. Vesiclepedia: a compendium for extracellular vesicles
475 with continuous community annotation. PLoS Biol **2012**; 10:e1001450.
476 29. Masyuk AI, Huang BQ, Ward CJ, et al. Biliary exosomes influence cholangiocyte
477 regulatory mechanisms and proliferation through interaction with primary cilia. Am J Physiol
478 Gastrointest Liver Physiol **2010**; 299:G990-9.
479 30. Rana S, Zoller M. Exosome target cell selection and the importance of exosomal
480 tetraspanins: a hypothesis. Biochem Soc Trans **2011**; 39:559-62.
481 31. Piratae S, Tesana S, Jones MK, et al. Molecular characterization of a tetraspanin from the
482 human liver fluke, *Opisthorchis viverrini*. PLoS Negl Trop Dis **2012**; 6:e1939.
483 32. Mulvenna J, Sripa B, Brindley PJ, et al. The secreted and surface proteomes of the adult
484 stage of the carcinogenic human liver fluke *Opisthorchis viverrini*. Proteomics **2010**;
485 10:1063-78.

33. Sripa B, Mairiang E, Thinkhamrop B, et al. Advanced periductal fibrosis from infection with the carcinogenic human liver fluke *Opisthorchis viverrini* correlates with elevated levels of interleukin-6. Hepatology **2009**; 50:1273-81.

34. Schafer M, Werner S. Cancer as an overhealing wound: an old hypothesis revisited. Nat Rev Mol Cell Bio **2008**; 9:628-38.

35. Sripa B, Brindley PJ, Mulvenna J, et al. The tumorigenic liver fluke *Opisthorchis viverrini*-multiple pathways to cancer. Trends Parasitol **2012**; 28:395-407.

36. Dvorak HF. Tumors: wounds that do not heal. Similarities between tumor stroma generation and wound healing. N Engl J Med **1986**; 315:1650-9.

37. Coniglio SJ, Zavarella S, Symons MH. Pak1 and Pak2 mediate tumor cell invasion through distinct signaling mechanisms. Mol Cell Biol **2008**; 28:4162-72.

38. Farkas AE, Capaldo CT, Nusrat A. Regulation of epithelial proliferation by tight junction proteins. Ann N Y Acad Sci **2012**; 1258:115-24.

39. Frankland-Searby S, Bhaumik SR. The 26S proteasome complex: an attractive target for cancer therapy. Biochim Biophys Acta **2012**; 1825:64-76.

40. Rastogi N, Mishra DP. Therapeutic targeting of cancer cell cycle using proteasome inhibitors. Cell Div **2012**; 7:26.

41. Morelli AE, Larregina AT, Shufesky WJ, et al. Endocytosis, intracellular sorting, and processing of exosomes by dendritic cells. Blood **2004**; 104:3257-66.

42. Rana S, Yue S, Stadel D, Zoller M. Toward tailored exosomes: the exosomal tetraspanin web contributes to target cell selection. Int J Biochem Cell Biol **2012**; 44:1574-84.

43. Loukas A, Tran M, Pearson MS. Schistosome membrane proteins as vaccines. Int J Parasitol **2007**; 37:257-63.

44. Dang Z, Yagi K, Oku Y, et al. A pilot study on developing mucosal vaccine against alveolar echinococcosis (AE) using recombinant tetraspanin 3: Vaccine efficacy and immunology. PLoS Negl Trop Dis **2012**; 6:e1570.

45. Joseph SK, Ramaswamy K. Single multivalent vaccination boosted by trickle larval infection confers protection against experimental lymphatic filariasis. Vaccine **2013**; 31:3320-6.

46. Tran MH, Pearson MS, Bethony JM, et al. Tetraspanins on the surface of *Schistosoma mansoni* are protective antigens against schistosomiasis. Nat Med **2006**; 12:835-40.

47. Conesa A, Gotz S, Garcia-Gomez JM, Terol J, Talon M, Robles M. Blast2GO: a universal tool for annotation, visualization and analysis in functional genomics research. Bioinformatics **2005**; 21:3674-6.

FIGURE LEGENDS

Figure 1. Extracellular vesicles (EVs) secreted by *Opisthorchis viverrini*. Transmission electron micrograph showing the presence of microvesicles after ultracentrifugation of *O. viverrini* excretory/secretory products. EV-like microvesicles of 40-100 nm can be observed.

Figure 2. Internalization of *Opisthorchis viverrini* secreted extracellular vesicles (EVs) by human cholangiocytes. Fluorescence images of Alexa Fluor 488-labeled EVs (green) internalized by H69 cholangiocytes (A). Cholangiocytes internalized the EVs within 1 h of co-culture and maximum internalization was observed by 6 h. Control cells were incubated with PBS. Hoescht dye (blue) was employed to label cell nuclei (A). 3D-Structured Illumination microscopy (3D-SIM) fluorescence image of the edge of a well-separated individual cholangiocyte after 6 h incubation with Alexa Fluor 488-stained EVs (green) (B). Lateral (xy) overview of cell showing EVs present within the cytoskeletal actin network (red) of the cell (B). Rendered axial (xz) view of inset in panel A revealed EVs between the apical and basal surfaces of the cell that were stained by phalloidin (red) (C).

Figure 3. *Opisthorchis viverrini* extracellular vesicles (EVs) drive proliferation of human cholangiocytes. *O. viverrini* EVs (open triangles) and excretory/secretory (ES) products (closed circles) promoted the proliferation of human cholangiocytes. Asterisks represent the time-point from which cell growth remained significantly different between test and control groups after each treatment. * $P<0.05$.

Figure 4. Comparison of proteins that were significantly regulated, and biological pathways regulated in cholangiocytes co-cultured with *Opisthorchis viverrini* extracellular vesicles (EVs). (A) Heatmap of the proteins from human cholangiocytes with a significant fold regulation after Kruskal-Wallis test and that underwent a 2-fold-change

549 (log_2=1.5) in at least one of the time-points assessed after incubation with EVs from *O.*
550 *viverrini*. (B) Top 25 Kyoto Encyclopedia of Genes and Genomes (KEGG) pathways
551 regulated after incubation with EVs. (C) Reactome pathways regulated after incubation with
552 EVs. Pathways that are involved in wound healing and cancer are indicated by red font.
553
554 **Figure 5. Blockade of uptake of *Opisthorchis viverrini* extracellular vesicles (EVs) by**
555 **antibodies to recombinant *Ov*-TSP-1**. Mouse antibodies raised to recombinant *Ov*-TSP-1
556 blocked the uptake of Alexa Fluor 488-labeled *O. viverrini* EVs by H69 cholangiocytes.
557 Fluorescence micrographs of internalized EVs co-cultured with H69 cholangiocytes in the
558 presence of anti-*Ov*-TSP-1 serum (A) or normal mouse serum (NMS) (B) at different
559 dilutions. A□□□–*Ov*-TSP-1 significantly reduced the binding and internalization of EVs at
560 all serum dilutions when measured as fluorescence intensity (C) when compared to NMS (D).
561 ***P<0.001; ****P<0.0001.
562
563 **Figure 6. IL-6 production by human cholangiocytes after internalisation of *Opisthorchis***
564 ***viverrini* extracellular vesicles (EVs)**. Human cholangiocytes produce significantly greater
565 levels of IL-6 after co-culture with *O. viverrini* EVs. IL-6 production was partially blocked
566 when EVs were incubated with antibodies against recombinant *Ov*-TSP-1 prior to cell culture.
567 *P<0.05; **P<0.01; ***P<0.001.
568 **Supplementary Materials.**
569
570 **Figure S1. Gene Ontology and Pfam analysis of proteins in *Opisthorchis viverrini***
571 **extracellular vesicles (EVs).** Gene Ontology terms according to biological process (A),
572 molecular function (B) and cellular component (C) assigned to the proteins present in *O.*
573 *viverrini* EVs. Bar graph showing the most frequently represented protein families (Pfam) in
574 in *O. viverrini* EVs (D).

Figure S2. Single Reaction Monitoring (SRM) analysis confirms the presence of specific extracellular vesicle (EV) proteins in the bile of *Opisthorchis viverrini* infected humans and hamsters. The peak area for each transition analysed in the different proteins is shown. Seven of the top 15 proteins identified in the EV proteomic analysis (based on number of peptides identified) were successfully quantified, including a tetraspanin-family member (TSP-2B). Protein names and target peptide sequences for SRM are indicated at the top and the bottom of each graph, respectively. The transitions identified are also indicated in each graph. Only proteins and peptides identified by LC-MS/MS in the proteomic analysis from EVs secreted by *O. viverrini* were pre-selected for the SRM analysis. The software Skyline® was used to select the best peptides and transitions based on default parameters. Peptides analysed were the following: Annexin (EGVSSILDMAK, VGQDVADIYDAGVGK), Hypothetical protein (FAQHGDQGLRRR), Myosin heavy chain (ANGMASQLER, MQGELQQLR, DVEDLESSLQK), Myosin regulatory chain (LDYNEFVTLIK), Taurocyamine kinase (LANAISELGK, TSFGGSLAQCVSHNAR), Tetraspanin 2-B (KLIDLIQK), Tubulin alpha (DAIDTISVIK).

Figure S3. Expression of cholangiocyte proteins in the phagosome pathway was altered by co-culture with *Opisthorchis viverrini* extracellular vesicles (EVs). Phagosome pathway mapping of significantly regulated (log_2=0.6) proteins (red boxes) identified from human cholangiocytes after incubation with EVs from *Opisthorchis viverrini* using the Kyoto Encyclopedia of Genes and Genomes (KEGG). Green boxes represent proteins in the phagosome pathway that were not identified or were identified but not significantly regulated by co-culture with EVs.

Figure S4. Functional interactions of cholangiocyte proteins associated with the "Apoptosis" pathway whose expression was affected by co-culture with *Opisthorchis viverrini* extracellular vesicles (EVs). STRING database [27] was used to identify protein-protein interactions associated with the apoptosis pathway for proteins from human cholangiocytes that were significantly regulated (log_2=0.6) after incubation with *O. viverrini* EVs.

Table S1. Proteins identified in extracellular vesicles of *Opisthorchis viverrini*. Mascot was used as the search engine; spectra were searched against the *O. viverrini* genome database [25] and hits were annotated using Blast2GO [47].

Table S2. Quantitative protein and peptide report of human cholangiocyte proteins after incubation with extracellular vesicles from *Opisthorchis viverrini*. Scaffold-generated report of the iTRAQ results showing the proteins identified by MASCOT and X! Tandem and peptides matching each protein.

Table S3. Reactome pathway. Human cholangiocyte proteins associated with Reactome pathways after incubation with *Opisthorchis viverrini* extracellular vesicles (EVs).

Table S4. Phagosome pathway. Human cholangiocyte proteins involved in the Phagosome pathway after incubation with *Opisthorchis viverrini* extracellular vesicles (EVs).

Table S5. Proteins related to wound healing and cancer pathways that were differentially regulated in human cholangiocytes after co-culture with extracellular vesicles (EVs) from *Opisthorchis viverrini*. Proteins significantly up- or downregulated in

626 cholangiocytes after incubation with EVs were subjected to functional enrichment analysis
627 using the Kyoto Encyclopedia of Genes and Genomes (KEGG). A $\log_2$=0.6 corresponding to
628 a 1.5-fold change in proteins with *P*-value <0.05 was considered to be significant.
629
630 **Supplementary Movie.** 3D-Structured Illumination microscopy (3D-SIM) fluorescence
631 video of an individual cholangiocyte after 6 h incubation with Alexa Fluor 488-stained EVs
632 (green). Cytoskeletal actin network was stained by phalloidin (red).
633

Figure 1
Click here to download Figure: Figure_1.tif

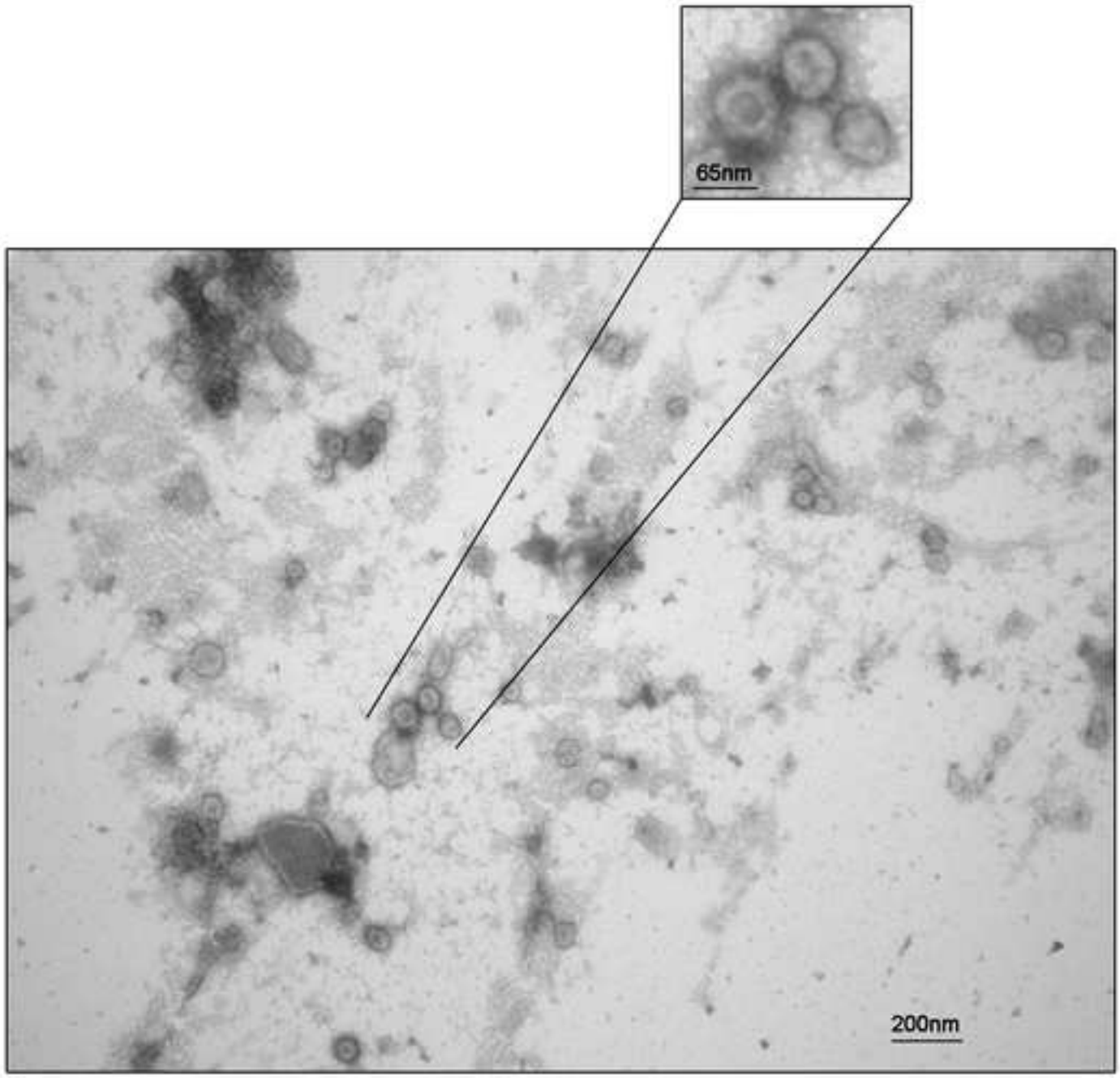

Figure 2
Click here to download Figure: Figure_2.tif

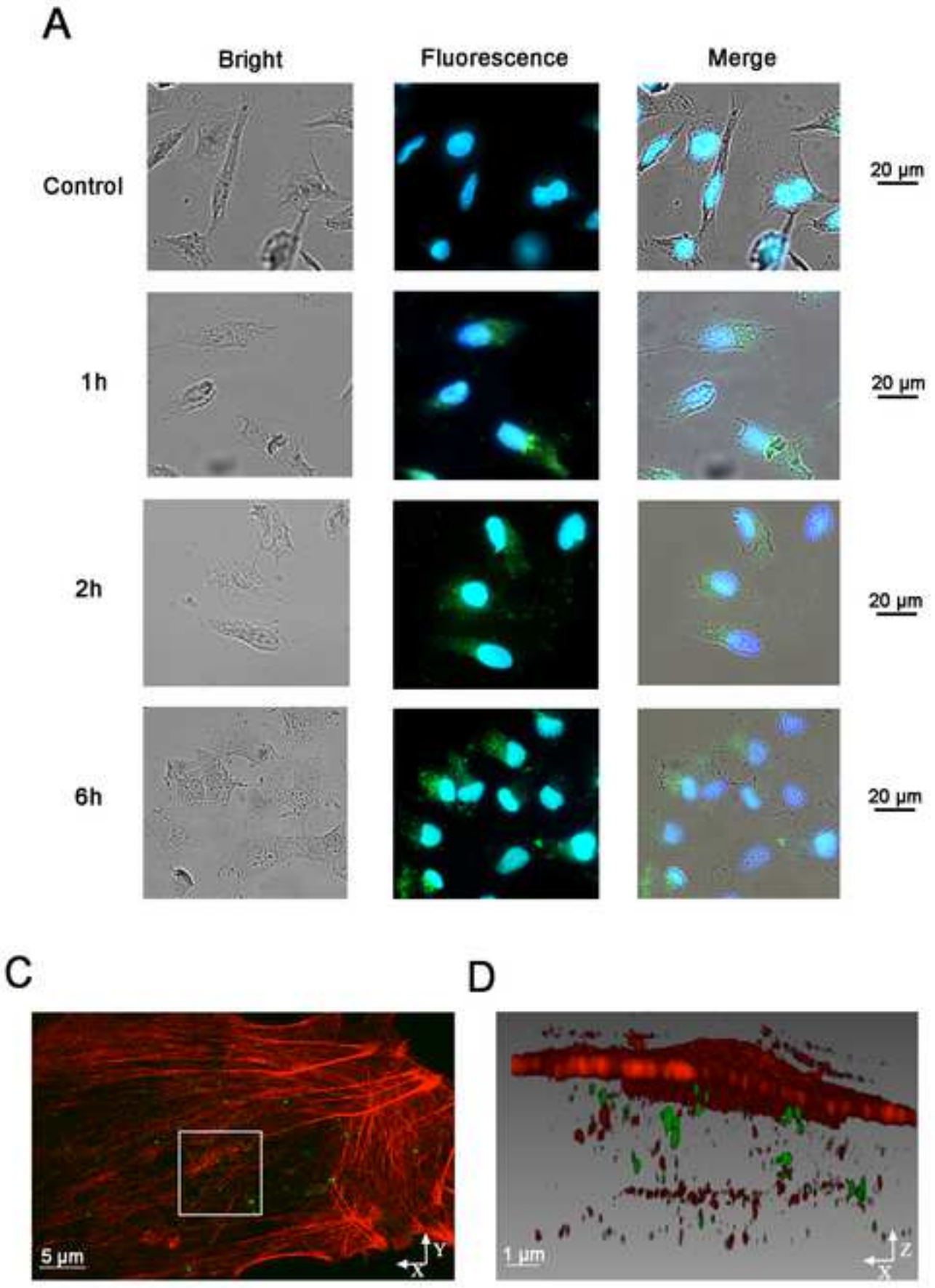

Figure 3
Click here to download Figure: Figure_3.tif

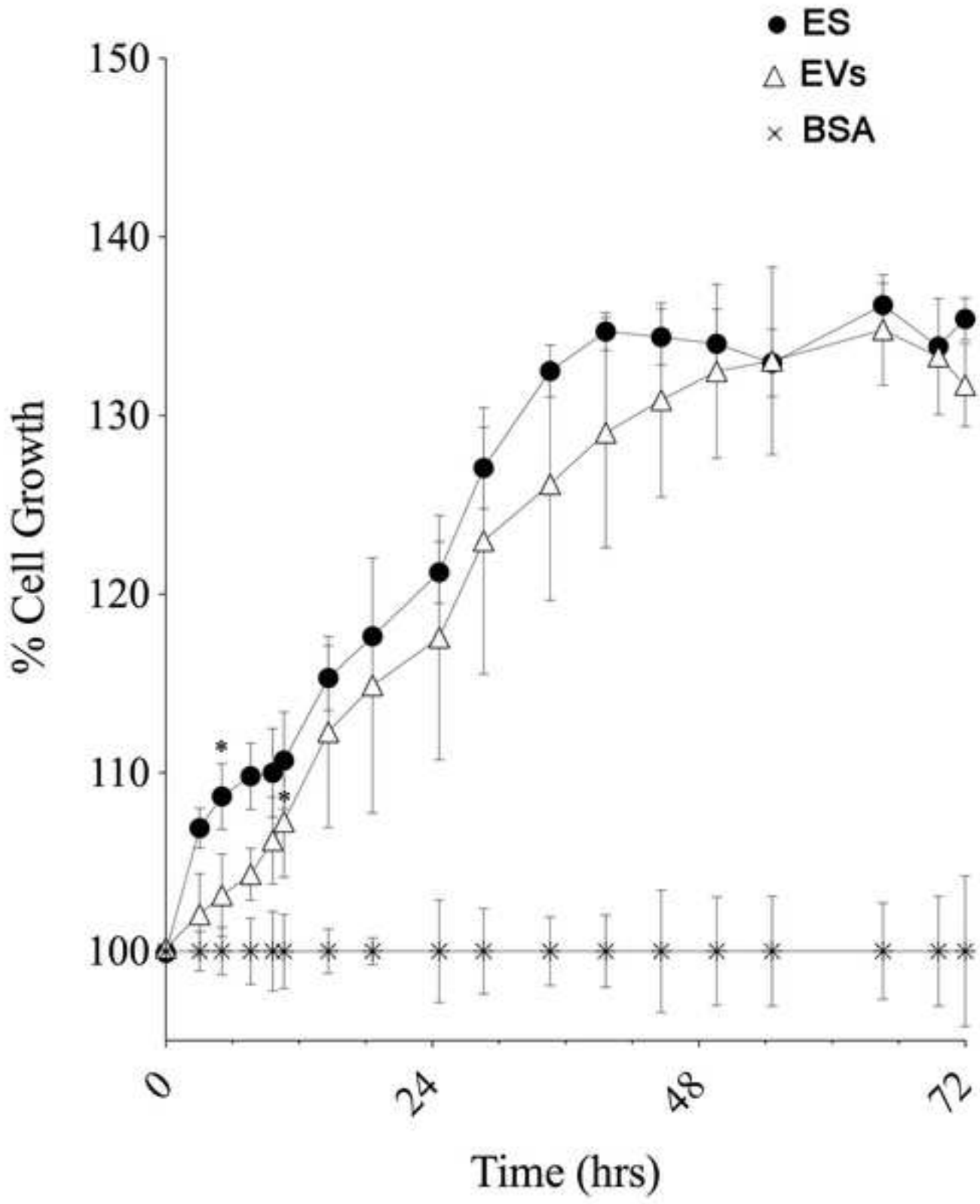

Figure 4
Click here to download Figure: Figure_4.tif

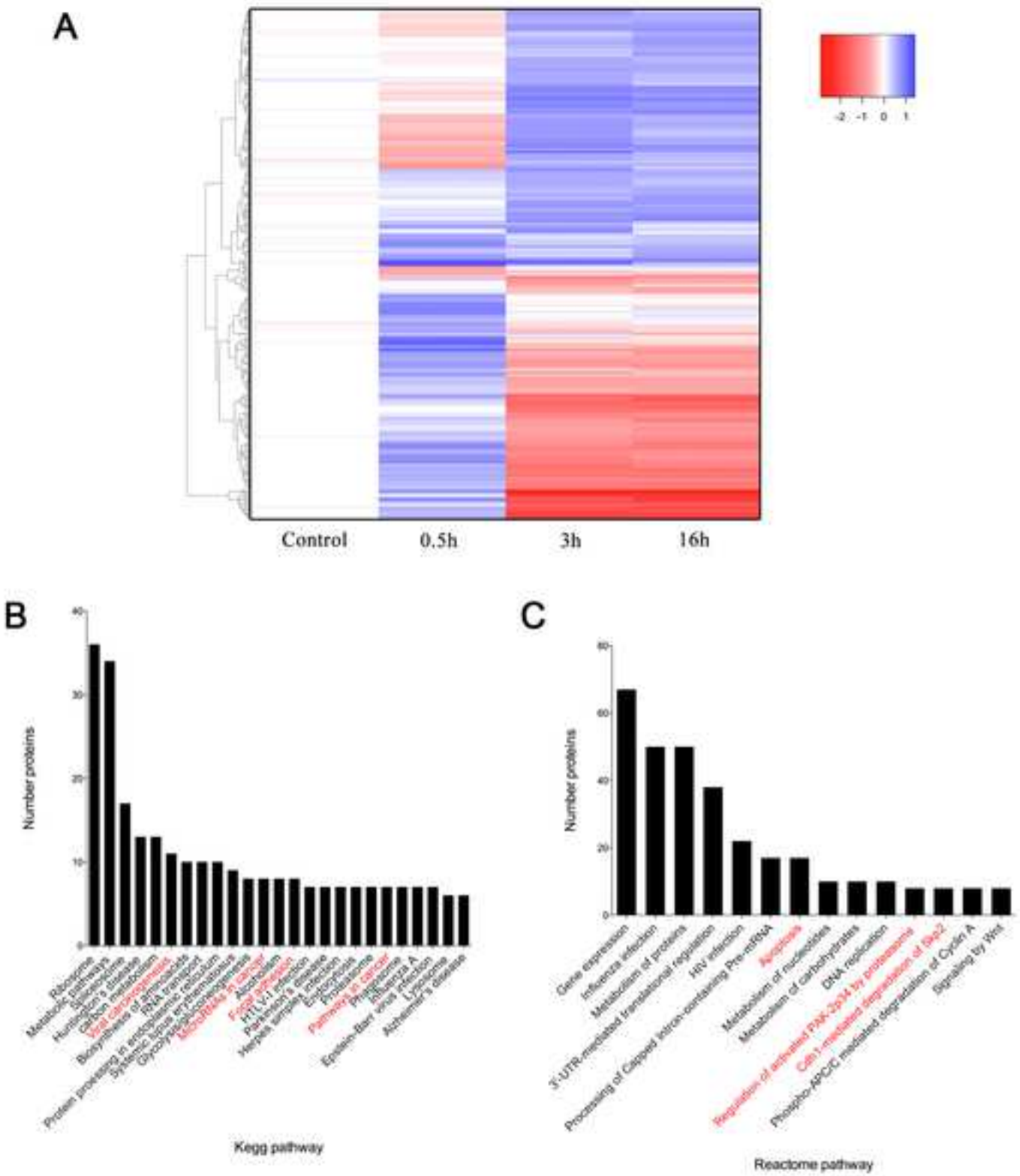

Figure 5
Click here to download Figure: Figure_5.tif

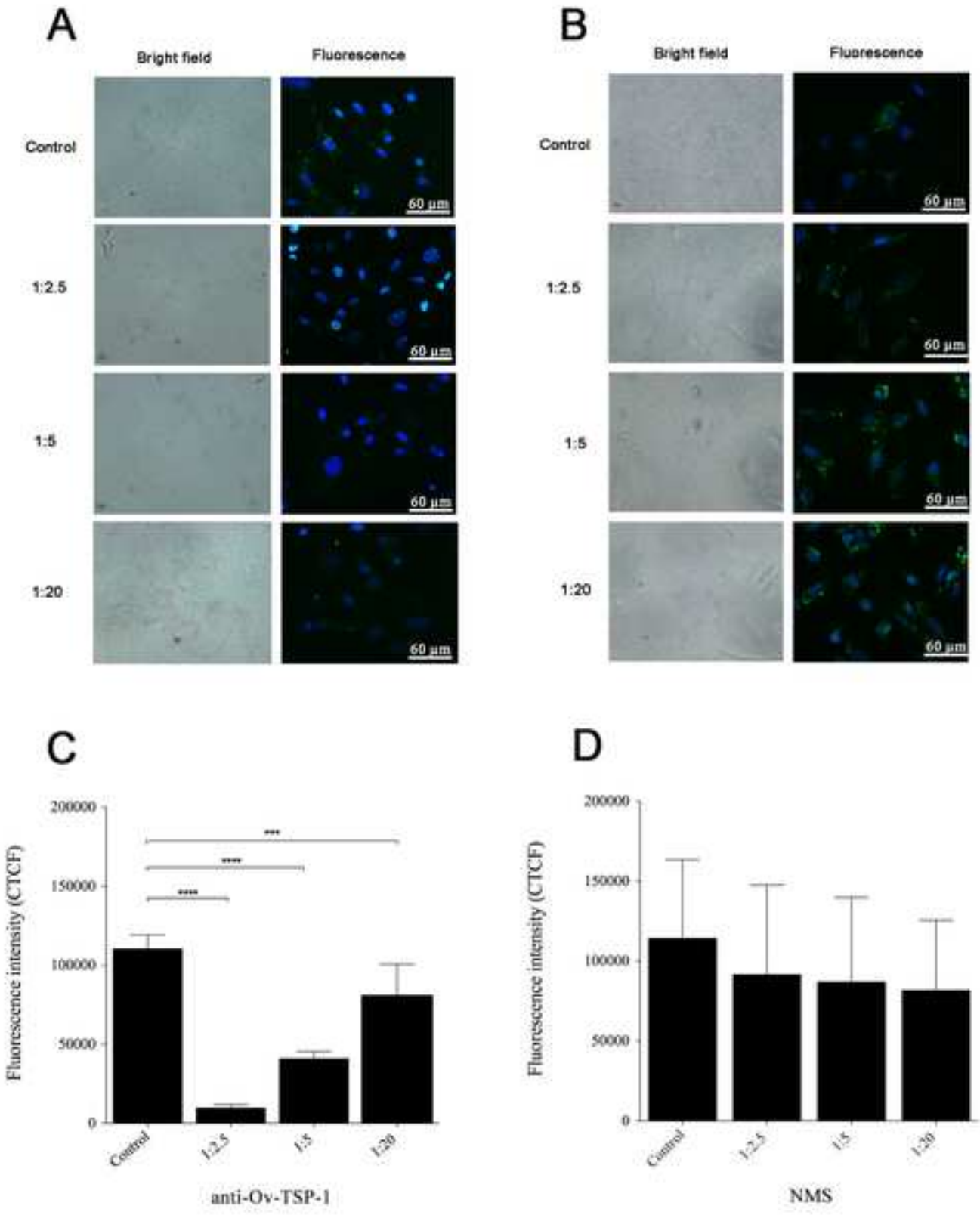

Figure 6
Click here to download Figure: Figure_6.tif

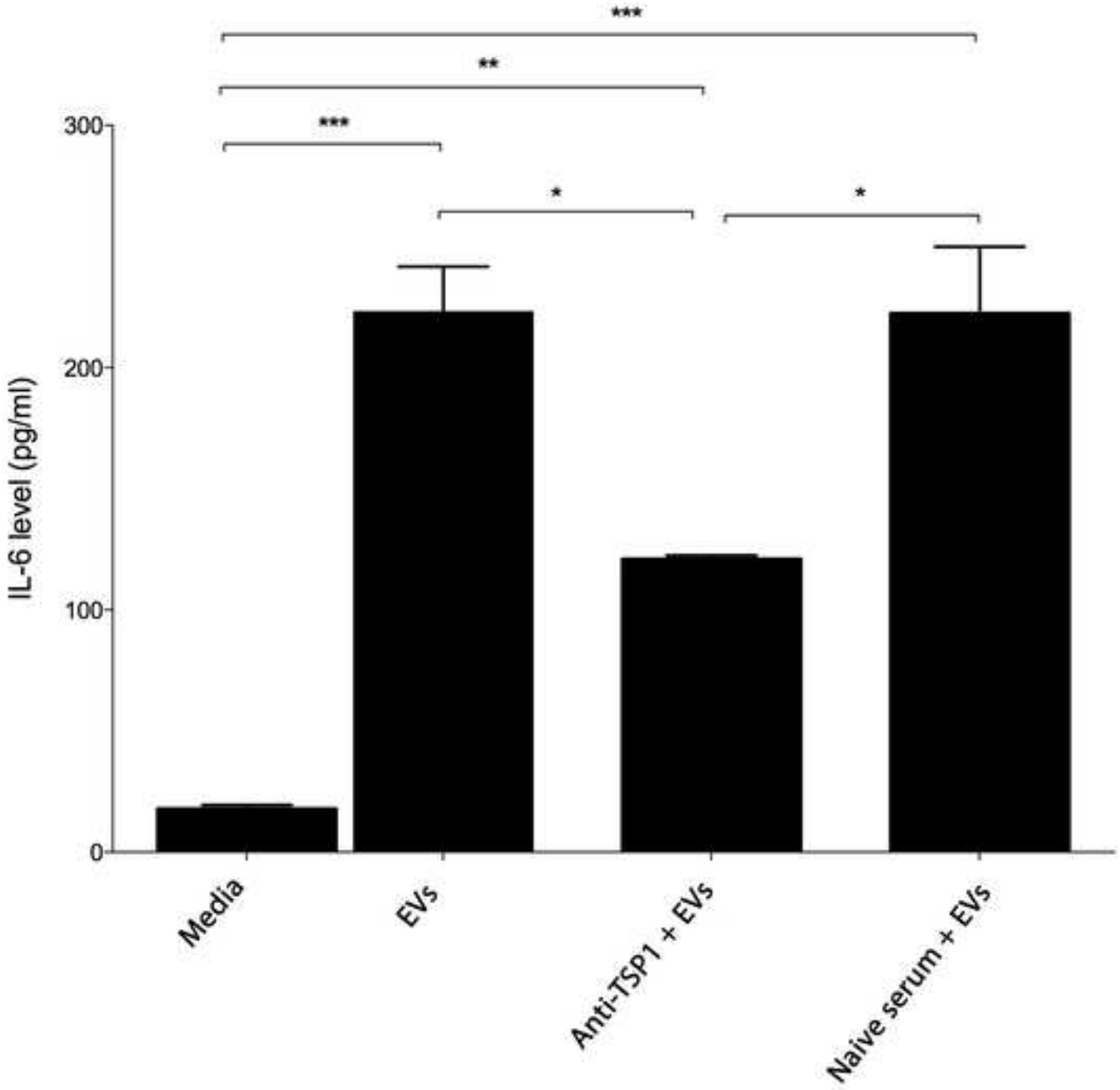

Supplementary Figure 1

Click here to download Figure: Supplementary_Figure1.tif

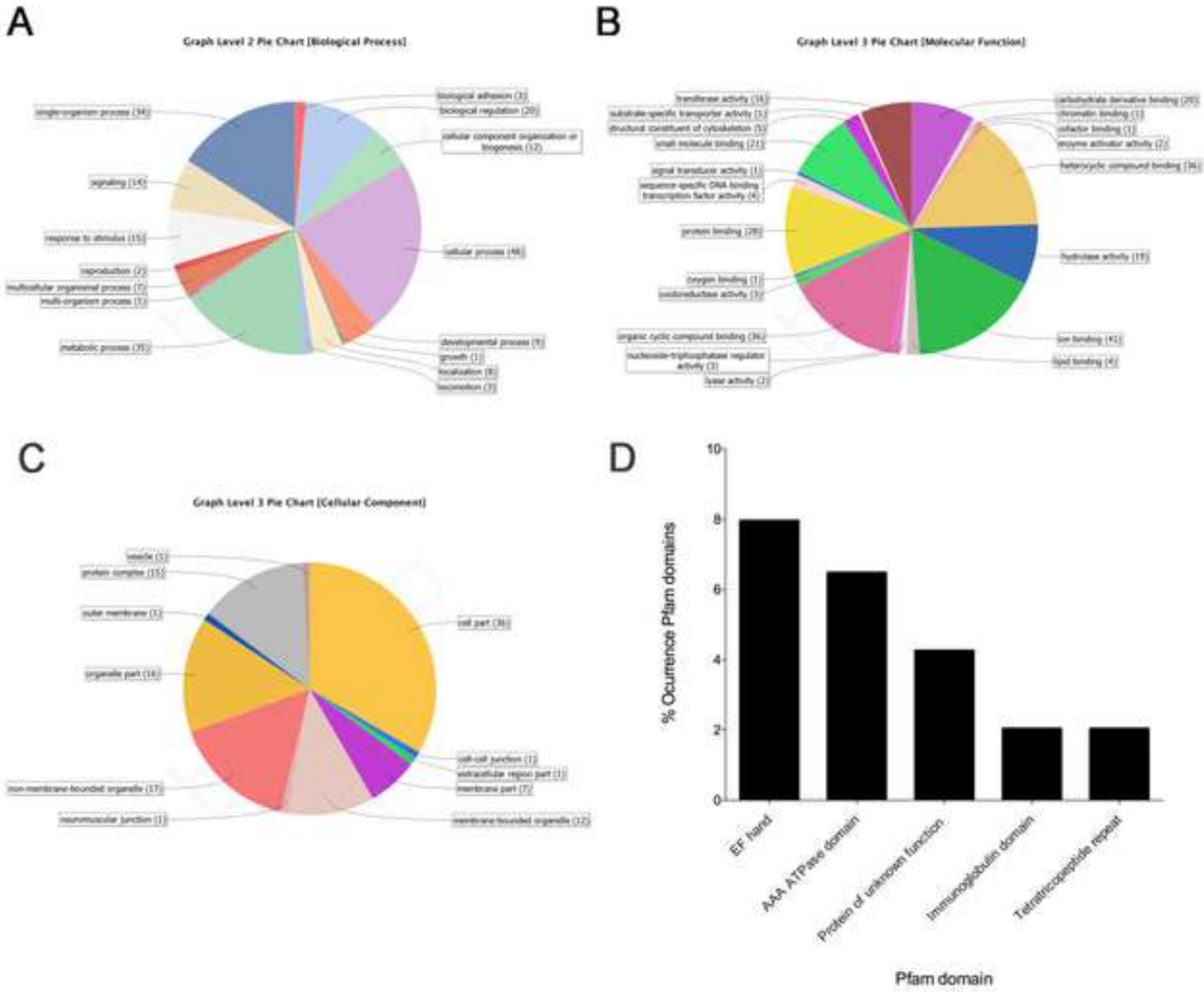

Supplementary Figure 2

Click here to download Figure: Supplementary_Figure2.tif

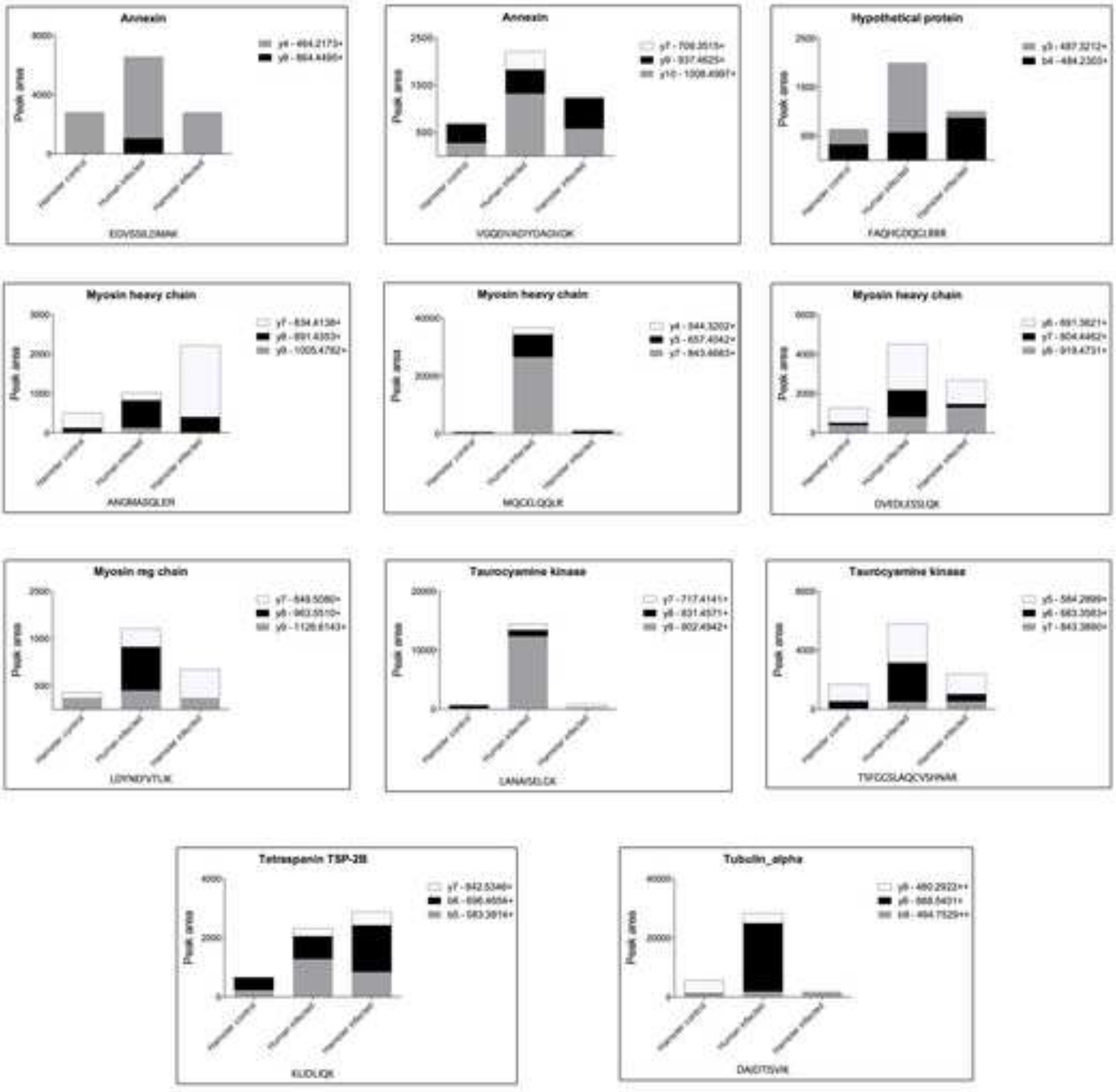

Supplementary Figure 3

Click here to download Figure: Supplementary_Figure3.tif

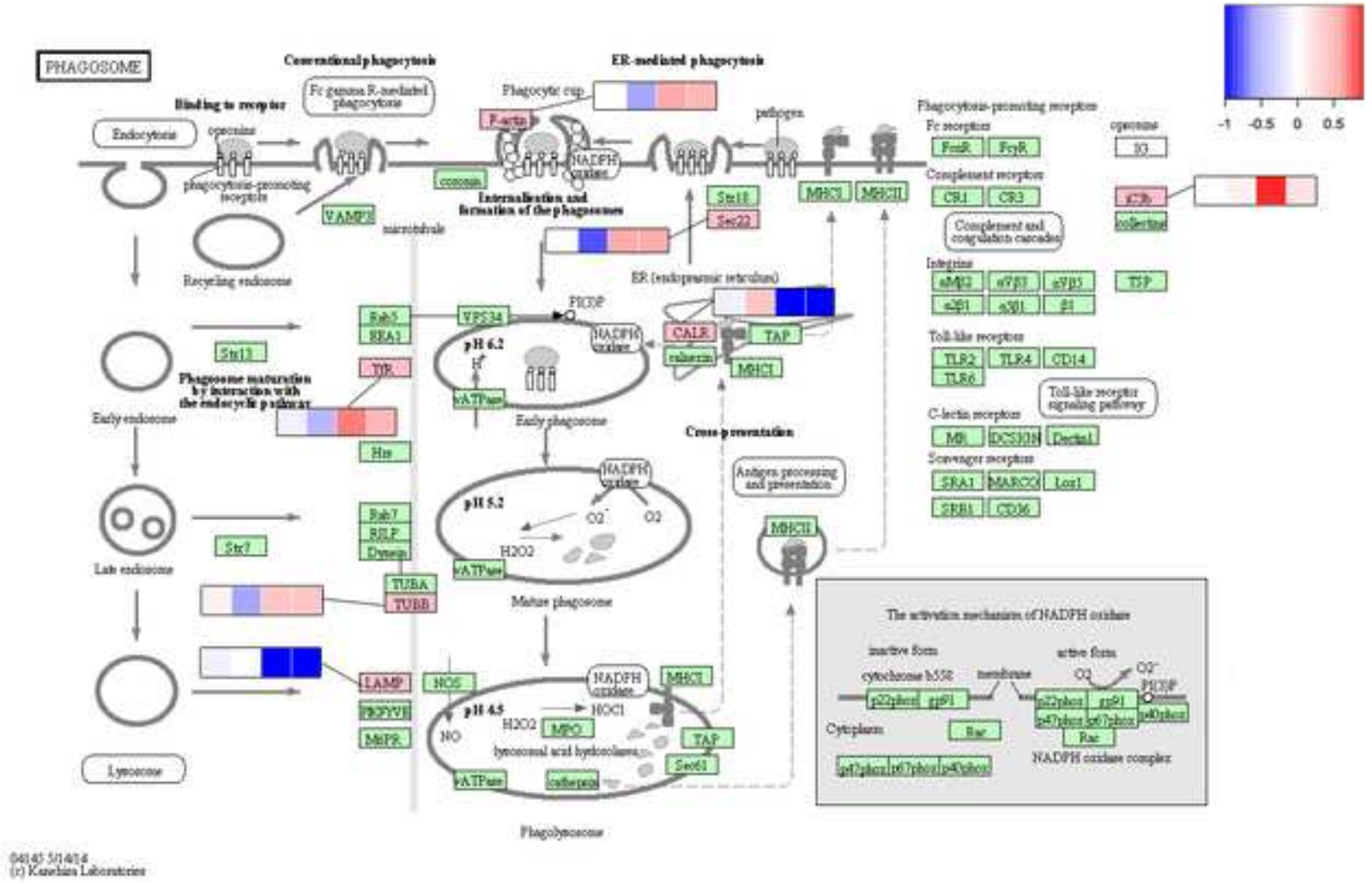

Supplementary Figure 4

Click here to download Figure: Supplementary_Figure4.tif

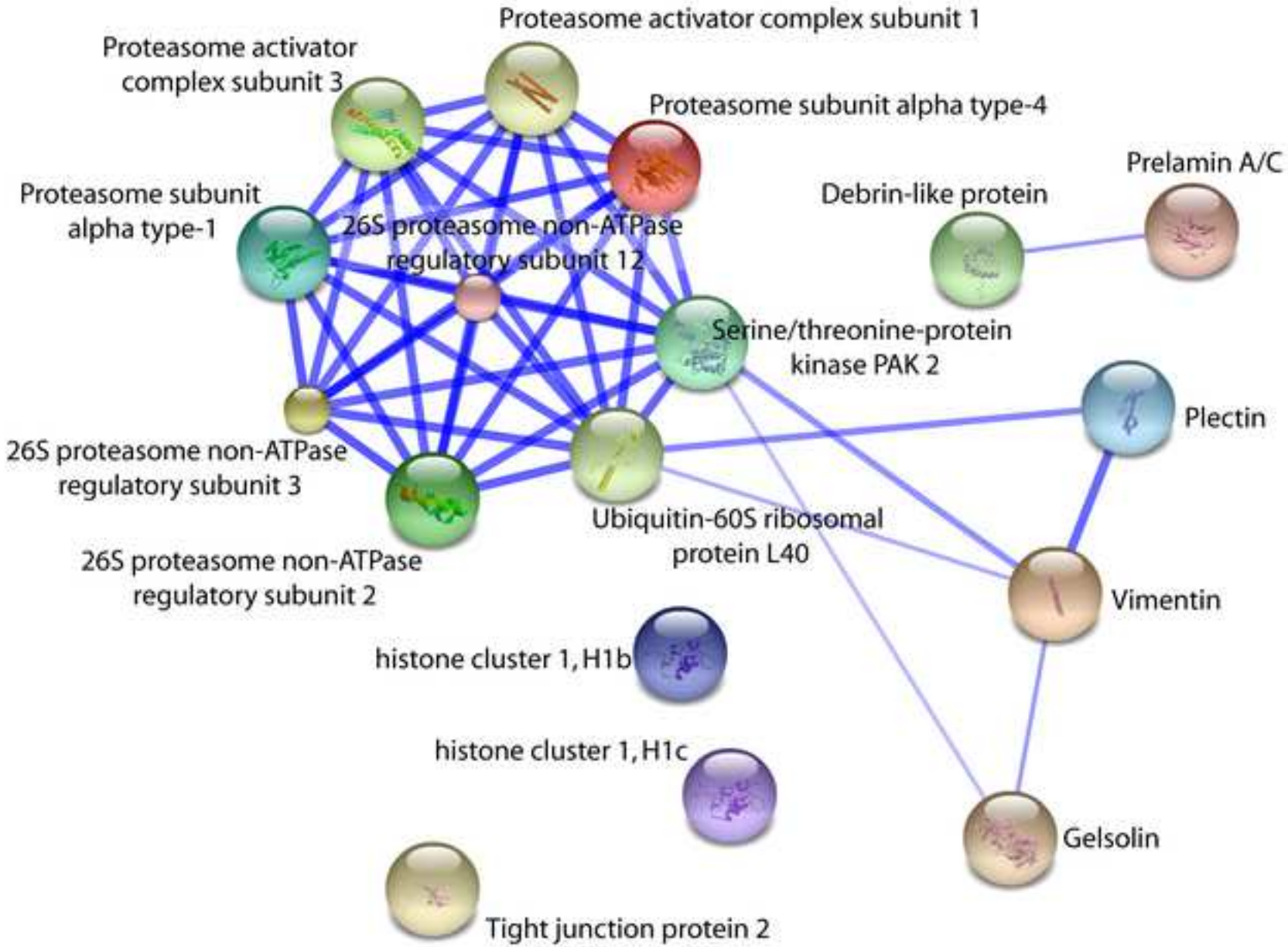

Table S1. Proteins identified in extracellular vesicles of *Opisthorchis viverr*

Seq. Name	BLAST Accession	BLAST hitName
T265_11028	gi|358253594	actin beta/gamma 1
T265_02106	gi|358332991	tubulin beta
T265_00284	gi|126116628	paramyosin
T265_06881	gi|22655518	AF527456_1calcium binding pr
T265_07359	gi|358336555	ubiquitin C
T265_09134	gi|358341210	annexin A7
T265_15787	gi|358334577	cathepsin D
T265_09973	gi|358340940	syntenin-1
T265_08714	gi|262213552	myosin regulatory light chain
T265_13308	gi|325513923	helminth defence molecule-1
T265_10526	gi|684407701	hypothetical protein T265_105
T265_15836	gi|684413836	hypothetical protein T265_158
T265_16303	gi|353229182	putative major vault protein
T265_08893	gi|358340880	annexin A7
T265_06253	gi|684390600	hypothetical protein T265_062
T265_03631	gi|358334667	tRNA (adenine-N(1)-)-methyltr
T265_05238	gi|684386456	hypothetical protein T265_052
T265_09955	gi|325459332	unknown transmembrane prot
T265_09952	gi|358333044	myosin heavy chain
T265_15563	gi|360043476	venom allergen-like (VAL) 8 pr
T265_15799	gi|685936383	Ras-related protein Rac1, parti
T265_03867	gi|20270894	AF461710_1myoglobin
T265_02259	gi|23428564	glutathione S-transferase
T265_08043	gi|358337609	tegumental protein
T265_08991	gi|358333925	Ras homolog gene family mem
T265_09265	gi|358337832	endophilin-B1
T265_10536	gi|684407743	hypothetical protein T265_105
T265_03615	gi|684379718	hypothetical protein T265_036
T265_04144	gi|684381871	hypothetical protein T265_041
T265_07169	gi|360044564	cript-related
T265_04047	gi|350023777	tubulin alpha chain
T265_07596	gi|358333877	taurocyamine kinase
T265_10204	gi|426308934	tetraspanin 2A
T265_13185	gi|684378098	hypothetical protein T265_131
T265_00358	gi|358253276	hypothetical protein CLF_1087
T265_01977	gi|358342015	COMPASS component SWD1
T265_04046	gi|358335874	tubulin alpha
T265_08065	gi|426308936	tetraspanin 2B
T265_09781	gi|358253835	DNA repair protein REV1, parti
T265_06356	gi|358335181	zinc finger protein 341
T265_10362	gi|226468366	Vesicle transport protein SFT2I

T265_02867	gi|358333977	myosin essential light chain str
T265_04527	gi|358332486	KRAB domain-containing zinc f
T265_08099	gi|904121	tropomyosin
T265_10125	gi|358254620	copine-8, partial
T265_08367	gi|358342140	hypothetical protein CLF_1033
T265_04851	gi|358336212	replication factor C subunit 3/5
T265_05756	gi|684388548	hypothetical protein T265_057
T265_13582	gi|58263527	14-3-3 protein
T265_07292	gi|358331798	tubulin alpha
T265_08188	gi|254587308	endonuclease-reverse transcri
T265_10730	gi|358339096	BRO1 domain-containing prote
T265_01105	gi|358333593	beta-arrestin
T265_03959	gi|358337668	hypothetical protein CLF_1096
T265_12534	gi|358333203	serine/threonine-protein kinas
T265_13848	gi|358254343	calcium-binding protein
T265_14319	gi|358333055	cyclin-dependent kinase-like
T265_01853	gi|360044613	putative merlin/moesin/ezrin/
T265_03292	gi|358334092	U3 small nucleolar RNA-associ
T265_06061	gi|153861719	heat shock protein 70
T265_06656	gi|358333984	hypothetical protein CLF_1080
T265_10899	gi|358342418	acetyl-CoA acyltransferase
T265_13810	gi|358340653	protein unc-80 homolog
T265_14094	gi|358332850	signal-induced proliferation-as
T265_14629	gi|685962441	Regulator of G-protein signalin
T265_00300	gi|358342642	pre-mRNA-splicing factor
T265_03216	gi|360044772	putative dead box ATP-depenc
T265_03979	gi|358335239	large subunit ribosomal protei
T265_08081	gi|358254618	coiled-coil domain-containing
T265_09935	gi|358336872	transitional endoplasmic reticu
T265_11598	gi|358253589	hypothetical protein CLF_1103
T265_11632	gi|358340214	spectrin beta chain
T265_14214	gi|358253196	calpain
T265_14955	gi|358332908	hypothetical protein CLF_1062
T265_01157	gi|358336587	sterol regulatory element-bind
T265_01206	gi|358253741	gamma-tubulin complex comp
T265_01323	gi|358332388	cullin 1
T265_01951	gi|358253292	serine/threonine-protein phos
T265_03269	gi|358336101	innexin unc-9
T265_05027	gi|353228659	putative serine-rich repeat pro
T265_06464	gi|358254922	protein tyrosine phosphatase r
T265_06544	gi|358334779	protocadherin-9
T265_06597	gi|358340957	protein CIP2A
T265_07346	gi|358341589	nuclear factor interleukin-3-re
T265_08700	gi|358332999	splicing factor arginine/serine-

T265_08792	gi|358339172	programmed cell death 6-inter
T265_09632	gi|358342856	polycomb protein Su(z)12
T265_10413	gi|358338282	integrin alpha-5
T265_15583	gi|358334974	coiled-coil domain-containing p
T265_05385	gi|358254660	ecdysone-induced protein 78C
T265_06055	gi|358338672	ankyrin repeat domain-contair
T265_09823	gi|358338574	patatin-like phospholipase dor
T265_12442	gi|358342089	exocyst complex component 6
T265_14563	gi|358336386	terminal uridylyltransferase 7
T265_14630	gi|358338747	zinc finger CCCH domain-conta
T265_15132	gi|358333293	ATPase family AAA domain-cor
T265_15342	gi|358341675	cell division cycle 2-like
T265_00630	gi|358340488	telomerase protein componen
T265_00976	gi|358252933	FH1/FH2 domain-containing pr
T265_02851	gi|358335297	neurofibromin 1
T265_04878	gi|684384900	hypothetical protein T265_048
T265_05525	gi|358340495	DNA polymerase alpha subunit
T265_11520	gi|358338356	Ca(2+)/calmodulin-responsive
T265_12500	gi|358340364	striated muscle preferentially e
T265_13055	gi|353229947	putative spectrin beta chain, b
T265_14174	gi|358254651	plectin, partial
T265_14303	gi|358255157	rootletin
T265_15051	gi|358342072	twitchin, partial

***ini* are diagnostic features of exosomes.** Mascot was used as the search engine; spectra were searc

BLAST Organism	SignalP	TMHMM	Exocarta homologue	Present in *O. viverrini*	E	#GOs
Clonorchis sinensis	N	N	Yes	No		7
Clonorchis sinensis	N	N	Yes	Yes		8
Clonorchis sinensis	N	N	No	Yes		3
Clonorchis sinensis	N	N	No	Yes		1
Clonorchis sinensis	N	N	Yes	No		1
Clonorchis sinensis	N	N	Yes	No		2
Clonorchis sinensis	N	N	Yes	No		2
Clonorchis sinensis	N	N	No	No		1
Fasciola hepatica	N	N	Yes	No		8
Fasciola hepatica	N	N	Yes	No		5
Opisthorchis viverrini	N	N	No	No		0
Opisthorchis viverrini	N	N	No	No		0
Schistosoma mansoni	N	N	Yes	Yes		3
Clonorchis sinensis	N	N	Yes	No		2
Opisthorchis viverrini	N	N	No	No		0
Clonorchis sinensis	N	N	No	No		4
Opisthorchis viverrini	N	N	No	No		0
Clonorchis sinensis	N	Y	No	No		0
Clonorchis sinensis	N	N	Yes	No		6
Schistosoma mansoni	N	N	No	Yes		1
Schistosoma haematobiu	N	N	Yes	No		6
Clonorchis sinensis	N	N	No	Yes		5
Opisthorchis viverrini	N	N	Yes	Yes		2
Clonorchis sinensis	N	N	No	Yes		3
Clonorchis sinensis	N	N	No	No		20
Clonorchis sinensis	N	N	Yes	Yes		2
Opisthorchis viverrini	N	N	No	No		0
Opisthorchis viverrini	N	N	No	No		0
Opisthorchis viverrini	N	Y	No	No		0
Schistosoma mansoni	N	N	No	No		0
Clonorchis sinensis	N	N	Yes	No		8
Clonorchis sinensis	N	N	No	No		6
Opisthorchis viverrini	N	Y	Yes	No		1
Opisthorchis viverrini	Y	N	No	No		0
Clonorchis sinensis	N	N	No	No		1
Clonorchis sinensis	N	N	No	No		1
Clonorchis sinensis	N	N	Yes	No		8
Opisthorchis viverrini	N	Y	Yes	No		1
Clonorchis sinensis	N	N	No	No		3
Clonorchis sinensis	N	N	No	No		7
Schistosoma japonicum	N	Y	No	No		2

Clonorchis sinensis	N	N	Yes	No	1
Clonorchis sinensis	N	N	Yes	No	2
Clonorchis sinensis	N	N	Yes	No	0
Clonorchis sinensis	N	N	Yes	No	4
Clonorchis sinensis	N	N	No	No	0
Clonorchis sinensis	N	N	Yes	No	3
Opisthorchis viverrini	N	N	No	No	0
Fasciola gigantica	N	N	Yes	Yes	2
Clonorchis sinensis	N	N	Yes	No	12
Schistosoma japonicum	N	N	No	No	4
Clonorchis sinensis	N	N	Yes	No	1
Clonorchis sinensis	N	N	No	No	1
Clonorchis sinensis	N	N	No	No	0
Clonorchis sinensis	N	N	Yes	No	4
Clonorchis sinensis	N	N	Yes	Yes	2
Clonorchis sinensis	N	N	Yes	No	3
Schistosoma mansoni	N	N	No	Yes	7
Clonorchis sinensis	N	N	Yes	No	2
Fasciola hepatica	N	N	Yes	No	2
Clonorchis sinensis	N	N	No	No	1
Clonorchis sinensis	N	N	Yes	No	14
Clonorchis sinensis	N	N	No	No	0
Clonorchis sinensis	N	N	No	No	3
Schistosoma haematobiu	N	N	No	No	1
Clonorchis sinensis	N	N	No	No	3
Schistosoma mansoni	N	N	Yes	No	4
Clonorchis sinensis	N	N	Yes	No	2
Clonorchis sinensis	N	N	No	No	4
Clonorchis sinensis	N	N	No	No	3
Clonorchis sinensis	N	N	No	No	1
Clonorchis sinensis	N	N	Yes	No	2
Clonorchis sinensis	N	N	Yes	Yes	4
Clonorchis sinensis	N	Y	No	No	0
Clonorchis sinensis	N	N	No	No	35
Clonorchis sinensis	N	N	No	No	3
Clonorchis sinensis	N	N	No	No	6
Clonorchis sinensis	N	N	Yes	No	1
Clonorchis sinensis	N	Y	No	No	1
Schistosoma mansoni	N	N	No	No	0
Clonorchis sinensis	N	N	No	No	3
Clonorchis sinensis	N	Y	No	No	4
Clonorchis sinensis	N	N	No	No	8
Clonorchis sinensis	N	N	No	No	3
Clonorchis sinensis	N	N	No	No	0

Clonorchis sinensis	N	N	Yes	No	1
Clonorchis sinensis	N	N	No	No	5
Clonorchis sinensis	Y	N	Yes	No	3
Clonorchis sinensis	N	N	No	No	5
Clonorchis sinensis	N	Y	No	No	8
Clonorchis sinensis	N	N	No	No	1
Clonorchis sinensis	N	N	Yes	No	2
Clonorchis sinensis	N	N	No	No	4
Clonorchis sinensis	N	N	No	No	3
Clonorchis sinensis	N	N	No	No	8
Clonorchis sinensis	N	N	Yes	No	4
Clonorchis sinensis	N	N	No	No	4
Clonorchis sinensis	N	N	No	No	3
Clonorchis sinensis	N	N	No	No	8
Clonorchis sinensis	Y	N	No	No	4
Opisthorchis viverrini	N	N	No	No	0
Clonorchis sinensis	N	N	No	No	5
Clonorchis sinensis	N	Y	No	No	3
Clonorchis sinensis	N	N	No	No	6
Schistosoma mansoni	N	N	No	No	31
Clonorchis sinensis	N	N	Yes	No	9
Clonorchis sinensis	Y	N	Yes	No	2
Clonorchis sinensis	N	N	No	No	5

:hed against the *O. viverrini* genome database [65] and hits were annotated using Blast2GO

GOs	Enzyme Codes	InterProScan	score	Number peptid	Score	emPAI
P:sarcomere	-	IPR004000 (PF	728.783	9	1040	1.05
C:microtubul	-	Coil (COILS); II	846.655	8	852	0.94
C:myofibril; C	-	Coil (COILS); C	1540.4	13	945	0.52
F:calcium ion	-	IPR002048 (SM	133.265	1	32	0.45
F:protein binding		IPR019956 (PF	303	2	147	0.43
F:calcium ion	-	IPR001464 (PF	678.707	4	213	0.39
F:aspartic-typ	EC:3.4.23	IPR001461 (PF	141.739	1	17	0.36
F:protein binding		IPR001478 (SM	287	3	216	0.34
P:DNA duple	EC:3.6.1	Coil (COILS); II	311.997	3	201	0.33
C:retromer complex; P:vacuola		Coil (COILS); M	50.447	2	84	0.32
-		no IPS match	100	1	14	0.31
-		no IPS match	99	1	38	0.31
P:eye develo	-	IPR002499 (PF	206	1	40	0.3
F:calcium ion	-	IPR001464 (PF	653.67	3	199	0.28
-		no IPS match	117	1	17	0.26
P:methylatio	-	IPR007316 (PF	207.223	1	15	0.24
-		no IPS match	134	1	27	0.24
-		Coil (COILS); C	191	5	261	0.22
C:myosin fila	-	Coil (COILS); C	3319.25	13	509	0.21
C:extracellular region		IPR001283 (PF	134.42	2	134	0.21
F:GTP binding; P:small GTPase		IPR001806 (PF	143	1	44	0.21
F:heme bindi	-	IPR011406 (PI	256.144	1	200	0.2
F:transferase	-	IPR004046 (PF	342.813	1	52	0.17
F:calcium ion	-	IPR011992 (PF	306.22	1	98	0.17
P:oviposition	-	IPR001806 (PF	293.123	1	20	0.17
C:cytoplasm;	-	Coil (COILS); II	263.848	1	50	0.17
-		no IPS match	188	1	15	0.17
-		no IPS match	182	1	25	0.16
-		CYTOPLASMIC	191	1	18	0.16
-		IPR019367 (PF	92	1	16	0.16
C:microtubul	-	Coil (COILS); II	800.431	2	56	0.14
F:metal ion b	EC:2.7.3.4	IPR022413 (G	567	3	70	0.14
C:integral to membrane		IPR000301 (PF	178.333	1	114	0.14
-		SIGNAL_PEPTI	211	1	44	0.14
F:zinc ion bin	-	IPR000433 (PF	368.622	1	23	0.13
F:protein binding		IPR001680 (SM	269	2	14	0.13
C:microtubul	-	Coil (COILS); II	753.051	2	44	0.13
C:integral to	-	IPR000301 (PF	336.265	1	39	0.13
P:DNA repair; F:DNA-directed D		no IPS match	91.2781	1	33	0.13
F:translation	EC:2.7.7.49	no IPS match	182.57	1	14	0.12
C:integral to	-	IPR007305 (PF	148.288	1	19	0.11

F:calcium ion	-	IPR011992 (G	370.933	1	147	0.1
F:nucleic acic	-	IPR015880 (SI	226.868	1	17	0.1
-		Coil (COILS); C	279	1	44	0.1
F:RNA bindin	EC:2.7.7.49	IPR010734 (PI	213.001	1	18	0.1
-		no IPS match	322	1	26	0.09
F:nucleoside-	EC:3.6.1.15	PF13177 (PFA	622.854	1	23	0.08
-		no IPS match	354	1	32	0.08
F:protein dor	-	IPR000308 (PI	338.191	1	46	0.08
C:cilium; F:pr	-	Coil (COILS); II	840.491	1	55	0.07
F:RNA binding; P:RNA-depende		no IPS match	101.679	1	13	0.07
C:membrane		IPR004328 (SI	286.96	1	34	0.07
P:signal trans	-	IPR000698 (PI	788.104	1	17	0.06
-		Coil (COILS); C	316	1	38	0.06
P:protein phc	EC:2.7.11	IPR000095 (SI	891.338	1	13	0.06
C:membrane	-	IPR002048 (SI	688.723	1	77	0.06
P:protein phc	EC:2.7.11	no IPS match	181.8	1	18	0.06
F:RNA-directe	EC:2.7.7.49	Coil (COILS); C	355.14	2	76	0.05
C:intracellula	-	Coil (COILS); C	946.806	1	17	0.05
F:ATP binding	-	IPR013126 (PI	1083.94	1	54	0.05
F:protein tyrosine phosphatase		IPR028472 (PA	415	1	19	0.05
C:mitochond	EC:4.2.1.17; EC:1.	IPR002155 (TI	573.933	1	19	0.05
-		Coil (COILS); P	344	1	14	0.05
F:GTPase acti	-	no IPS match	996.882	1	21	0.05
P:termination of G-protein cou		IPR000342 (PI	185	1	27	0.05
P:mRNA proc	-	IPR003107 (SI	1461.82	1	28	0.04
F:helicase act	-	IPR001650 (SI	716.457	1	17	0.04
C:ribosome; I	-	Coil (COILS); II	780.015	1	17	0.04
C:cytoplasm; C:cytoskeleton; P:		Coil (COILS); C	78.1814	1	15	0.04
F:nucleoside-	EC:3.6.1.15	IPR003338 (SI	1365.9	1	28	0.04
C:cell wall		TRANSMEMBI	58.5362	2	29	0.04
F:actin bindir	-	Coil (COILS); C	1178.7	2	20	0.04
C:intracellula	-	Coil (COILS); II	1535.39	1	28	0.04
-		CYTOPLASMIC	375	1	16	0.04
F:sequence-s	EC:3.1.4.11	Coil (COILS); II	817.765	1	19	0.03
C:microtubul	-	no IPS match	1664.82	1	18	0.03
C:SCF ubiquit	-	IPR016158 (SI	1125.92	1	17	0.03
F:calcium ion	-	IPR011992 (PI	1578.15	1	24	0.03
C:gap junctio	-	IPR000990 (PI	803.897	1	30	0.03
-		no IPS match	323	1	14	0.03
F:protein tyr	EC:3.1.3.48	IPR000980 (PI	1274.61	1	14	0.03
C:integral to	-	IPR002126 (PI	1865.51	1	33	0.03
F:RNA bindin	EC:2.7.7.49	Coil (COILS); II	207.608	1	28	0.03
F:sequence-s	-	Coil (COILS); C	1566.21	1	16	0.03
-		Coil (COILS); C	365	1	17	0.03

F:protein binding	Coil (COILS); II	334	1	41	0.03
F:binding; P:r	-	IPR019135 (PI	159.844	1	17	0.03
C:integrin co	-	IPR000413 (PI	1672.14	1	16	0.03
P:system dev	-	Coil (COILS); C	330.872	1	17	0.03
P:steroid hor	-	IPR000008 (PI	804.668	1	22	0.02
F:protein binding	IPR002110 (SI	846	1	14	0.02
P:phosphatid	EC:3.1.1.5	IPR000595 (SI	2380.13	1	19	0.02
P:vesicle doc	-	IPR007225 (PI	1456.04	1	18	0.02
F:zinc ion bin	-	IPR001878 (SI	3256.08	1	31	0.02
F:RNA-direct	EC:2.7.7.49	Coil (COILS); II	1535.78	1	18	0.02
F:nucleoside-	EC:3.6.1.15	Coil (COILS); II	1464.51	1	18	0.02
P:protein ph	EC:2.7.11	IPR002290 (SI	1755.34	1	20	0.02
F:RNA bindin	-	IPR001680 (SI	580.096	1	18	0.01
P:cell migrati	-	Coil (COILS); C	3016.1	1	20	0.01
C:intracellula	-	IPR001936 (SI	4016.08	1	19	0.01
-	no IPS match	2654	1	24	0.01
F:DNA-direct	EC:2.7.7.7	Coil (COILS); C	2401.71	1	20	0.01
P:intracellula	-	IPR001054 (SI	5421.67	1	20	0.01
F:Rho guanyl	-	Coil (COILS); C	5958.64	1	22	0.01
P:axon midlir	-	Coil (COILS); C	3063.86	1	20	0.01
P:anatomical	-	Coil (COILS); C	4715.6	1	21	0.01
P:centrosom	-	Coil (COILS); C	1859.73	1	13	0.01
F:protein binding; F:ATP bindin	PR00014 (PRII	20387	2	18	0.01

[66].

Seq. Length	#Hits	min. eValue	mean Similarity
358	20	0	93.80%
474	20	0	91.50%
871	20	0	93.05%
70	20	3.23E-40	67.50%
152	20	2.40E-103	99.95%
342	20	0	68.90%
86	3	7.42E-56	78.67%
302	20	0	61.45%
295	20	0	90.30%
202	17	4.42E-146	66.24%
100	1	8.01E-64	100.00%
99	2	5.38E-64	89.50%
101	20	4.75E-68	79.55%
354	20	0	69.45%
117	1	4.07E-82	100.00%
124	20	1.42E-84	69.70%
134	1	8.74E-79	100.00%
727	20	0	55.45%
1932	20	0	84.95%
298	20	0	61.20%
142	20	2.35E-99	72.10%
150	20	1.67E-104	66.00%
177	20	2.23E-126	63.20%
175	20	1.81E-112	59.80%
175	20	1.45E-111	80.40%
173	20	2.45E-95	57.90%
188	20	3.13E-135	74.00%
182	20	3.13E-127	71.35%
191	5	1.02E-137	82.00%
186	20	7.69E-135	85.10%
435	20	0	94.15%
655	20	0	82.50%
223	20	4.71E-154	66.35%
211	4	3.53E-154	70.25%
218	9	3.90E-149	64.89%
477	20	0	80.45%
473	20	0	90.00%
230	20	3.20E-149	66.00%
230	20	2.45E-170	73.40%
233	20	3.28E-159	83.50%
279	20	0	82.35%

300	20	0	85.80%
291	20	0	71.00%
284	20	7.91E-152	90.35%
314	20	0	77.30%
322	20	0	57.65%
367	20	0	80.10%
354	5	5.95E-136	66.60%
355	20	0	79.65%
451	20	0	93.15%
397	20	0	62.95%
436	20	0	60.25%
469	20	0	51.85%
499	20	0	54.65%
478	20	0	67.00%
516	20	0	77.65%
483	2	0	95.50%
1059	20	0	86.60%
561	20	0	62.50%
653	20	0	95.00%
553	20	0	78.15%
584	20	0	81.80%
610	20	0	78.20%
608	20	0	75.55%
628	20	0	54.05%
763	20	0	81.95%
744	20	0	66.60%
801	20	0	57.35%
648	20	0	56.80%
827	20	0	90.05%
1567	20	0	59.85%
1305	20	0	58.55%
756	20	0	73.05%
756	7	0	66.71%
1060	20	0	76.65%
918	20	0	68.45%
966	20	0	64.85%
929	20	0	79.25%
969	20	0	81.05%
895	5	0	67.60%
860	20	0	65.50%
1115	20	0	47.10%
1136	20	0	85.20%
936	20	0	75.30%
975	20	0	65.90%

1068	20	0	57.00%
1163	20	0	55.15%
1021	20	0	59.95%
969	20	0	58.45%
1255	20	0	54.50%
1991	20	0	56.55%
1619	20	0	62.65%
1660	20	0	58.60%
1835	20	0	54.90%
1736	20	0	95.10%
1613	20	0	69.25%
1571	20	0	88.35%
3231	20	0	56.05%
2026	20	0	64.15%
3568	20	0	72.90%
2654	2	0	74.50%
3052	20	0	62.65%
3148	20	0	58.00%
5487	20	0	53.75%
2421	20	0	77.70%
3288	20	0	56.55%
2198	20	0	59.90%
6861	1	0	100%

Table S2. Quantitative protein and peptide report of human cholangiocyte proteins after in

Microvesicles Quantitative Sample report created on 26/08/2014
Experiment: Microvesicles
Identification Criteria: unknown
Scaffold Version: Scaffold_4.2.1
Quantification Type: iTRAQ 8-Plex
Peak Quantitation Measurement: Centroided Peak Intensity
Peak List Generator: Analyst
Version: 2.0
Charge States Calculated: True
Deisotoped: True
Textual Annotation: unknown
Database Set: 2 Databases
Database Name: a subset of the SwissProt_2013_09 da
Version: 2013_09
Taxonomy: All Entries
Number of Proteins: 17420
Database Name: the SwissProt_2013_09 database
Version: 2013_09
Taxonomy: Homo sapiens
Number of Proteins: 20272
Does database contain common contaminants?: Yes
Search Engine Set: 2 Search Engines
Search Engine: Mascot
Version: 2.4.0
Samples: All Samples
Fragment Tolerance: 0.50 Da (Monoisotc
Parent Tolerance: 0.50 Da (Monoisotopic
Fixed Modifications: +304 on Kn (iTRAQ8
Variable Modifications: +16 on M (Oxidat
Database: the SwissProt_2013_09 databa
Digestion Enzyme: Trypsin
Max Missed Cleavages: 2
Probability Model:
mascot_daemon_merge (e
mascot_daemon_merge (e
Search Engine: X! Tandem
Version: CYCLONE (2010.12.01.1)
Samples: All Samples
Fragment Tolerance: 0.50 Da (Monoisotc
Parent Tolerance: 0.50 Da (Monoisotopic
Fixed Modifications: +304 on Kn (iTRAQ8
Variable Modifications: -18 on n (Glu->py

Database: a subset of the SwissProt_201
Digestion Enzyme: Trypsin
Max Missed Cleavages: 2
Probability Model:
mascot_daemon_merge (e
mascot_daemon_merge (e
Scaffold: Version: Scaffold_4.2.1
Modification Metadata Set: 1541 modifications
Source: C:\Program Files\Scaffold 4\para
Comment:
Protein Grouping Strategy: Experiment-wide grouping
Peptide Thresholds: 95.0% minimum
Protein Thresholds: 99.9% minimum and 2 peptides m
Peptide FDR: 0.8% (Decoy)
Protein FDR: 1.2% (Decoy)

Purity Correction Set: unknown
Default iTRAQ 8-Plex Purity Correction:
Purity Correction Values: [0.000,0.000,0.929,0.0689,0.
Samples Applied To: All Samples
Quantitation Preferences: unknown
Minimum Value Preference:
Use Minimum Absolute Intensity: false
Minimum Absolute Intensity: 0.0
Minimum Value: 0.01
Model Preference:
Model Type: Intensity-Based Normalization
Condenser Preference:
Use Intensity Weighting: true
Use Standard Deviation Estimation: true
Use Non-Exclusive Peptides: false
Intensity-Based Normalization Preference:
Calculation Type: Median
Quant Uniqueness Model: Unique Peptides
Use Inter Experiment Normalization: true
Use Intra Sample Normalization: true
Use Peptide Normalization: true
Use Protein Reference Normalization: true
Use Protein Average As Reference: true
Use Iterative Normalization: true
View Preference:
View Type: Log2 Ratio
Normalization Factors: unknown
Inter-Experiment Normalization Factors:

Javi_microvesicles: -0.000

Intra-Sample Normalization Factors:

Javi_microvesicles: [0.609,1.40,55.7,55.7,-1.14,55.7,-1.

Quantitative Test: unknown

Quantitative Test: Kruskal-Wallis Test (P-Value)

Microvesicles Displaying:Log2 Fold Change

#	Visible?	Starred?	Identified Prc	Accession Nu	Molecular W	Protein Grou
1	TRUE	Empty	Serum album	ALBU_HUMA	69 kDa	TRUE
2	TRUE	Empty	Cluster of Act	ACTB_HUMA	42 kDa	TRUE
3	TRUE	Empty	Cluster of His	H2B1M_HUM	14 kDa	TRUE
4	TRUE	Empty	Cluster of My	MYH9_HUMA	227 kDa	TRUE
5	TRUE	Empty	Neuroblast di	AHNK_HUMA	629 kDa	TRUE
6	TRUE	Empty	Cluster of Vin	VIME_HUMA	54 kDa	TRUE
7	TRUE	Empty	Cluster of Gly	G3P_HUMAN	36 kDa	TRUE
8	TRUE	Empty	Cluster of Tul	TBB5_HUMA	50 kDa	TRUE
9	TRUE	Empty	Histone H4 O	H4_HUMAN	11 kDa	
10	TRUE	Empty	Cluster of He	HS90B_HUM	83 kDa	TRUE
11	TRUE	Empty	Cluster of An	ANXA2_HUM	39 kDa	TRUE
12	TRUE	Empty	Plectin OS=H	PLEC_HUMAN	532 kDa	TRUE
13	TRUE	Empty	Cluster of Fil	FLNA_HUMA	281 kDa	TRUE
14	TRUE	Empty	Cluster of Tul	TBA1A_HUM	50 kDa	TRUE
15	TRUE	Empty	Cluster of Elo	EF1A1_HUMA	50 kDa	TRUE
16	TRUE	Empty	Cluster of Mc	MOES_HUMA	68 kDa	TRUE
17	TRUE	Empty	Nucleolin OS=	NUCL_HUMA	77 kDa	TRUE
18	TRUE	Empty	Cluster of His	H31T_HUMA	16 kDa	TRUE
19	TRUE	Empty	Cluster of Ub	RL40_HUMAN	15 kDa	TRUE
20	TRUE	Empty	Prelamin-A/C	LMNA_HUMA	74 kDa	TRUE
21	TRUE	Empty	Cluster of He	HSP7C_HUM	71 kDa	TRUE
22	TRUE	Empty	Cluster of Pyr	KPYM_HUMA	58 kDa	TRUE
23	TRUE	Empty	Annexin A5 C	ANXA5_HUM	36 kDa	TRUE
24	TRUE	Empty	Peptidyl-prol	PPIA_HUMAN	18 kDa	TRUE
25	TRUE	Empty	10 kDa heat s	CH10_HUMA	11 kDa	
26	TRUE	Empty	Cluster of Ker	K1C18_HUMA	48 kDa	TRUE
27	TRUE	Empty	Cluster of Alp	ENOA_HUMA	47 kDa	TRUE
28	TRUE	Empty	Cluster of Alp	ACTN4_HUM	105 kDa	TRUE
29	TRUE	Empty	Cluster of His	H12_HUMAN	21 kDa	TRUE
30	TRUE	Empty	Protein disulf	PDIA1_HUMA	57 kDa	TRUE
31	TRUE	Empty	60 kDa heat s	CH60_HUMA	61 kDa	TRUE
32	TRUE	Empty	Cluster of L-la	LDHA_HUMA	37 kDa	TRUE
33	TRUE	Empty	Spectrin alph	SPTN1_HUM	285 kDa	TRUE
34	TRUE	Empty	Cluster of Ph	PGK1_HUMA	45 kDa	TRUE
35	TRUE	Empty	Protein disulf	PDIA3_HUMA	57 kDa	TRUE

36	TRUE	Empty	Elongation fa	EF2_HUMAN	95 kDa	TRUE
37	TRUE	Empty	78 kDa gluco	GRP78_HUM	72 kDa	TRUE
38	TRUE	Empty	Cluster of Tra	TAGL2_HUM	22 kDa	TRUE
39	TRUE	Empty	Cluster of RN	RBMX_HUM	42 kDa	TRUE
40	TRUE	Empty	Cluster of 14-	1433Z_HUM	28 kDa	TRUE
41	TRUE	Empty	Triosephosph	TPIS_HUMAN	31 kDa	
42	TRUE	Empty	ATP synthase	ATPB_HUMA	57 kDa	TRUE
43	TRUE	Empty	Nucleophosm	NPM_HUMAN	33 kDa	TRUE
44	TRUE	Empty	Microtubule-	MAP4_HUM	121 kDa	
45	TRUE	Empty	Cluster of En	ENPL_HUMAN	92 kDa	TRUE
46	TRUE	Empty	Cluster of Sta	STMN1_HUM	17 kDa	TRUE
47	TRUE	Empty	Cluster of He	HNRPC_HUM	34 kDa	TRUE
48	TRUE	Empty	Heterogeneo	ROA2_HUMA	37 kDa	TRUE
49	TRUE	Empty	Heterogeneo	HNRPK_HUM	51 kDa	TRUE
50	TRUE	Empty	DNA-dependi	PRKDC_HUM	469 kDa	TRUE
51	TRUE	Empty	Ribosome-bir	RRBP1_HUM	152 kDa	TRUE
52	TRUE	Empty	MRO2B_HUM	MRO2B_HUM	?	TRUE
53	TRUE	Empty	Cluster of Cal	CALM_HUMA	17 kDa	TRUE
54	TRUE	Empty	Cluster of Spe	SPTB2_HUM	275 kDa	TRUE
55	TRUE	Empty	Profilin-1 OS=	PROF1_HUM	15 kDa	
56	TRUE	Empty	Cluster of 40S	RS10_HUMAN	19 kDa	TRUE
57	TRUE	Empty	Calreticulin O	CALR_HUMA	48 kDa	
58	TRUE	Empty	Cluster of He	ROA1_HUMA	39 kDa	TRUE
59	TRUE	Empty	Talin-1 OS=H	TLN1_HUMAN	270 kDa	TRUE
60	TRUE	Empty	Stress-induce	STIP1_HUMA	63 kDa	TRUE
61	TRUE	Empty	Heat shock pr	HSPB1_HUM	23 kDa	
62	TRUE	Empty	Peroxiredoxir	PRDX6_HUM	25 kDa	TRUE
63	TRUE	Empty	Peptidyl-prol	PPIB_HUMAN	24 kDa	TRUE
64	TRUE	Empty	40S ribosoma	RS19_HUMAN	16 kDa	
65	TRUE	Empty	T-complex pr	TCPG_HUMA	61 kDa	
66	TRUE	Empty	Cluster of Fru	ALDOA_HUM	39 kDa	TRUE
67	TRUE	Empty	ATP synthase	ATPA_HUMA	60 kDa	TRUE
68	TRUE	Empty	Histone H1.5	H15_HUMAN	23 kDa	TRUE
69	TRUE	Empty	Alpha-2-HS-g	FETUA_HUM	39 kDa	
70	TRUE	Empty	40S ribosoma	RS9_HUMAN	23 kDa	TRUE
71	TRUE	Empty	Proteasome s	PSME1_HUM	29 kDa	
72	TRUE	Empty	Cluster of Cla	CLH1_HUMAN	192 kDa	TRUE
73	TRUE	Empty	Transitional e	TERA_HUMAN	89 kDa	TRUE
74	TRUE	Empty	Protein S100-	S10A6_HUM	10 kDa	
75	TRUE	Empty	Cluster of AD	ADT2_HUMA	33 kDa	TRUE
76	TRUE	Empty	40S ribosoma	RS16_HUMAN	16 kDa	
77	TRUE	Empty	L-lactate deh	LDHB_HUMA	37 kDa	TRUE
78	TRUE	Empty	40S ribosoma	RS3A_HUMAN	30 kDa	
79	TRUE	Empty	Ras GTPase-a	IQGA1_HUM	189 kDa	TRUE

80	TRUE	Empty	X-ray repair c	XRCC6_HUM	70 kDa	TRUE
81	TRUE	Empty	Cluster of Hig	HMGB1_HUM	25 kDa	TRUE
82	TRUE	Empty	Translational	GCN1L_HUM	293 kDa	TRUE
83	TRUE	Empty	Cytoplasmic c	DYHC1_HUM	532 kDa	TRUE
84	TRUE	Empty	Stress-70 pro	GRP75_HUM	74 kDa	TRUE
85	TRUE	Empty	Cluster of Prc	TGM2_HUM	77 kDa	TRUE
86	TRUE	Empty	Cluster of He	HBA_HUMAN	15 kDa	TRUE
87	TRUE	Empty	Cluster of Col	COF1_HUMA	19 kDa	TRUE
88	TRUE	Empty	40S ribosoma	RS18_HUMAN	18 kDa	
89	TRUE	Empty	Galectin-1 OS	LEG1_HUMAN	15 kDa	
90	TRUE	Empty	Prohibitin-2 C	PHB2_HUMA	33 kDa	
91	TRUE	Empty	Cluster of 40S	RS4X_HUMAN	30 kDa	TRUE
92	TRUE	Empty	Calnexin OS=	CALX_HUMAN	68 kDa	TRUE
93	TRUE	Empty	Heterogeneo	HNRPM_HUM	78 kDa	
94	TRUE	Empty	Cluster of Lac	TRFL_HUMAN	78 kDa	TRUE
95	TRUE	Empty	Cluster of His	H2A2B_HUM	14 kDa	TRUE
96	TRUE	Empty	Myosin light p	MYL6_HUMA	17 kDa	
97	TRUE	Empty	60S ribosoma	RL4_HUMAN	48 kDa	TRUE
98	TRUE	Empty	Cluster of Trc	TPM3_HUMA	33 kDa	TRUE
99	TRUE	Empty	Cluster of Nu	YBOX1_HUM	36 kDa	TRUE
100	TRUE	Empty	60S ribosoma	RL3_HUMAN	46 kDa	TRUE
101	TRUE	Empty	Cluster of Glu	G6PI_HUMAN	63 kDa	TRUE
102	TRUE	Empty	Cluster of Trc	TPM1_HUMA	33 kDa	TRUE
103	TRUE	Empty	Cystatin-B OS	CYTB_HUMA	11 kDa	
104	TRUE	Empty	Malate dehyc	MDHM_HUM	36 kDa	
105	TRUE	Empty	Protein S100-	S10AA_HUM	11 kDa	TRUE
106	TRUE	Empty	Thioredoxin C	THIO_HUMA	12 kDa	
107	TRUE	Empty	Calpastatin O	ICAL_HUMAN	77 kDa	
108	TRUE	Empty	Elongation fa	EF1G_HUMA	50 kDa	
109	TRUE	Empty	Neutral alpha	GANAB_HUM	107 kDa	
110	TRUE	Empty	Serine/argini	SRSF1_HUMA	28 kDa	TRUE
111	TRUE	Empty	60S ribosoma	RL6_HUMAN	33 kDa	TRUE
112	TRUE	Empty	Annexin A6 C	ANXA6_HUM	76 kDa	TRUE
113	TRUE	Empty	ATP-citrate s	ACLY_HUMA	121 kDa	TRUE
114	TRUE	Empty	40S ribosoma	RS7_HUMAN	22 kDa	TRUE
115	TRUE	Empty	60S ribosoma	RL23A_HUM	18 kDa	
116	TRUE	Empty	Vinculin OS=H	VINC_HUMA	124 kDa	
117	TRUE	Empty	Heterogeneo	ROAA_HUMA	36 kDa	TRUE
118	TRUE	Empty	Far upstream	FUBP2_HUM	73 kDa	TRUE
119	TRUE	Empty	C-1-tetrahydr	C1TC_HUMA	102 kDa	
120	TRUE	Empty	Annexin A1 C	ANXA1_HUM	39 kDa	TRUE
121	TRUE	Empty	Cluster of 60S	RL13A_HUM	24 kDa	TRUE
122	TRUE	Empty	Transketolase	TKT_HUMAN	68 kDa	TRUE
123	TRUE	Empty	Calumenin OS	CALU_HUMA	37 kDa	TRUE

124	TRUE	Empty	Cluster of He	HBB_HUMAN	16 kDa	TRUE
125	TRUE	Empty	Eukaryotic tra	IF4H_HUMAN	27 kDa	TRUE
126	TRUE	Empty	40S ribosoma	RS13_HUMAN	17 kDa	TRUE
127	TRUE	Empty	Glucosidase 2	GLU2B_HUM	59 kDa	TRUE
128	TRUE	Empty	Cluster of Hig	HMGB2_HUM	24 kDa	TRUE
129	TRUE	Empty	Cluster of Eul	IF4A1_HUMA	46 kDa	TRUE
130	TRUE	Empty	60S ribosoma	RL13_HUMAN	24 kDa	
131	TRUE	Empty	Peptidyl-prol	FKBP3_HUMA	25 kDa	TRUE
132	TRUE	Empty	Myosin regul	ML12A_HUM	20 kDa	TRUE
133	TRUE	Empty	T-complex pr	TCPQ_HUMA	60 kDa	
134	TRUE	Empty	40S ribosoma	RS15A_HUM	15 kDa	
135	TRUE	Empty	Glycine--tRNA	SYG_HUMAN	83 kDa	TRUE
136	TRUE	Empty	Plasminogen	PAIRB_HUMA	45 kDa	
137	TRUE	Empty	60S ribosoma	RL7_HUMAN	29 kDa	TRUE
138	TRUE	Empty	Nuclear ubiqu	NUCKS_HUM	27 kDa	
139	TRUE	Empty	ATPase inhibi	ATIF1_HUMA	12 kDa	
140	TRUE	Empty	Procollagen-l	PLOD2_HUM	85 kDa	
141	TRUE	Empty	40S ribosoma	RS25_HUMAN	14 kDa	
142	TRUE	Empty	Cluster of 6-p	K6PF_HUMAN	85 kDa	TRUE
143	TRUE	Empty	Cluster of Eul	IF5A1_HUMA	17 kDa	TRUE
144	TRUE	Empty	Cluster of Ser	2AAA_HUMA	65 kDa	TRUE
145	TRUE	Empty	Fatty acid syn	FAS_HUMAN	273 kDa	TRUE
146	TRUE	Empty	Lupus La prot	LA_HUMAN	47 kDa	
147	TRUE	Empty	Cluster of 60S	RL26_HUMAN	17 kDa	TRUE
148	TRUE	Empty	Protein disulf	PDIA4_HUMA	73 kDa	
149	TRUE	Empty	Cluster of Dih	DPYL2_HUMA	62 kDa	TRUE
150	TRUE	Empty	Protein S100-	S10AB_HUM	12 kDa	
151	TRUE	Empty	Fascin OS=Ho	FSCN1_HUM	55 kDa	
152	TRUE	Empty	Protein DJ-1 (	PARK7_HUM	20 kDa	TRUE
153	TRUE	Empty	Cluster of Ph	PGAM1_HUM	29 kDa	TRUE
154	TRUE	Empty	Heterogeneo	HNRPU_HUM	91 kDa	
155	TRUE	Empty	60S acidic rib	RLA0_HUMAN	34 kDa	
156	TRUE	Empty	60S ribosoma	RL10_HUMAN	25 kDa	
157	TRUE	Empty	Staphylococc	SND1_HUMA	102 kDa	
158	TRUE	Empty	Cluster of Nu	NDKB_HUMA	17 kDa	TRUE
159	TRUE	Empty	Non-histone	HMGN2_HUM	9 kDa	TRUE
160	TRUE	Empty	Nuclear mito	NUMA1_HUM	238 kDa	TRUE
161	TRUE	Empty	Glycogen pho	PYGB_HUMA	97 kDa	TRUE
162	TRUE	Empty	60S ribosoma	RL31_HUMAN	14 kDa	TRUE
163	TRUE	Empty	Dolichyl-diph	RPN1_HUMA	69 kDa	
164	TRUE	Empty	40S ribosoma	RS3_HUMAN	27 kDa	
165	TRUE	Empty	Tropomyosin	TPM4_HUMA	29 kDa	TRUE
166	TRUE	Empty	28 kDa heat-	HAP28_HUM	21 kDa	
167	TRUE	Empty	Programmed	PDCD5_HUM	14 kDa	TRUE

168	TRUE	Empty	Non-POU dor	NONO_HUM/	54 kDa	TRUE
169	TRUE	Empty	60S ribosoma	RL5_HUMAN	34 kDa	
170	TRUE	Empty	Cluster of Spl	DX39B_HUM/	49 kDa	TRUE
171	TRUE	Empty	Thioredoxin c	TXND5_HUM	48 kDa	
172	TRUE	Empty	RNA-binding	EWS_HUMAN	68 kDa	TRUE
173	TRUE	Empty	Glutathione S	GSTO1_HUM	28 kDa	
174	TRUE	Empty	Periplakin OS	PEPL_HUMAN	205 kDa	TRUE
175	TRUE	Empty	Epiplakin OS=	EPIPL_HUMA	556 kDa	TRUE
176	TRUE	Empty	Polymerase I	PTRF_HUMAI	43 kDa	TRUE
177	TRUE	Empty	Arginine--tRN	SYRC_HUMAI	75 kDa	
178	TRUE	Empty	Exportin-2 OS	XPO2_HUMA	110 kDa	
179	TRUE	Empty	T-complex pr	TCPE_HUMAI	60 kDa	
180	TRUE	Empty	Platelet-activ	PA1B3_HUM/	26 kDa	
181	TRUE	Empty	Elongation fa	EFTU_HUMAI	50 kDa	TRUE
182	TRUE	Empty	Eukaryotic tra	IF4B_HUMAN	69 kDa	
183	TRUE	Empty	Splicing facto	SFPQ_HUMA	76 kDa	TRUE
184	TRUE	Empty	Protein disulf	PDIA6_HUM/	48 kDa	
185	TRUE	Empty	Alpha-2-macr	A2MG_HUM/	163 kDa	TRUE
186	TRUE	Empty	Inter-alpha-tr	ITIH2_HUMA	106 kDa	
187	TRUE	Empty	60S acidic rib	RLA2_HUMAI	12 kDa	
188	TRUE	Empty	Single-strand	SSBP_HUMAI	17 kDa	
189	TRUE	Empty	DnaJ homolo	DNJC8_HUM/	30 kDa	
190	TRUE	Empty	40S ribosoma	RS2_HUMAN	31 kDa	
191	TRUE	Empty	Elongation fa	EF1B_HUMAI	25 kDa	TRUE
192	TRUE	Empty	Caveolin-1 OS	CAV1_HUMA	20 kDa	
193	TRUE	Empty	Non-histone	HMGN1_HUM	11 kDa	TRUE
194	TRUE	Empty	Cluster of T-c	TCPZ_HUMAI	58 kDa	TRUE
195	TRUE	Empty	Peptidyl-prol	FKBP5_HUM/	51 kDa	
196	TRUE	Empty	Cluster of AD	ARF3_HUMAI	21 kDa	TRUE
197	TRUE	Empty	Cluster of Pol	PCBP1_HUM/	37 kDa	TRUE
198	TRUE	Empty	Transaldolase	TALDO_HUM	38 kDa	TRUE
199	TRUE	Empty	Ubiquitin-ass	UBP2L_HUM/	115 kDa	
200	TRUE	Empty	Small nuclear	RUXGL_HUM	9 kDa	
201	TRUE	Empty	Serine hydro	GLYM_HUMA	56 kDa	
202	TRUE	Empty	Interleukin er	ILF2_HUMAN	43 kDa	
203	TRUE	Empty	Caldesmon O	CALD1_HUM/	93 kDa	TRUE
204	TRUE	Empty	Eukaryotic tra	EIF3B_HUMA	92 kDa	
205	TRUE	Empty	D-3-phospho	SERA_HUMAI	57 kDa	
206	TRUE	Empty	60S ribosoma	RL8_HUMAN	28 kDa	TRUE
207	TRUE	Empty	Cluster of Pu	PSA_HUMAN	103 kDa	TRUE
208	TRUE	Empty	Citrate synth	CISY_HUMAN	52 kDa	TRUE
209	TRUE	Empty	ATP-depende	DDX1_HUMA	82 kDa	
210	TRUE	Empty	Cluster of Ub	UB2V1_HUM	16 kDa	TRUE
211	TRUE	Empty	Serine/argini	SRSF3_HUMA	19 kDa	TRUE

212	TRUE	Empty	LIM and SH3	LASP1_HUMA	30 kDa	
213	TRUE	Empty	DNA replicati	MCM4_HUM	97 kDa	TRUE
214	TRUE	Empty	14-3-3 protei	1433E_HUMA	29 kDa	TRUE
215	TRUE	Empty	Eukaryotic tra	EIF3A_HUMA	167 kDa	TRUE
216	TRUE	Empty	DNA replicati	MCM7_HUM	81 kDa	
217	TRUE	Empty	Reticulocalbi	RCN1_HUMA	39 kDa	TRUE
218	TRUE	Empty	Ubiquitin-like	UBA1_HUMA	118 kDa	
219	TRUE	Empty	Trifunctional	ECHB_HUMA	51 kDa	
220	TRUE	Empty	Ran-specific (	RANG_HUMA	23 kDa	
221	TRUE	Empty	Flap endonuc	FEN1_HUMA	43 kDa	
222	TRUE	Empty	Rab GDP diss	GDIB_HUMA	51 kDa	
223	TRUE	Empty	Lamin-B2 OS=	LMNB2_HUM	68 kDa	TRUE
224	TRUE	Empty	DNA replicati	MCM5_HUM	82 kDa	
225	TRUE	Empty	Aspartate--tR	SYDC_HUMA	57 kDa	
226	TRUE	Empty	14-3-3 protei	1433F_HUMA	28 kDa	TRUE
227	TRUE	Empty	ADP-ribosylat	ARF4_HUMA	21 kDa	TRUE
228	TRUE	Empty	Extended syn	ESYT1_HUMA	123 kDa	TRUE
229	TRUE	Empty	Kinectin OS=H	KTN1_HUMA	156 kDa	TRUE
230	TRUE	Empty	Cluster of UV	RD23B_HUM	43 kDa	TRUE
231	TRUE	Empty	60S ribosoma	RL19_HUMAN	23 kDa	TRUE
232	TRUE	Empty	Serine/arginin	SRSF7_HUMA	27 kDa	TRUE
233	TRUE	Empty	40S ribosoma	RSSA_HUMA	33 kDa	TRUE
234	TRUE	Empty	Aspartate am	AATM_HUMA	48 kDa	
235	TRUE	Empty	60S ribosoma	RL27_HUMAN	16 kDa	
236	TRUE	Empty	60S ribosoma	RL28_HUMAN	16 kDa	
237	TRUE	Empty	Serpin H1 OS=	SERPH_HUM	46 kDa	TRUE
238	TRUE	Empty	T-complex pr	TCPD_HUMA	58 kDa	
239	TRUE	Empty	Alpha-2-macr	AMRP_HUMA	41 kDa	
240	TRUE	Empty	Catenin delta	CTND1_HUM	108 kDa	
241	TRUE	Empty	Glutamine--tI	SYQ_HUMAN	88 kDa	
242	TRUE	Empty	Annexin A3 C	ANXA3_HUM	36 kDa	TRUE
243	TRUE	Empty	Glucose-6-ph	G6PD_HUMA	59 kDa	
244	TRUE	Empty	Mitochondria	IMMT_HUMA	84 kDa	TRUE
245	TRUE	Empty	Nucleobindin	NUCB1_HUM	54 kDa	TRUE
246	TRUE	Empty	GTP-binding r	RAN_HUMAN	24 kDa	
247	TRUE	Empty	Cluster of DN	TOP2B_HUM	183 kDa	TRUE
248	TRUE	Empty	Protein CDV3	CDV3_HUMA	27 kDa	TRUE
249	TRUE	Empty	DNA replicati	MCM2_HUM	102 kDa	TRUE
250	TRUE	Empty	Proactivator p	SAP_HUMAN	58 kDa	
251	TRUE	Empty	T-complex pr	TCPA_HUMA	60 kDa	
252	TRUE	Empty	Dynactin sub	DCTN2_HUM	44 kDa	TRUE
253	TRUE	Empty	Zyxin OS=Hor	ZYX_HUMAN	61 kDa	
254	TRUE	Empty	Proliferating	PCNA_HUMA	29 kDa	
255	TRUE	Empty	Septin-9 OS=H	SEPT9_HUMA	65 kDa	TRUE

256	TRUE	Empty	Thioredoxin c	TXD12_HUM	19 kDa	
257	TRUE	Empty	Cluster of Ald	AK1C2_HUM	37 kDa	TRUE
258	TRUE	Empty	Adenylyl cycl	CAP1_HUMA	52 kDa	
259	TRUE	Empty	Lamin-B1 OS=	LMNB1_HUM	66 kDa	TRUE
260	TRUE	Empty	Voltage-depe	VDAC1_HUM	31 kDa	TRUE
261	TRUE	Empty	X-ray repair c	XRCC5_HUM	83 kDa	TRUE
262	TRUE	Empty	60S ribosoma	RL14_HUMAN	23 kDa	TRUE
263	TRUE	Empty	Serine protea	HTRA1_HUM	51 kDa	
264	TRUE	Empty	Cluster of SW	SMCA5_HUM	122 kDa	TRUE
265	TRUE	Empty	Cluster of He	HXK1_HUMA	102 kDa	TRUE
266	TRUE	Empty	Cluster of Ins	IF2B3_HUMA	64 kDa	TRUE
267	TRUE	Empty	Peroxiredoxir	PRDX2_HUM	22 kDa	TRUE
268	TRUE	Empty	Parathymosir	PTMS_HUMA	12 kDa	
269	TRUE	Empty	Reticulon-4 C	RTN4_HUMA	130 kDa	TRUE
270	TRUE	Empty	Biliverdin red	BIEA_HUMAN	33 kDa	TRUE
271	TRUE	Empty	Chloride intra	CLIC1_HUMA	27 kDa	TRUE
272	TRUE	Empty	Cluster of Co	H2AY_HUMA	40 kDa	TRUE
273	TRUE	Empty	DNA replicati	MCM3_HUM	91 kDa	TRUE
274	TRUE	Empty	60S ribosoma	RL23_HUMAN	15 kDa	
275	TRUE	Empty	Adenosylhom	SAHH_HUMA	48 kDa	TRUE
276	TRUE	Empty	Thrombospor	TSP1_HUMAN	129 kDa	TRUE
277	TRUE	Empty	40S ribosoma	RS24_HUMAN	15 kDa	
278	TRUE	Empty	Cluster of Kin	KINH_HUMAN	110 kDa	TRUE
279	TRUE	Empty	Splicing facto	SF3B2_HUMA	100 kDa	TRUE
280	TRUE	Empty	Cytochrome c	CYC_HUMAN	12 kDa	
281	TRUE	Empty	Multifunctior	PUR6_HUMA	47 kDa	
282	TRUE	Empty	Vitronectin O	VTNC_HUMA	54 kDa	
283	TRUE	Empty	DNA replicati	MCM6_HUM	93 kDa	
284	TRUE	Empty	Desmoplakin	DESP_HUMAN	332 kDa	TRUE
285	TRUE	Empty	Trifunctional	PUR2_HUMA	108 kDa	
286	TRUE	Empty	40S ribosoma	RS14_HUMAN	16 kDa	
287	TRUE	Empty	40S ribosoma	RS12_HUMAN	15 kDa	
288	TRUE	Empty	Eukaryotic tra	EIF3F_HUMA	38 kDa	
289	TRUE	Empty	Beta-2-micro	B2MG_HUMA	14 kDa	
290	TRUE	Empty	UPF0568 pro	CN166_HUM	28 kDa	
291	TRUE	Empty	rRNA 2'-O-me	FBRL_HUMAN	34 kDa	TRUE
292	TRUE	Empty	Heterogeneo	HNRPQ_HUM	70 kDa	TRUE
293	TRUE	Empty	Acidic leucine	AN32B_HUM	29 kDa	TRUE
294	TRUE	Empty	Small nuclear	SMD3_HUMA	14 kDa	
295	TRUE	Empty	Proteasome a	PSME3_HUM	30 kDa	
296	TRUE	Empty	Peroxiredoxir	PRDX1_HUM	22 kDa	TRUE
297	TRUE	Empty	40S ribosoma	RS6_HUMAN	29 kDa	TRUE
298	TRUE	Empty	Exportin-1 OS	XPO1_HUMA	123 kDa	TRUE
299	TRUE	Empty	CD44 antigen	CD44_HUMA	82 kDa	

300	TRUE	Empty	Cluster of Int	ILF3_HUMAN	95 kDa	TRUE
301	TRUE	Empty	Integrin beta	ITB1_HUMAN	88 kDa	TRUE
302	TRUE	Empty	Leucine-rich I	LPPRC_HUMA	158 kDa	TRUE
303	TRUE	Empty	Cluster of Ra	RAB10_HUM	23 kDa	TRUE
304	TRUE	Empty	40S ribosoma	RS23_HUMAN	16 kDa	
305	TRUE	Empty	Proliferation-	PA2G4_HUM	44 kDa	
306	TRUE	Empty	Aldose reduc	ALDR_HUMA	36 kDa	
307	TRUE	Empty	Destrin OS=H	DEST_HUMAN	19 kDa	TRUE
308	TRUE	Empty	Cluster of Cy	CD2A1_HUM	17 kDa	TRUE
309	TRUE	Empty	Cytochrome c	COX5B_HUM	14 kDa	
310	TRUE	Empty	Basigin OS=H	BASI_HUMAN	42 kDa	
311	TRUE	Empty	Clathrin light	CLCA_HUMAN	27 kDa	
312	TRUE	Empty	Polyadenylat	PABP3_HUM	70 kDa	TRUE
313	TRUE	Empty	Lysophospha	PCAT1_HUM	59 kDa	
314	TRUE	Empty	Gelsolin OS=H	GELS_HUMAN	86 kDa	
315	TRUE	Empty	TATA-binding	RBP56_HUM	62 kDa	TRUE
316	TRUE	Empty	Alpha-fetopr	FETA_HUMAN	69 kDa	TRUE
317	TRUE	Empty	Hepatoma-de	HDGF_HUMA	27 kDa	TRUE
318	TRUE	Empty	Eukaryotic tra	IF4G1_HUMA	175 kDa	TRUE
319	TRUE	Empty	Splicing facto	SF3B1_HUMA	146 kDa	TRUE
320	TRUE	Empty	Cluster of Prc	PSA7_HUMAN	28 kDa	TRUE
321	TRUE	Empty	Cluster of U1	SNRPA_HUM	31 kDa	TRUE
322	TRUE	Empty	Apoptotic chr	ACINU_HUM	152 kDa	
323	TRUE	Empty	Deoxyuridine	DUT_HUMAN	27 kDa	
324	TRUE	Empty	Malate dehyc	MDHC_HUM	36 kDa	
325	TRUE	Empty	Phosphate ca	MPCP_HUMA	40 kDa	TRUE
326	TRUE	Empty	Prohibitin OS	PHB_HUMAN	30 kDa	
327	TRUE	Empty	Cluster of Pol	PTBP1_HUM	57 kDa	TRUE
328	TRUE	Empty	Glycogen phc	PYGL_HUMAN	97 kDa	TRUE
329	TRUE	Empty	Heterogeneo	ROA3_HUMA	40 kDa	TRUE
330	TRUE	Empty	Serine/argini	SRSF6_HUMA	40 kDa	TRUE
331	TRUE	Empty	Tight junctior	ZO2_HUMAN	134 kDa	TRUE
332	TRUE	Empty	Cysteine and	CSRP1_HUM	21 kDa	
333	TRUE	Empty	Cluster of Put	LC7L2_HUMA	47 kDa	TRUE
334	TRUE	Empty	Coatomer sul	COPD_HUMA	57 kDa	
335	TRUE	Empty	Sulfide:quino	SQRD_HUMA	50 kDa	
336	TRUE	Empty	T-complex pr	TCPH_HUMA	59 kDa	TRUE
337	TRUE	Empty	Proteasome s	PSA1_HUMAN	30 kDa	
338	TRUE	Empty	60S ribosoma	RL35A_HUM	13 kDa	
339	TRUE	Empty	NAD(P)H deh	NQO1_HUMA	31 kDa	
340	TRUE	Empty	Cullin-associa	CAND1_HUM	136 kDa	TRUE
341	TRUE	Empty	Importin subu	IMB1_HUMA	97 kDa	
342	TRUE	Empty	Galectin-3 OS	LEG3_HUMAN	26 kDa	
343	TRUE	Empty	Leucine-rich r	LRC59_HUM	35 kDa	

344	TRUE	Empty	Nucleobindin	NUCB2_HUM	50 kDa	TRUE
345	TRUE	Empty	Protein trans	SC23A_HUM	86 kDa	TRUE
346	TRUE	Empty	Vacuolar prot	VPS35_HUM	92 kDa	
347	TRUE	Empty	Histone H2A.'	H2AV_HUMA	14 kDa	TRUE
348	TRUE	Empty	Heterogeneo	HNRPD_HUM	38 kDa	TRUE
349	TRUE	Empty	CD166 antige	CD166_HUM	65 kDa	
350	TRUE	Empty	Coatomer sul	COPG1_HUM	98 kDa	TRUE
351	TRUE	Empty	Double-stran	DSRAD_HUM	136 kDa	
352	TRUE	Empty	Hypoxanthine	HPRT_HUMA	25 kDa	TRUE
353	TRUE	Empty	60S ribosoma	RL10A_HUM	25 kDa	TRUE
354	TRUE	Empty	Tumor protei	TPD54_HUM	22 kDa	TRUE
355	TRUE	Empty	Voltage-depe	VDAC2_HUM	32 kDa	TRUE
356	TRUE	Empty	Hematologica	HN1L_HUMA	20 kDa	
357	TRUE	Empty	AP-1 complex	AP1G1_HUM	91 kDa	
358	TRUE	Empty	Complement	CO3_HUMAN	187 kDa	TRUE
359	TRUE	Empty	DnaJ homolo	DNJB1_HUM	38 kDa	TRUE
360	TRUE	Empty	Dolichyl-diph	OST48_HUM	51 kDa	
361	TRUE	Empty	60S ribosoma	RL38_HUMAN	8 kDa	
362	TRUE	Empty	Transferrin re	TFR1_HUMAN	85 kDa	TRUE
363	TRUE	Empty	WD repeat-co	WDR1_HUM	66 kDa	
364	TRUE	Empty	Inorganic pyr	IPYR_HUMAN	33 kDa	TRUE
365	TRUE	Empty	Cluster of AP-	AP2A1_HUM	108 kDa	TRUE
366	TRUE	Empty	E3 ubiquitin-p	TRIPC_HUMA	220 kDa	
367	TRUE	Empty	Flavin reducta	BLVRB_HUM	22 kDa	
368	TRUE	Empty	26S proteaso	PSMD2_HUM	100 kDa	
369	TRUE	Empty	Tyrosine-prot	PTN1_HUMA	50 kDa	
370	TRUE	Empty	Signal recogn	SRP14_HUM	15 kDa	
371	TRUE	Empty	Activated RN	TCP4_HUMAN	14 kDa	
372	TRUE	Empty	Actin-related	ARPC4_HUM	20 kDa	
373	TRUE	Empty	CAD protein (	PYR1_HUMAN	243 kDa	TRUE
374	TRUE	Empty	Brain acid sol	BASP1_HUM	23 kDa	TRUE
375	TRUE	Empty	ATP-depende	DHX9_HUMA	141 kDa	TRUE
376	TRUE	Empty	Hypoxia up-re	HYOU1_HUM	111 kDa	TRUE
377	TRUE	Empty	Phosphoserin	SERC_HUMAN	40 kDa	TRUE
378	TRUE	Empty	Heterogeneo	HNRH3_HUM	37 kDa	
379	TRUE	Empty	Nuclear autoa	NASP_HUMA	85 kDa	TRUE
380	TRUE	Empty	Glutathione r	GSHR_HUMA	56 kDa	
381	TRUE	Empty	Macrophage	MIF_HUMAN	12 kDa	
382	TRUE	Empty	Sorting nexin	SNX12_HUM	20 kDa	TRUE
383	TRUE	Empty	Cluster of Chi	CBX3_HUMA	21 kDa	TRUE
384	TRUE	Empty	T-complex pr	TCPB_HUMAN	57 kDa	
385	TRUE	Empty	THO complex	THOC4_HUM	27 kDa	
386	TRUE	Empty	Peroxiredoxir	PRDX5_HUM	22 kDa	
387	TRUE	Empty	Procollagen g	GT251_HUM	72 kDa	

388	TRUE	Empty	FACT comple:	SSRP1_HUM/	81 kDa	TRUE
389	TRUE	Empty	Myristoylatec	MARCS_HUM	32 kDa	
390	TRUE	Empty	B-cell receptc	BAP31_HUM/	28 kDa	
391	TRUE	Empty	Glutathione S	GSTP1_HUM/	23 kDa	
392	TRUE	Empty	Cytoplasmic a	ACOC_HUMA	98 kDa	TRUE
393	TRUE	Empty	6-phosphofru	K6PP_HUMAI	86 kDa	
394	TRUE	Empty	Nucleoprotei	TPR_HUMAN	267 kDa	TRUE
395	TRUE	Empty	Nucleoside di	NDKA_HUMA	17 kDa	TRUE
396	TRUE	Empty	Insulin-like gr	IBP7_HUMAN	29 kDa	
397	TRUE	Empty	WW domain-	WBP11_HUM	70 kDa	TRUE
398	TRUE	Empty	Tight junctior	ZO1_HUMAN	195 kDa	TRUE
399	TRUE	Empty	Thyroid horm	TR150_HUM/	109 kDa	TRUE
400	TRUE	Empty	ATP synthase	ATP5J_HUMA	13 kDa	
401	TRUE	Empty	Immortalizati	IMUP_HUMA	11 kDa	TRUE
402	TRUE	Empty	Ataxin-10 OS:	ATX10_HUM/	53 kDa	
403	TRUE	Empty	Trifunctional	ECHA_HUMA	83 kDa	
404	TRUE	Empty	Cluster of Ras	RB11A_HUM/	24 kDa	TRUE
405	TRUE	Empty	40S ribosoma	RS28_HUMAI	8 kDa	
406	TRUE	Empty	High mobility	HMGA1_HUM	12 kDa	TRUE
407	TRUE	Empty	SH3 domain-l	SH3L1_HUM/	13 kDa	
408	TRUE	Empty	NADH-cytoch	NB5R3_HUM	34 kDa	
409	TRUE	Empty	Epidermal gr(	EGFR_HUMA	134 kDa	
410	TRUE	Empty	Protein SET C	SET_HUMAN	33 kDa	
411	TRUE	Empty	Endoplasmic	ERP29_HUM/	29 kDa	
412	TRUE	Empty	Cathepsin D (	CATD_HUMA	45 kDa	
413	TRUE	Empty	Prothymosin	PTMA_HUM/	12 kDa	
414	TRUE	Empty	Acidic leucine	AN32A_HUM	29 kDa	TRUE
415	TRUE	Empty	Dihydrolipoyl	ODO2_HUM/	49 kDa	
416	TRUE	Empty	60S ribosoma	RL12_HUMAI	18 kDa	
417	TRUE	Empty	Coatomer sul	COPB2_HUM	102 kDa	
418	TRUE	Empty	Phenylalanin	SYFA_HUMAI	58 kDa	
419	TRUE	Empty	Barrier-to-au	BAF_HUMAN	10 kDa	
420	TRUE	Empty	Annexin A8 C	ANXA8_HUM	37 kDa	
421	TRUE	Empty	ATP synthase	ATPG_HUMA	33 kDa	
422	TRUE	Empty	Heterochrom	HP1B3_HUM/	61 kDa	
423	TRUE	Empty	Nascent poly	NACA_HUMA	23 kDa	
424	TRUE	Empty	Polyadenylat	PABP4_HUM/	71 kDa	TRUE
425	TRUE	Empty	Vesicle-traffic	SC22B_HUM/	25 kDa	
426	TRUE	Empty	Transmembra	TMM43_HUM	45 kDa	
427	TRUE	Empty	Cluster of His	SYHC_HUMA	57 kDa	TRUE
428	TRUE	Empty	Protein diaph	DIAP1_HUM/	141 kDa	TRUE
429	TRUE	Empty	Protein CYR6	CYR61_HUM/	42 kDa	
430	TRUE	Empty	Cluster of Se	SEPT7_HUM/	51 kDa	TRUE
431	TRUE	Empty	40S ribosoma	RS17L_HUM/	16 kDa	TRUE

432	TRUE	Empty	ATP-binding c	ABCF1_HUM	96 kDa	
433	TRUE	Empty	Actin-binding	ANLN_HUMA	124 kDa	TRUE
434	TRUE	Empty	Clathrin light	CLCB_HUMAI	25 kDa	
435	TRUE	Empty	Band 4.1-like	E41L1_HUM	99 kDa	TRUE
436	TRUE	Empty	Bifunctional p	PUR9_HUMA	65 kDa	TRUE
437	TRUE	Empty	Isoleucine--tF	SYIC_HUMAN	145 kDa	TRUE
438	TRUE	Empty	Proteasome s	PSB6_HUMAI	25 kDa	
439	TRUE	Empty	Atlastin-3 OS	ATLA3_HUM	61 kDa	
440	TRUE	Empty	Coiled-coil do	CC124_HUM	26 kDa	
441	TRUE	Empty	Drebrin OS=H	DREB_HUMA	71 kDa	
442	TRUE	Empty	Na(+)/H(+) ex	NHRF1_HUM	39 kDa	
443	TRUE	Empty	Methionine a	MAT2B_HUM	38 kDa	
444	TRUE	Empty	Endoplasmic	ERMP1_HUM	100 kDa	
445	TRUE	Empty	Heterogeneo	HNRH2_HUM	49 kDa	TRUE
446	TRUE	Empty	Growth facto	GRB2_HUMA	25 kDa	
447	TRUE	Empty	Transcription	TCAL3_HUM	23 kDa	
448	TRUE	Empty	CD109 antige	CD109_HUM	162 kDa	TRUE
449	TRUE	Empty	60S ribosoma	RL24_HUMAI	18 kDa	TRUE
450	TRUE	Empty	Nicotinamide	NNMT_HUM	30 kDa	
451	TRUE	Empty	Thioredoxin d	TXD17_HUM	14 kDa	
452	TRUE	Empty	A-kinase anch	AKA12_HUM	191 kDa	
453	TRUE	Empty	Nucleolar RN	DDX21_HUM	87 kDa	TRUE
454	TRUE	Empty	Microtubule-	MAP1B_HUM	271 kDa	TRUE
455	TRUE	Empty	Programmed	PDC6I_HUM	96 kDa	
456	TRUE	Empty	Thioredoxin-d	PRDX3_HUM	28 kDa	
457	TRUE	Empty	Ubiquitin carl	UBP5_HUMA	96 kDa	TRUE
458	TRUE	Empty	Macrophage-	CAPG_HUMA	38 kDa	TRUE
459	TRUE	Empty	Protein S100-	S10AD_HUM	11 kDa	
460	TRUE	Empty	Very-long-ch	TECR_HUMAI	36 kDa	TRUE
461	TRUE	Empty	Nicotinamide	NAMPT_HUM	56 kDa	
462	TRUE	Empty	PDZ and LIM	PDLI5_HUMA	64 kDa	
463	TRUE	Empty	Eukaryotic pe	ERF1_HUMAI	49 kDa	TRUE
464	TRUE	Empty	Importin subu	IMA1_HUMA	58 kDa	TRUE
465	TRUE	Empty	Coatomer sul	COPB_HUMA	107 kDa	
466	TRUE	Empty	26S proteaso	PSMD3_HUM	61 kDa	
467	TRUE	Empty	Proteasome s	PSA3_HUMAI	28 kDa	TRUE
468	TRUE	Empty	Cluster of Fra	FXR1_HUMAI	70 kDa	TRUE
469	TRUE	Empty	Coatomer sul	COPA_HUMA	138 kDa	TRUE
470	TRUE	Empty	Myb-binding	MBB1A_HUM	149 kDa	TRUE
471	TRUE	Empty	RNA-binding	RBM8A_HUM	20 kDa	
472	TRUE	Empty	60S ribosoma	RL18A_HUM	21 kDa	
473	TRUE	Empty	60S ribosoma	RL7A_HUMAI	30 kDa	TRUE
474	TRUE	Empty	Translocator	TSPOA_HUM	19 kDa	
475	TRUE	Empty	Phenylalanin	SYFB_HUMAI	66 kDa	

476	TRUE	Empty	RuvB-like 2 O	RUVB2_HUM	51 kDa	
477	TRUE	Empty	Calcium-bind	SCMC1_HUM	53 kDa	
478	TRUE	Empty	60S ribosoma	RL27A_HUM	17 kDa	
479	TRUE	Empty	ATP-depende	RECQ1_HUM	73 kDa	
480	TRUE	Empty	Microtubule-	MARE1_HUM	30 kDa	TRUE
481	TRUE	Empty	Mesencephal	MANF_HUM	21 kDa	
482	TRUE	Empty	Ras-related p	RAB7A_HUM	23 kDa	TRUE
483	TRUE	Empty	Ubiquitin carl	UCHL1_HUM	25 kDa	
484	TRUE	Empty	PC4 and SFRS	PSIP1_HUMA	60 kDa	TRUE
485	TRUE	Empty	Phosphatidyl	PEBP1_HUM	21 kDa	TRUE
486	TRUE	Empty	EH domain-c	EHD2_HUMA	61 kDa	TRUE
487	TRUE	Empty	Putative pre-	DHX15_HUM	91 kDa	
488	TRUE	Empty	Integrin alpha	ITA3_HUMAN	117 kDa	
489	TRUE	Empty	Major vault p	MVP_HUMAN	99 kDa	
490	TRUE	Empty	PDZ and LIM	PDLI1_HUMA	36 kDa	TRUE
491	TRUE	Empty	SAP domain-c	SARNP_HUM	24 kDa	TRUE
492	TRUE	Empty	Eukaryotic tra	EIF3C_HUMA	105 kDa	
493	TRUE	Empty	26S proteaso	PSD11_HUM	47 kDa	
494	TRUE	Empty	RNA-binding	RBM14_HUM	69 kDa	TRUE
495	TRUE	Empty	60S ribosoma	RL17_HUMAN	21 kDa	TRUE
496	TRUE	Empty	Latent-transf	LTBP2_HUM	195 kDa	
497	TRUE	Empty	Pre-mRNA-pr	PRP8_HUMA	274 kDa	
498	TRUE	Empty	RuvB-like 1 O	RUVB1_HUM	50 kDa	TRUE
499	TRUE	Empty	26S proteaso	PSMD8_HUM	40 kDa	
500	TRUE	Empty	Probable ATP	DDX17_HUM	80 kDa	TRUE
501	TRUE	Empty	Eukaryotic tra	IF5_HUMAN	49 kDa	
502	TRUE	Empty	Testin OS=Ho	TES_HUMAN	48 kDa	TRUE
503	TRUE	Empty	Tubulin-speci	TBCA_HUMA	13 kDa	
504	TRUE	Empty	Probable ATP	DDX5_HUMA	69 kDa	TRUE
505	TRUE	Empty	Ribonucleosi	RIR1_HUMAN	90 kDa	TRUE
506	TRUE	Empty	Cytosolic acyl	BACH_HUMA	42 kDa	
507	TRUE	Empty	Vesicular inte	LMAN2_HUM	40 kDa	
508	TRUE	Empty	SYNE2_HUM	SYNE2_HUM	?	TRUE
509	TRUE	Empty	Cluster of Ser	PAK2_HUMA	58 kDa	TRUE
510	TRUE	Empty	Vacuolar prot	VPS29_HUM	21 kDa	
511	TRUE	Empty	Asparagine--t	SYNC_HUMA	63 kDa	TRUE
512	TRUE	Empty	Very long-cha	ACADV_HUM	70 kDa	TRUE
513	TRUE	Empty	26S protease	PRS8_HUMAN	46 kDa	TRUE
514	TRUE	Empty	Sorting nexin	SNX1_HUMA	59 kDa	TRUE
515	TRUE	Empty	Protein-L-iso	PIMT_HUMA	25 kDa	
516	TRUE	Empty	Acetyl-CoA a	THIC_HUMAN	41 kDa	
517	TRUE	Empty	DNA damage	DDB1_HUMA	127 kDa	
518	TRUE	Empty	Calponin-3 O	CNN3_HUMA	36 kDa	TRUE
519	TRUE	Empty	U2 small nucl	RU2A_HUMA	28 kDa	

520	TRUE	Empty	Actin-related	ARP2_HUMA	45 kDa	
521	TRUE	Empty	Ras-related p	RAP1B_HUM	21 kDa	TRUE
522	TRUE	Empty	Transcription	TCRG1_HUM	124 kDa	
523	TRUE	Empty	Ras suppress	RSU1_HUMA	32 kDa	
524	TRUE	Empty	AP-3 comple	AP3B1_HUM	121 kDa	TRUE
525	TRUE	Empty	26S proteaso	PSD12_HUM	53 kDa	
526	TRUE	Empty	Ubiquitin-cor	UBE2N_HUM	17 kDa	TRUE
527	TRUE	Empty	Septin-2 OS=I	SEPT2_HUM	41 kDa	TRUE
528	TRUE	Empty	Transcription	TIF1B_HUMA	89 kDa	
529	TRUE	Empty	Actin-related	ARPC2_HUM	34 kDa	TRUE
530	TRUE	Empty	Ubiquitin thic	OTUB1_HUM	31 kDa	
531	TRUE	Empty	Eukaryotic tra	IF2P_HUMAN	139 kDa	
532	TRUE	Empty	Collagen alph	COGA1_HUM	158 kDa	TRUE
533	TRUE	Empty	Small EDRK-ri	SERF2_HUM	7 kDa	TRUE
534	TRUE	Empty	Cluster of N-a	NAA10_HUM	26 kDa	TRUE
535	TRUE	Empty	Nexilin OS=H	NEXN_HUMA	81 kDa	TRUE
536	TRUE	Empty	Heterogeneo	HNRL1_HUM	96 kDa	
537	TRUE	Empty	4F2 cell-surfa	4F2_HUMAN	68 kDa	TRUE
538	TRUE	Empty	Adipocyte pla	APMAP_HUM	46 kDa	
539	TRUE	Empty	Ubiquitin carl	UBP14_HUM	56 kDa	
540	TRUE	Empty	26S protease	PRS6A_HUM	49 kDa	
541	TRUE	Empty	Lysosome-ass	LAMP2_HUM	45 kDa	
542	TRUE	Empty	Eukaryotic tra	IF2A_HUMAN	36 kDa	
543	TRUE	Empty	Trans-Golgi n	TGON2_HUM	51 kDa	
544	TRUE	Empty	26S protease	PRS7_HUMAN	49 kDa	
545	TRUE	Empty	Unconventior	MYO1C_HUM	122 kDa	TRUE
546	TRUE	Empty	Interleukin-18	IL18_HUMAN	22 kDa	
547	TRUE	Empty	A-kinase anch	AKAP2_HUM	95 kDa	TRUE
548	TRUE	Empty	Lactoylglutath	LGUL_HUMA	21 kDa	
549	TRUE	Empty	Integrin beta-	ITB4_HUMAN	202 kDa	
550	TRUE	Empty	NSFL1 cofact	NSF1C_HUM	41 kDa	
551	TRUE	Empty	40S ribosoma	RS20_HUMAN	13 kDa	
552	TRUE	Empty	Dolichyl-diph	RPN2_HUMA	69 kDa	TRUE
553	TRUE	Empty	Peptidyl-prol	FKB1A_HUM	12 kDa	TRUE
554	TRUE	Empty	Twinfilin-1 OS	TWF1_HUMA	40 kDa	
555	TRUE	Empty	Laminin subu	LAMA5_HUM	400 kDa	
556	TRUE	Empty	Nucleolar prc	NOP58_HUM	60 kDa	
557	TRUE	Empty	Nuclear migra	NUDC_HUM	38 kDa	TRUE
558	TRUE	Empty	Dolichyl-diph	STT3A_HUM	81 kDa	TRUE
559	TRUE	Empty	dCTP pyroph	DCTP1_HUM	19 kDa	
560	TRUE	Empty	Reticulocalbi	RCN2_HUMA	37 kDa	
561	TRUE	Empty	Pyridoxal kina	PDXK_HUMA	35 kDa	
562	TRUE	Empty	NADPH--cyto	NCPR_HUMA	77 kDa	
563	TRUE	Empty	DNA (cytosin	DNMT1_HUM	183 kDa	TRUE

564	TRUE	Empty	S-adenosylm	METK2_HUM	44 kDa	TRUE
565	TRUE	Empty	Cell division c	CDC5L_HUM	92 kDa	TRUE
566	TRUE	Empty	UTP20_HUM	UTP20_HUM	?	TRUE
567	TRUE	Empty	Ribosome ma	SBDS_HUMA	29 kDa	
568	TRUE	Empty	Cluster of Prc	PSA4_HUMA	29 kDa	TRUE
569	TRUE	Empty	26S proteaso	PSMD6_HUM	46 kDa	
570	TRUE	Empty	Electron tran	ETFB_HUMA	28 kDa	
571	TRUE	Empty	U6 snRNA-as	LSM3_HUMA	12 kDa	
572	TRUE	Empty	Fibrinogen ga	FIBG_HUMA	52 kDa	
573	TRUE	Empty	Vesicle-fusing	NSF_HUMAN	83 kDa	
574	TRUE	Empty	Eukaryotic tra	IF6_HUMAN	27 kDa	TRUE
575	TRUE	Empty	Ras GTPase-a	G3BP1_HUM	52 kDa	TRUE
576	TRUE	Empty	Alcohol dehy	AK1A1_HUM	37 kDa	
577	TRUE	Empty	Secernin-1 O	SCRN1_HUM	46 kDa	TRUE
578	TRUE	Empty	Cluster of AP-	AP2B1_HUM	105 kDa	TRUE
579	TRUE	Empty	Cluster of Trc	TMOD3_HUM	40 kDa	TRUE
580	TRUE	Empty	Drebrin-like p	DBNL_HUMA	48 kDa	
581	TRUE	Empty	RNA-binding	FUS_HUMAN	53 kDa	TRUE
582	TRUE	Empty	60S ribosoma	RL18_HUMA	22 kDa	
583	TRUE	Empty	Sorting and a	SAM50_HUM	52 kDa	TRUE
584	TRUE	Empty	ERO1-like prc	ERO1A_HUM	54 kDa	
585	TRUE	Empty	Cytochrome b	QCR1_HUMA	53 kDa	
586	TRUE	Empty	Amine oxidas	AOFA_HUMA	60 kDa	
587	TRUE	Empty	Cluster of GT	SAR1A_HUM	22 kDa	TRUE
588	TRUE	Empty	Calponin-2 O	CNN2_HUMA	34 kDa	TRUE
589	TRUE	Empty	RNA-binding	RALY_HUMA	32 kDa	
590	TRUE	Empty	Actin-related	ARP3_HUMA	47 kDa	
591	TRUE	Empty	Insulin-like gr	IF2B2_HUMA	66 kDa	TRUE
592	TRUE	Empty	40S ribosoma	RS11_HUMA	18 kDa	
593	TRUE	Empty	COP9 signalo	CSN4_HUMA	46 kDa	
594	TRUE	Empty	UBX domain-	UBXN1_HUM	33 kDa	TRUE
595	TRUE	Empty	Hippocalcin-li	HPCL1_HUM	22 kDa	
596	TRUE	Empty	Collagen alph	CO4A5_HUM	161 kDa	
597	TRUE	Empty	Elongation fa	EF1D_HUMA	31 kDa	TRUE
598	TRUE	Empty	Heterogeneo	HNRPR_HUM	71 kDa	TRUE
599	TRUE	Empty	Cleavage stim	CSTF2_HUM	61 kDa	TRUE
600	TRUE	Empty	Long-chain-fa	ACSL1_HUM	78 kDa	TRUE
601	TRUE	Empty	ATP synthase	ATPD_HUMA	17 kDa	TRUE
602	TRUE	Empty	DnaJ homolo	DNJC9_HUM	30 kDa	
603	TRUE	Empty	Palladin OS=H	PALLD_HUM	151 kDa	TRUE
604	TRUE	Empty	Cytoplasmic F	CYFP1_HUM	145 kDa	TRUE
605	TRUE	Empty	Cell surface g	MUC18_HUM	72 kDa	
606	TRUE	Empty	Glycerol-3-ph	GPDM_HUM	81 kDa	
607	TRUE	Empty	Nicastrin OS=	NICA_HUMA	78 kDa	

608	TRUE	Empty	39S ribosoma	RM38_HUMA	45 kDa	
609	TRUE	Empty	RNA-binding	RBM12_HUM	97 kDa	TRUE
610	TRUE	Empty	Cluster of sp|	MRCKG_HUM	?	TRUE
611	TRUE	Empty	Double-stran	STAU1_HUM	63 kDa	TRUE
612	TRUE	Empty	Protein PRRC	PRC2A_HUM	229 kDa	
613	TRUE	Empty	Transgelin OS	TAGL_HUMA	23 kDa	
614	TRUE	Empty	Cluster of EH	EHD1_HUMA	61 kDa	TRUE
615	TRUE	Empty	Actin-binding	ABLM1_HUM	88 kDa	
616	TRUE	Empty	ATP synthase	ATP5L_HUM	11 kDa	TRUE
617	TRUE	Empty	Splicing facto	U2AF2_HUM	54 kDa	
618	TRUE	Empty	Isocitrate deh	IDHP_HUMA	51 kDa	TRUE
619	TRUE	Empty	Sortilin OS=H	SORT_HUMA	92 kDa	TRUE
620	TRUE	Empty	Leukotriene A	LKHA4_HUM	69 kDa	
621	TRUE	Empty	Polyadenylat	PABP2_HUM	33 kDa	
622	TRUE	Empty	Cluster of Tra	RHOA_HUM	22 kDa	TRUE
623	TRUE	Empty	Isovaleryl-Co	IVD_HUMAN	46 kDa	
624	TRUE	Empty	Cluster of E3	RBP2_HUMA	358 kDa	TRUE
625	TRUE	Empty	Eukaryotic tra	EIF3J_HUMA	29 kDa	
626	TRUE	Empty	Gem-associat	GEMI5_HUM	169 kDa	
627	TRUE	Empty	5'-nucleotida	5NTD_HUMA	63 kDa	TRUE
628	TRUE	Empty	Transcription	ELOB_HUMA	13 kDa	
629	TRUE	Empty	Thioredoxin-r	TMX1_HUM	32 kDa	
630	TRUE	Empty	PEST proteol	PCNP_HUMA	19 kDa	
631	TRUE	Empty	Alpha/beta h	ABHEB_HUM	22 kDa	
632	TRUE	Empty	Cluster of Dy	DYN2_HUMA	98 kDa	TRUE
633	TRUE	Empty	Protein FAM1	F136A_HUM	16 kDa	
634	TRUE	Empty	DnaJ homolo	DJB11_HUM	41 kDa	
635	TRUE	Empty	Probable heli	SETX_HUMA	303 kDa	
636	TRUE	Empty	Lysosomal al	MA2B1_HUM	114 kDa	TRUE
637	TRUE	Empty	Tryptophan--	SYWC_HUM	53 kDa	
638	TRUE	Empty	Serpin B6 OS=	SPB6_HUMA	43 kDa	TRUE
639	TRUE	Empty	Coactosin-lik	COTL1_HUM	16 kDa	
640	TRUE	Empty	Plakophilin-2	PKP2_HUMA	97 kDa	
641	TRUE	Empty	Heterogeneo	HNRPF_HUM	46 kDa	TRUE
642	TRUE	Empty	Purine nuclec	PNPH_HUMA	32 kDa	
643	TRUE	Empty	Probable ATP	DDX6_HUMA	54 kDa	
644	TRUE	Empty	Tubulin-foldi	TBCB_HUMA	27 kDa	
645	TRUE	Empty	PRKC apopto	PAWR_HUM	37 kDa	TRUE
646	TRUE	Empty	Enoyl-CoA hy	ECHM_HUM	31 kDa	
647	TRUE	Empty	RNA-binding	RNPS1_HUM	34 kDa	
648	TRUE	Empty	26S protease	PRS6B_HUM	47 kDa	TRUE
649	TRUE	Empty	Regulator of	RMD1_HUM	36 kDa	TRUE
650	TRUE	Empty	Prefoldin sub	PFD2_HUMA	17 kDa	
651	TRUE	Empty	Phosphoserir	SERB_HUMA	25 kDa	

652	TRUE	Empty	Signal peptid	SC11A_HUM	21 kDa	
653	TRUE	Empty	N(G),N(G)-dir	DDAH1_HUM	31 kDa	TRUE
654	TRUE	Empty	Serine--tRNA	SYSC_HUMAN	59 kDa	
655	TRUE	Empty	Interferon-in	IFIT2_HUMAN	55 kDa	TRUE
656	TRUE	Empty	Structural ma	SMC4_HUMA	147 kDa	TRUE
657	TRUE	Empty	Copine-1 OS=	CPNE1_HUM	59 kDa	
658	TRUE	Empty	Integrin-linke	ILK_HUMAN	51 kDa	
659	TRUE	Empty	Procollagen-l	PLOD3_HUM	85 kDa	
660	TRUE	Empty	Mannosyl-oli	MOGS_HUM	92 kDa	
661	TRUE	Empty	Melanoma-as	MAGD2_HUM	65 kDa	
662	TRUE	Empty	Aminopeptid	AMPN_HUM	110 kDa	
663	TRUE	Empty	Methionine--	SYMC_HUMA	101 kDa	
664	TRUE	Empty	Nucleosome	NP1L1_HUM	45 kDa	TRUE
665	TRUE	Empty	GDP-L-fucose	FCL_HUMAN	36 kDa	
666	TRUE	Empty	Far upstream	FUBP1_HUM	68 kDa	TRUE
667	TRUE	Empty	Acylamino-ac	ACPH_HUMA	81 kDa	
668	TRUE	Empty	Proteasomal	ADRM1_HUM	42 kDa	
669	TRUE	Empty	sp|P02461|C	CO3A1_HUM	?	
670	TRUE	Empty	Annexin A4 C	ANXA4_HUM	36 kDa	TRUE
671	TRUE	Empty	Collagen alph	CO6A1_HUM	109 kDa	
672	TRUE	Empty	Electron tran	ETFA_HUMAN	35 kDa	
673	TRUE	Empty	SPEG_HUMA	SPEG_HUMA	?	
674	TRUE	Empty	Tyrosine--tRN	SYYC_HUMAN	59 kDa	
675	TRUE	Empty	39S ribosoma	RM12_HUMA	21 kDa	
676	TRUE	Empty	Serine/argini	SRSF9_HUMA	26 kDa	TRUE
677	TRUE	Empty	Collagen alph	CO2A1_HUM	142 kDa	TRUE
678	TRUE	Empty	Profilin-2 OS=	PROF2_HUM	15 kDa	
679	TRUE	Empty	AH receptor-i	AIP_HUMAN	38 kDa	
680	TRUE	Empty	Adenylate kir	KAD1_HUMA	22 kDa	
681	TRUE	Empty	Heterogeneo	HNRPL_HUM	64 kDa	TRUE
682	TRUE	Empty	Sideroflexin-1	SFXN1_HUM	36 kDa	
683	TRUE	Empty	Probable rRN	EBP2_HUMAN	35 kDa	
684	TRUE	Empty	Selenide, wat	SPS1_HUMAN	43 kDa	
685	TRUE	Empty	Peptidyl-prol	FKBP2_HUM	16 kDa	
686	TRUE	Empty	Collagen alph	CO7A1_HUM	295 kDa	
687	TRUE	Empty	Collagen alph	CO5A3_HUM	172 kDa	
688	TRUE	Empty	Threonine--tF	SYTC_HUMAN	83 kDa	TRUE
689	TRUE	Empty	Phosphatidyli	PIPNB_HUM	32 kDa	
690	TRUE	Empty	EMILIN-2 OS=	EMIL2_HUM	116 kDa	
691	TRUE	Empty	Protein phos	PP1R7_HUM	42 kDa	
692	TRUE	Empty	sp|P08572|C	CO4A2_HUM	?	
693	TRUE	Empty	Glutathione S	GSTK1_HUM	25 kDa	
694	TRUE	Empty	DMWD_HUM	DMWD_HUM	?	TRUE
695	TRUE	Empty	Serine/threor	PPP6_HUMA	35 kDa	TRUE

696	TRUE	Empty	F-actin-cappi	CAZA1_HUM	33 kDa	TRUE
697	TRUE	Empty	14-3-3 protei	1433S_HUM	28 kDa	TRUE
698	TRUE	Empty	Polyglutamin	PQBP1_HUM	30 kDa	
699	TRUE	Empty	Phosphopant	COAC_HUMA	22 kDa	
700	TRUE	Empty	Rho guanine	ARHG7_HUM	90 kDa	
701	TRUE	Empty	Cluster of Put	RS26L_HUM	13 kDa	TRUE
702	TRUE	Empty	Alpha-centra	ACTZ_HUMA	43 kDa	TRUE
703	TRUE	Empty	Zinc finger pr	ZN207_HUM	51 kDa	
704	TRUE	Empty	sp|Q32P51|F	RA1L2_HUM	?	
705	TRUE	Empty	Huntingtin-in	HYPK_HUMA	15 kDa	

END OF FILE

ıcubation with exosomes from *Opisthorchis viverrini* **.** Scaffold-generated report of the iTRAQ

atabase

›pic)
:)
plex)
tion), +57 on C (Carbamidomethyl), +304 on Y (iTRAQ8plex)
ase (selected for Homo sapiens, 2013_09, 20272 entries)

xosomes_A): LFDR Model, Classifier data: Bayes, Good (50%) m:44.4/s:12.7 m:31.8/s:0.995 m:N
xosomes_B): LFDR Model, Classifier data: Bayes, Good (50%) m:45.3/s:12.8 m:31.8/s:0.983 m:N

›pic)
:)
plex)
/ro-Glu), -17 on n (Ammonia-loss), -17 on n (Gln->pyro-Glu), +16 on M (Oxidation), +57 on C (Ca

3_09 database

xosomes_A): LFDR Model, Classifier data: Bayes, Good (50%) m:41.4/s:6.69 m:3.25/s:1.08 m:0.3
xosomes_B): LFDR Model, Classifier data: Bayes, Good (50%) m:41.0/s:6.78 m:3.17/s:1.12 m:0.3

meters\unimod.xml

with protein cluster analysis

inimum

00220]; [0.000,0.00940,0.930,0.0590,0.00160]; [0.000,0.0188,0.931,0.0490,0.001000]; [0.000,0.

.72,0.794]

Kruskal-Wall	Taxonomy	Control	0.5h	3h	16h
95% (< 0.000	unknown	0	0.8	-1.5	-2.2
95% (< 0.000	unknown	0	-0.6	0.6	0.5
95% (< 0.000	unknown	0.2	-0.1	0.6	0.5
95% (< 0.000	unknown	0	0.5	0.3	0.6
95% (< 0.000	unknown	0	1	-0.3	-0.1
95% (< 0.000	unknown	0	0.3	0.5	0.7
95% (< 0.000	unknown	-0.1	-0.5	0.8	0.7
95% (< 0.000	unknown	-0.1	-0.6	0.3	0.4
95% (< 0.000	unknown	0.1	-0.8	0.6	0.5
95% (< 0.000	unknown	-0.1	-0.5	0.6	0.4
95% (< 0.000	unknown	-0.1	-0.4	0.4	0.6
95% (< 0.000	unknown	0.1	0.4	0.3	0.6
95% (< 0.000	unknown	0	0	0.3	0.5
95% (< 0.000	unknown	-0.1	-0.4	0.4	0.3
95% (< 0.000	unknown	0.1	-0.4	0.7	0.6
95% (< 0.000	unknown	0	0.3	0.2	0.4
95% (< 0.000	unknown	0	0.5	-0.6	-0.6
95% (< 0.000	unknown	0	-0.6	0.8	0.8
95% (< 0.000	unknown	-0.2	0.6	-0.2	0
95% (< 0.000	unknown	0	1	0	0.2
95% (< 0.000	unknown	0	-0.1	0.3	0.2
95% (< 0.000	unknown	0	-0.3	0.7	0.8
95% (< 0.000	unknown	0.1	-0.1	0	0.1
95% (< 0.000	unknown	0	-0.1	0.2	0.2
95% (< 0.000	unknown	0	0.6	-1.1	-1.1
95% (< 0.000	unknown	0	0.4	0.2	0.5
95% (< 0.000	unknown	0	-0.5	0.7	0.5
95% (< 0.000	unknown	0	-0.2	0.3	0.4
95% (< 0.000	unknown	0	0.4	0	0.1
95% (< 0.000	unknown	0	-0.4	-0.3	-0.5
95% (< 0.000	unknown	0	-0.1	0.3	0.2
95% (< 0.000	unknown	0	-0.6	0.8	0.6
95% (< 0.000	unknown	0.1	0.4	0.1	0.1
95% (< 0.000	unknown	0	-0.5	0.7	0.5
95% (< 0.000	unknown	0	0.1	-0.1	-0.2

95% (< 0.000	unknown	0	-0.2	0.8	0.7
95% (< 0.000	unknown	0	0.3	-0.1	-0.2
95% (< 0.000	unknown	0	0	0	0
95% (< 0.000	unknown	0	0.8	-1.2	-1.2
95% (< 0.000	unknown	0	-0.1	-0.4	-0.4
95% (< 0.000	unknown	0	-0.2	0.4	0.4
95% (< 0.000	unknown	0	0	0.1	0
95% (< 0.000	unknown	0	0.4	-0.4	-0.5
95% (< 0.000	unknown	0	0.7	-0.6	-0.4
95% (< 0.000	unknown	0	-0.5	0.2	0.1
95% (< 0.000	unknown	0	0.6	-1.7	-1.8
95% (< 0.000	unknown	0	0.7	-0.3	-0.3
95% (< 0.000	unknown	0	0.6	-0.4	-0.3
95% (< 0.000	unknown	0	0.8	0.1	0
95% (< 0.000	unknown	0	0.1	0.5	0.4
95% (< 0.000	unknown	0	1.2	-0.2	-0.2
95% (< 0.000	unknown	0	0.1	-0.9	-0.7
95% (< 0.000	unknown	0	0.8	-2.9	-2.8
95% (< 0.000	unknown	0	0	0.4	0.6
95% (< 0.000	unknown	0	0.3	0.3	0.2
95% (< 0.000	unknown	0	0.4	-0.5	-0.4
95% (< 0.000	unknown	0	0.5	-1	-1.2
95% (< 0.000	unknown	-0.1	0.6	-0.4	-0.2
95% (0.0013	unknown	0.1	0.3	0.3	0.3
95% (< 0.000	unknown	0.1	0.3	-0.8	-0.9
95% (< 0.000	unknown	0	-0.1	0.2	0.3
95% (< 0.000	unknown	0	-0.6	0.1	-0.1
95% (< 0.000	unknown	0	0.2	0	0.1
95% (< 0.000	unknown	0	0	-0.5	-0.6
95% (< 0.000	unknown	-0.1	0	0.3	0.3
95% (< 0.000	unknown	0	-0.2	0.6	0.6
95% (< 0.000	unknown	0	0	0.4	0.4
95% (< 0.000	unknown	0	0.6	0.1	0.1
95% (< 0.000	unknown	0	0.6	-1.3	-1.7
95% (< 0.000	unknown	0	-0.3	0.7	0.5
95% (< 0.000	unknown	0	0.1	-0.7	-0.9
95% (< 0.000	unknown	-0.1	-0.2	0.5	0.5
95% (< 0.000	unknown	0	0	0.5	0.7
95% (< 0.000	unknown	0	0.5	-1.5	-1.1
95% (< 0.000	unknown	-0.2	-0.5	0.6	0.5
95% (< 0.000	unknown	0	-0.2	0.5	0.5
95% (< 0.000	unknown	0	-0.5	0.6	0.5
95% (< 0.000	unknown	0	-0.1	0.6	0.6
95% (< 0.000	unknown	-0.1	-0.1	0.5	0.3

95% (< 0.000	unknown	0	-0.3	0.7	0.5
95% (< 0.000	unknown	0	0	-1.4	-1.4
95% (0.0011)	unknown	0	0.3	-0.6	-0.6
95% (< 0.000	unknown	0.1	0.2	0.5	0.4
95% (< 0.000	unknown	0	0.2	0.3	0.3
95% (< 0.000	unknown	-0.1	0	0.7	0.7
95% (< 0.000	unknown	0	-0.1	0.1	-0.6
95% (< 0.000	unknown	0	0.4	-0.5	-0.3
95% (< 0.000	unknown	0	-0.5	0.6	0.6
95% (< 0.000	unknown	0	0	-0.4	-0.2
95% (< 0.000	unknown	0	-0.2	0.5	0.5
95% (< 0.000	unknown	0	-0.6	0.7	0.6
95% (< 0.000	unknown	0	-0.5	0.2	0
95% (< 0.000	unknown	0	0.2	0.4	0.4
95% (< 0.000	unknown	0	1.3	1	0.3
95% (0.040)	unknown	0	0.5	0.6	0.4
95% (< 0.000	unknown	0	0.2	-1.8	-1.9
95% (< 0.000	unknown	0	0	0.7	0.6
95% (< 0.000	unknown	0	0.6	-1.6	-1.6
95% (< 0.000	unknown	0	0.8	-1.9	-2
95% (< 0.000	unknown	0	0.2	0.6	0.7
95% (< 0.000	unknown	0	-0.2	0.9	0.8
95% (< 0.000	unknown	0	0.2	-2.2	-2.3
95% (< 0.000	unknown	0	0.9	-1.2	-1
95% (< 0.000	unknown	0	0.1	0.2	0.3
95% (< 0.000	unknown	0	0.3	-1.1	-1
95% (< 0.000	unknown	0	0.5	-1.3	-1.3
95% (< 0.000	unknown	0	0.7	-1.5	-1.4
95% (< 0.000	unknown	0	0.3	0.6	0.4
95% (< 0.000	unknown	0	-0.4	0.7	0.5
95% (< 0.000	unknown	0	0.3	-0.5	-0.6
95% (< 0.000	unknown	0	-0.4	0.8	0.5
75% (0.14)	unknown	0.2	0	0.2	0.2
95% (< 0.000	unknown	0	0	0.6	0.7
95% (< 0.000	unknown	-0.1	0.3	0.1	0.1
95% (< 0.000	unknown	0	0.6	0	-0.1
95% (< 0.000	unknown	0.1	0.4	-0.2	0
95% (< 0.000	unknown	0	0.4	-0.7	-0.9
95% (< 0.000	unknown	0	0.3	0	0
95% (< 0.000	unknown	0	0	0.5	0.7
95% (< 0.000	unknown	0	0.4	0.3	0.3
95% (< 0.000	unknown	0	-0.1	0.5	0.4
95% (< 0.000	unknown	0	-0.3	0.6	0.6
95% (< 0.000	unknown	0	0.4	-2.6	-2.6

95% (< 0.000	unknown	0	0.1	-0.1	-0.5
95% (< 0.000	unknown	0	0.4	-0.6	-0.6
95% (< 0.000	unknown	0	0	0.6	0.6
95% (< 0.000	unknown	0	0.4	-1.2	-1.2
95% (< 0.000	unknown	0	0.2	-1.6	-1.7
95% (< 0.000	unknown	0	0	0.6	0.5
95% (< 0.000	unknown	0	0	0.6	0.5
95% (< 0.000	unknown	0	0.5	-1.2	-1.2
95% (< 0.000	unknown	0	0.5	-1.3	-1.2
95% (< 0.000	unknown	0	-0.1	0.4	0.5
95% (< 0.000	unknown	0	0.1	0.5	0.4
95% (< 0.000	unknown	0	-0.4	0.7	0.6
95% (< 0.000	unknown	0	0.5	-0.8	-0.9
95% (< 0.000	unknown	0	0.2	0.2	0.1
95% (< 0.000	unknown	0	0	-1.3	-1.4
95% (< 0.000	unknown	0	0.4	-1.3	-1.1
95% (< 0.000	unknown	0	-0.4	0.7	0.5
95% (< 0.000	unknown	0.2	0.1	0.6	0.4
75% (0.065)	unknown	0	-0.1	0.3	0.4
95% (< 0.000	unknown	0	0.4	-0.6	-0.7
95% (< 0.000	unknown	0	-0.3	0.3	0.2
95% (< 0.000	unknown	-0.1	0.1	0.6	0.7
95% (< 0.000	unknown	0	0.2	-0.4	-0.6
95% (< 0.000	unknown	0	0.5	0.3	0.2
95% (< 0.000	unknown	0	0.1	-0.2	-0.2
95% (< 0.000	unknown	0	0.1	0.4	0.4
95% (< 0.000	unknown	0	0.5	-2.1	-1.8
95% (< 0.000	unknown	0	0.6	0.3	0.4
95% (< 0.000	unknown	0	0	-0.1	-0.1
95% (< 0.000	unknown	0	-0.4	0.5	0.5
95% (< 0.000	unknown	0.1	-0.1	0.7	0.8
95% (< 0.000	unknown	0	-0.4	0.7	0.6
95% (< 0.000	unknown	0	0.4	0.6	0.6
95% (< 0.000	unknown	0	0.3	0.3	0.3
95% (0.023)	unknown	0	-0.2	0.1	0.1
95% (< 0.000	unknown	0	0.2	-2.2	-2
95% (< 0.000	unknown	0	1.2	0.5	0.5
95% (< 0.000	unknown	0	0.4	0.4	0.6
95% (< 0.000	unknown	0	-0.1	-0.5	-0.6
95% (< 0.000	unknown	0	0.1	0.5	0.5
95% (< 0.000	unknown	0	0	0.5	0.3
95% (< 0.000	unknown	0	0.5	-2	-2
95% (< 0.000	unknown	0	0.8	-1.1	-1.3
95% (< 0.000	unknown	0	0.5	-1.1	-1.1

95% (0.0001(	unknown	0	0.2	0.3	0.3
95% (< 0.000	unknown	0	-0.1	0.6	0.5
95% (< 0.000	unknown	-0.1	-0.2	0.4	0.6
95% (< 0.000	unknown	0	0	-0.3	-0.3
95% (< 0.000	unknown	0	0.5	-1	-0.9
95% (< 0.000	unknown	0	0.2	0.4	0.3
95% (< 0.000	unknown	-0.1	0.7	0.2	0.4
0% (NaN)	unknown	No Values	No Values	No Values	No Values
95% (< 0.000	unknown	0	0.2	-0.3	-0.3
95% (< 0.000	unknown	0	-0.1	0.7	0.8
95% (0.0001!	unknown	0	-0.2	0.5	0.6
95% (< 0.000	unknown	0	0.1	0.9	0.7
75% (0.092)	unknown	-0.1	0.1	0.1	0.2
95% (< 0.000	unknown	0	0.1	0.5	0.4
95% (< 0.000	unknown	0	0.7	-0.6	-0.6
95% (< 0.000	unknown	0	0.5	0.1	0.2
95% (< 0.000	unknown	0	-0.1	0.2	0.2
95% (< 0.000	unknown	0	-0.8	0.9	0.2
95% (< 0.000	unknown	0	0.2	0.6	0
95% (< 0.000	unknown	0	0.3	-1.4	-1.8
95% (< 0.000	unknown	0	0.8	-0.4	-0.4
95% (< 0.000	unknown	0	0.7	-0.8	-0.9
95% (< 0.000	unknown	0	-0.3	0.8	0.7
95% (< 0.000	unknown	0	0.3	-0.7	-0.8
95% (< 0.000	unknown	0	-0.6	0.6	0.8
95% (< 0.000	unknown	0	0.4	-1.5	-1.7
95% (< 0.000	unknown	0	-0.4	0.6	0.5
95% (0.0009!	unknown	0	0.1	0.3	-0.1
95% (< 0.000	unknown	0	-0.1	0.4	0.4
95% (< 0.000	unknown	0	-0.3	0.5	0.4
95% (< 0.000	unknown	0	-0.2	0.3	0.2
95% (< 0.000	unknown	0	0.8	-0.4	-0.6
95% (< 0.000	unknown	0	0.5	0	0
95% (< 0.000	unknown	0	-0.1	0.5	0.7
95% (< 0.000	unknown	0	0	0.5	0.7
95% (< 0.000	unknown	0	0.8	-1	-0.9
95% (< 0.000	unknown	0	0.1	0.5	0.5
95% (< 0.000	unknown	0.1	0	0.6	0.6
95% (< 0.000	unknown	0	-0.1	0.8	0.8
95% (0.0082)	unknown	-0.1	0.3	0.4	0.5
95% (< 0.000	unknown	0	-0.5	0.9	0.8
95% (< 0.000	unknown	0	0.3	0.5	0.4
95% (< 0.000	unknown	0	0.2	0	0.1
95% (< 0.000	unknown	0	-0.6	-0.2	0.2

95% (< 0.000	unknown	0	0.7	-0.5	-0.5
95% (< 0.000	unknown	0.1	0.3	0.6	0.6
95% (< 0.000	unknown	0	0.2	-0.5	-0.6
0% (0.28)	unknown	0	0.2	0.2	0.2
95% (0.0091	unknown	0	0.4	0.1	0.2
95% (< 0.000	unknown	0	0.4	-2	-2.1
95% (< 0.000	unknown	0	-0.3	0.2	0.3
95% (< 0.000	unknown	0	-0.1	0.5	0.5
95% (< 0.000	unknown	0	0.5	-0.7	-1.2
0% (0.11)	unknown	0	0.3	0.3	0.3
95% (< 0.000	unknown	0	-0.5	0.6	0.4
95% (< 0.000	unknown	0	0.7	-0.1	-0.1
95% (< 0.000	unknown	-0.1	0.1	0.4	0.5
95% (< 0.000	unknown	0	-0.1	0.6	0.7
95% (< 0.000	unknown	-0.1	0	0.1	0.3
95% (< 0.000	unknown	0	-0.2	0.4	0
95% (< 0.000	unknown	0	-0.3	0.8	0.9
95% (< 0.000	unknown	0	0.1	0.5	0.6
95% (< 0.000	unknown	0	0.4	-0.9	-1
95% (< 0.000	unknown	0	0	0.9	1
95% (< 0.000	unknown	0	-0.6	-0.6	-0.3
95% (0.0012	unknown	0	0.5	0.4	0.3
95% (< 0.000	unknown	0	0.1	0.4	0.4
95% (< 0.000	unknown	0	1	0.9	0.8
95% (< 0.000	unknown	0	-0.6	0.8	0.6
95% (< 0.000	unknown	0	0	0.1	0
95% (< 0.000	unknown	0	-0.3	1	0.9
95% (< 0.000	unknown	0	0.1	-1.4	-1.6
95% (< 0.000	unknown	0.1	-0.1	0.3	0.6
95% (< 0.000	unknown	0	0.4	0.3	0.6
95% (0.021)	unknown	0	-0.1	0	0.2
95% (0.0061	unknown	0	0	0.1	-0.2
95% (0.012)	unknown	0	0.6	0.5	0.7
95% (< 0.000	unknown	0	0.4	-1.2	-1.3
95% (< 0.000	unknown	0	-0.3	0.4	0.4
95% (0.0019	unknown	0	0	0.5	0.4
95% (< 0.000	unknown	0	0.5	-1.2	-1.3
95% (< 0.000	unknown	0	-0.2	0.6	0.6
95% (< 0.000	unknown	0	0.8	-2.4	-2.4
95% (0.0086	unknown	0	0.1	0.3	0.2
95% (< 0.000	unknown	0	0.3	-0.5	-0.6
95% (< 0.000	unknown	0	0.9	0.2	0.2
95% (< 0.000	unknown	0	-0.2	0.4	0.3
95% (< 0.000	unknown	0	0	0.7	0.7

95% (< 0.000	unknown	0	0.3	-1.1	-1.1
95% (< 0.000	unknown	0	-0.5	0.3	0.1
95% (< 0.000	unknown	0	0	0.5	0.5
95% (< 0.000	unknown	0	0.4	0.2	0.4
95% (< 0.000	unknown	0	-0.1	0.6	0.5
95% (< 0.000	unknown	0	-0.2	0.6	0.7
95% (< 0.000	unknown	0	-0.3	0.8	0.7
95% (0.015)	unknown	0	-0.2	-0.2	0
75% (0.047)	unknown	0	-0.1	0	0.1
0% (0.076)	unknown	0	0.5	0.3	0.1
95% (< 0.000	unknown	0	0	0.5	0.5
95% (< 0.000	unknown	0	0.1	-0.1	-0.1
95% (< 0.000	unknown	0	0.6	-2	-2
95% (0.0001	unknown	0	0.2	0.2	0.3
95% (< 0.000	unknown	0	0	0	0.1
95% (< 0.000	unknown	0	0	0.8	0.7
95% (< 0.000	unknown	-0.1	0.2	0.6	0.6
75% (0.12)	unknown	0.1	0.4	0.6	0.4
95% (< 0.000	unknown	0	0	0.7	0.7
95% (< 0.000	unknown	0	0.1	0.6	0.5
95% (0.0035	unknown	-0.2	0.1	0.2	0.1
95% (< 0.000	unknown	0	-0.2	0.5	0.2
95% (0.0002	unknown	0	0.1	0.4	0.4
95% (0.0009	unknown	0	0.3	0.2	0.4
95% (< 0.000	unknown	0	0.2	-0.5	-0.5
95% (< 0.000	unknown	0	-0.2	1	0.7
95% (0.0004	unknown	0	-0.1	0.3	-0.1
95% (< 0.000	unknown	0	0	0.3	0.3
0% (0.75)	unknown	0	1.1	0.4	0.5
95% (0.0001	unknown	0	0	0.6	0.6
95% (0.011)	unknown	0	0.2	0.2	0.2
95% (< 0.000	unknown	0	0.1	-0.2	-0.1
95% (< 0.000	unknown	0	0	0.4	0.3
95% (< 0.000	unknown	0	0.2	-1.5	-1.3
95% (< 0.000	unknown	0	0.4	-0.4	-0.5
95% (< 0.000	unknown	-0.1	0.5	0.4	0.4
95% (< 0.000	unknown	0	0.2	0.1	0.1
95% (< 0.000	unknown	0	0.1	-0.4	-0.6
95% (< 0.000	unknown	0	0.2	0.6	0.7
95% (0.0005	unknown	0.1	0.6	0.5	0.2
95% (0.0001	unknown	0	0.2	0.1	0.2
95% (0.022)	unknown	0	0.3	0.5	0.2
95% (< 0.000	unknown	0	-0.3	0.6	0.3
95% (< 0.000	unknown	0	0.1	-0.2	-0.2

95% (< 0.000	unknown	0	0.4	0.2	0.4
95% (< 0.000	unknown	0	-0.4	-0.1	-0.2
95% (0.040)	unknown	0	0.2	0.6	0.4
95% (0.0013	unknown	0	0.2	0.5	0.4
95% (< 0.000	unknown	0	0.1	0.7	0.6
95% (< 0.000	unknown	0	0.3	0.5	0.4
95% (0.028)	unknown	0	0.3	0.7	0.8
95% (< 0.000	unknown	0	-0.2	0	0
95% (< 0.000	unknown	0	1.2	-0.6	-0.4
95% (< 0.000	unknown	0	0.3	-1.6	-1.4
95% (0.0042	unknown	0	-0.1	-0.3	-0.2
95% (< 0.000	unknown	0	0.8	-1.1	-0.8
95% (< 0.000	unknown	0	0.6	0.2	0.4
95% (< 0.000	unknown	0	0.1	0.4	0.5
95% (0.0040	unknown	0	0.7	0.4	0.4
95% (< 0.000	unknown	0	0.8	-1.2	-0.9
95% (< 0.000	unknown	0	0.8	-0.9	-1.3
95% (< 0.000	unknown	0	0.9	-1	-1.2
75% (0.0054	unknown	0	0.3	0.4	0.2
95% (< 0.000	unknown	0	0.5	0.3	0.4
0% (0.15)	unknown	0	0	-0.2	-0.1
95% (0.0089	unknown	0	-0.1	-0.3	-0.4
75% (0.069)	unknown	0	1.1	0.9	0.9
95% (< 0.000	unknown	0	0.2	-0.4	-0.5
95% (< 0.000	unknown	0	-0.2	0.3	0.4
95% (< 0.000	unknown	-0.1	-0.3	0.6	0.7
95% (0.0041	unknown	0	0.2	0.2	0.2
95% (< 0.000	unknown	0.1	0.2	0.5	0.4
95% (< 0.000	unknown	0	-0.3	0.5	0.5
95% (< 0.000	unknown	0	0.5	0	0
95% (< 0.000	unknown	0	-0.2	0.1	0.1
95% (0.011)	unknown	0	0.1	0.5	0.6
95% (< 0.000	unknown	0	0	-0.8	-0.5
95% (< 0.000	unknown	0	-0.1	0.4	0.6
95% (< 0.000	unknown	0	-0.1	0.3	0.3
95% (< 0.000	unknown	0	0.3	0.6	0.4
95% (0.0002	unknown	0	-0.1	0.4	0.4
95% (< 0.000	unknown	0	-0.1	0.8	0.8
95% (< 0.000	unknown	0	-0.2	0.9	0.8
95% (< 0.000	unknown	0	0.2	0.6	0.6
95% (< 0.000	unknown	0	0.3	0.3	0.1
95% (< 0.000	unknown	0	-0.3	0.3	0.1
95% (< 0.000	unknown	0	0.1	-0.2	0
95% (< 0.000	unknown	0	-0.4	0.5	0.5

95% (< 0.000	unknown	0	0.5	-1.8	-1.8
0% (0.11)	unknown	0	0.1	0.1	0.1
0% (0.053)	unknown	0	0.1	0.3	0.3
95% (< 0.000	unknown	0	0	0.5	0.6
95% (< 0.000	unknown	0	0.3	-0.6	-0.6
95% (< 0.000	unknown	0	-0.5	-1.1	-1.2
95% (< 0.000	unknown	0	-0.5	0.7	0.6
95% (< 0.000	unknown	0	0.3	0.6	0.5
95% (0.0001	unknown	0	-0.1	0.2	0.4
95% (< 0.000	unknown	0	-0.1	0.6	0.4
95% (< 0.000	unknown	0	0.1	-0.7	-0.6
95% (< 0.000	unknown	0	0.4	0.7	0.6
95% (< 0.000	unknown	0	0.7	-1.2	-1
75% (0.29)	unknown	-0.1	0.2	0.5	0.5
95% (0.0004	unknown	0	0.1	0.9	0.2
95% (0.0013	unknown	0	0.5	0.3	0.3
95% (< 0.000	unknown	0	0.3	0.3	0.5
95% (0.0001	unknown	0	0.5	-0.5	-0.5
95% (< 0.000	unknown	0	-0.4	0.8	0.6
95% (< 0.000	unknown	0	0	0.3	-0.1
95% (< 0.000	unknown	0	0.7	0.5	-0.5
95% (< 0.000	unknown	0	0	0.5	0.6
0% (0.92)	unknown	0	0	0	0
0% (0.17)	unknown	0	0	-0.1	-0.1
95% (< 0.000	unknown	0	-0.3	0.6	0.5
95% (0.024)	unknown	0	0	0.2	0.2
95% (< 0.000	unknown	0	-0.1	-0.1	0
95% (< 0.000	unknown	0	0.2	0	0.2
95% (< 0.000	unknown	0	-0.2	0.4	0.5
0% (0.12)	unknown	-0.6	3.7	3.9	3.6
95% (< 0.000	unknown	0.1	0.5	-1.8	-2.1
95% (0.0026	unknown	0	0.1	0.4	0.5
0% (0.36)	unknown	0	0.2	0	0
95% (< 0.000	unknown	-0.1	0.3	0.5	0.5
95% (< 0.000	unknown	0	0.3	-0.5	-0.3
95% (0.0002	unknown	0	0.2	-0.4	-0.5
95% (0.0023	unknown	0.1	0.2	0.6	0.5
95% (< 0.000	unknown	0	-0.4	0.3	0.2
0% (0.18)	unknown	0	-0.2	0.1	0.2
95% (< 0.000	unknown	0	0.2	-0.7	-0.9
95% (< 0.000	unknown	0	0	0.4	0.2
95% (< 0.000	unknown	0	0.7	-0.7	-0.8
95% (< 0.000	unknown	0	0	0.1	0.2
95% (0.021)	unknown	0	0	0.1	0.5

95% (< 0.000	unknown	0	0.1	0.5	0.6
95% (0.0054)	unknown	0	0	-1.3	-1.2
0% (0.54)	unknown	0	0.3	0.2	0
95% (< 0.000	unknown	0	-0.9	0.1	0.2
95% (< 0.000	unknown	0	0	0.5	0.5
95% (< 0.000	unknown	0	0.3	0.6	0.6
95% (0.0007	unknown	0	0.6	-0.2	0.1
95% (< 0.000	unknown	0	-0.2	0.2	0
95% (< 0.000	unknown	0	0.4	-1.2	-1.2
95% (< 0.000	unknown	0	-0.6	-0.3	-0.4
0% (0.12)	unknown	-0.4	3.4	1.5	2.4
95% (0.0002	unknown	0	0.2	-0.1	0.3
95% (< 0.000	unknown	0	0.5	-2.1	-2
95% (< 0.000	unknown	0	-0.1	-0.6	-0.1
95% (< 0.000	unknown	-0.1	-0.1	0.4	0.3
95% (0.0017)	unknown	0	-0.2	0.7	0.5
95% (0.026)	unknown	0	-0.2	0.2	0.3
95% (< 0.000	unknown	0	0.9	-0.6	-0.6
95% (< 0.000	unknown	0	0.9	-1.2	-1.1
95% (0.0001	unknown	0	0.6	-1.2	-1.4
95% (< 0.000	unknown	0	-0.4	0.3	0.3
95% (< 0.000	unknown	0	0	0.5	0.5
95% (< 0.000	unknown	0	0.6	-1.3	-1.5
95% (< 0.000	unknown	0	0.2	-0.8	-0.8
95% (< 0.000	unknown	0	-0.5	-0.1	0
95% (< 0.000	unknown	0	0.8	-1.9	-2.2
95% (< 0.000	unknown	0	0.4	-0.9	-1
95% (0.019)	unknown	0	0.2	0.8	0.8
95% (< 0.000	unknown	0	-0.5	0.4	0.3
0% (0.59)	unknown	0	0.4	0.2	0.1
95% (0.048)	unknown	0	-0.1	0.2	0.3
95% (< 0.000	unknown	0	0.3	-0.8	-1
0% (0.36)	unknown	0.2	0	-0.1	0.2
95% (< 0.000	unknown	0	-0.1	0.4	0.6
95% (< 0.000	unknown	0	0.7	0.3	0.7
95% (< 0.000	unknown	0	0.4	-0.7	-0.6
0% (0.32)	unknown	0	0.3	0.4	0.3
95% (< 0.000	unknown	0	-0.9	0.5	0.5
95% (0.0046)	unknown	0	0.1	0.3	0.2
95% (0.0052)	unknown	0	0.4	0	0.4
0% (0.28)	unknown	0	0.3	0.2	0.2
95% (< 0.000	unknown	0	0.6	0	0.2
95% (< 0.000	unknown	0	-0.6	0.6	0.5
95% (< 0.000	unknown	0	0	0.6	0.4

95% (< 0.000	unknown	0	0.1	0.7	0.8
95% (< 0.000	unknown	0	-0.1	0.5	0.4
95% (< 0.000	unknown	0	0.6	-1	-1
95% (< 0.000	unknown	0.1	0.8	0.3	0.4
95% (< 0.000	unknown	-0.1	-0.2	0.5	0.4
95% (< 0.000	unknown	0	0.3	1	0.8
75% (0.026)	unknown	0	0.3	0	-0.2
95% (< 0.000	unknown	0	0.1	0.4	0.8
95% (< 0.000	unknown	0	0.7	-0.8	-0.9
95% (< 0.000	unknown	0	-0.3	-0.4	-0.3
95% (< 0.000	unknown	0	0.2	-0.3	-0.2
75% (0.031)	unknown	0	0.2	0.3	0.2
0% (0.21)	unknown	0.1	2.7	1.9	2.4
95% (0.0048)	unknown	0	-0.3	0.4	0.4
95% (< 0.000	unknown	0	0.6	-0.6	-0.7
95% (< 0.000	unknown	0	0.7	-0.9	-0.7
95% (0.0059)	unknown	0	-0.4	0.1	0.1
95% (< 0.000	unknown	0	-0.7	0.6	0.5
95% (0.0002	unknown	0	0.2	-0.3	-0.2
95% (< 0.000	unknown	0	0.2	-0.1	-0.1
95% (0.014)	unknown	0	0.8	-0.1	-0.3
95% (< 0.000	unknown	0	-0.6	1	0.7
95% (< 0.000	unknown	0	0.4	0	0
95% (0.015)	unknown	0	0.3	0.4	0.2
95% (0.042)	unknown	0	0.2	0	0
0% (0.58)	unknown	0	0.2	0	0.2
95% (0.0011)	unknown	0	0.2	-0.2	-0.2
95% (< 0.000	unknown	0	0.3	-1.7	-1.6
0% (0.12)	unknown	0	0	0.2	0.2
0% (0.18)	unknown	0	-0.7	-0.1	0.2
95% (< 0.000	unknown	0	0.7	-0.1	0.2
95% (< 0.000	unknown	0	-0.2	0.7	0.6
75% (0.057)	unknown	0	-0.3	0.5	0.4
75% (0.072)	unknown	0	0.4	0.2	0.2
95% (0.035)	unknown	0	1	0.9	0.9
95% (< 0.000	unknown	0	0.2	0.2	0.2
0% (0.12)	unknown	0	-0.1	0.3	0.3
95% (< 0.000	unknown	0	-0.5	0.7	0.4
95% (0.0001	unknown	0	0.4	0.7	0.5
95% (< 0.000	unknown	0	0.6	-0.8	-0.7
95% (< 0.000	unknown	0	0.1	0.8	0.6
95% (< 0.000	unknown	0	-0.1	0.6	0.5
95% (< 0.000	unknown	0	0	0.5	0.5
95% (< 0.000	unknown	0	-0.1	0.3	0.2

95% (< 0.000	unknown	0	0.2	0.6	0.4
95% (< 0.000	unknown	0	-0.1	0.2	0.2
95% (0.0003	unknown	0	0.1	0.5	0.1
0% (0.29)	unknown	0	0.2	0.2	0.1
95% (< 0.000	unknown	0	0.6	0	0
95% (< 0.000	unknown	0	0	-1.4	-1.5
75% (< 0.000	unknown	0	-0.3	0	-0.1
95% (0.0043	unknown	0	0.3	0	0.1
95% (< 0.000	unknown	0	0.3	-0.5	-0.2
95% (< 0.000	unknown	0	0.2	-0.2	-0.1
95% (0.0001	unknown	0	0.5	-0.1	0.1
95% (< 0.000	unknown	0	0.2	0.7	0.7
95% (0.0011	unknown	0	-0.5	0.3	0.4
95% (< 0.000	unknown	0	0	0.9	0.7
95% (< 0.000	unknown	0	-0.2	-0.5	-0.3
95% (< 0.000	unknown	0	0.3	-0.7	-0.6
95% (0.0073	unknown	0	0.3	0.4	0.4
0% (0.93)	unknown	0	0.1	0	0.1
0% (0.51)	unknown	0	0.2	0.1	-0.4
95% (< 0.000	unknown	0	-0.5	1	0.5
95% (< 0.000	unknown	0	0.9	-0.1	-0.2
0% (0.59)	unknown	0	0.1	0.2	0.5
95% (0.011)	unknown	0	-0.1	0.5	0.5
0% (0.095)	unknown	0	0.6	-0.1	-0.1
95% (< 0.000	unknown	0	-0.3	0.7	0.7
0% (0.39)	unknown	0	-0.1	0.2	0
95% (< 0.000	unknown	0	0.1	0.3	0.5
95% (< 0.000	unknown	0	0.6	-1.3	-1.3
0% (0.27)	unknown	0	0.1	0.1	0.3
95% (< 0.000	unknown	0	-0.3	0.7	0.7
95% (< 0.000	unknown	0	0.9	-0.1	-0.1
95% (0.0005	unknown	0	0	0.4	0.4
75% (0.12)	unknown	0	0.9	-1.6	-2.3
95% (< 0.000	unknown	0	0.9	0.5	0.6
95% (0.0023	unknown	-0.1	0.1	0.5	0.6
75% (0.034)	unknown	0	0.7	0.8	0.2
0% (0.32)	unknown	0.1	0.4	0.4	0.3
95% (0.0049	unknown	0	0	0.4	0.1
95% (< 0.000	unknown	-0.1	1.4	1.2	0.8
0% (0.11)	unknown	0	0	0	0.1
0% (0.27)	unknown	0	0.1	0.4	0.7
95% (0.016)	unknown	0	-0.4	0.7	0.4
95% (0.0028	unknown	0	0.2	-0.4	0
95% (0.025)	unknown	0	0.3	0.1	0.2

95% (< 0.000	unknown	0	0.3	0.4	0.4
95% (< 0.000	unknown	0	0.1	0.4	0.4
95% (0.048)	unknown	0.1	0.6	0.7	0.2
0% (0.96)	unknown	0	0.1	0	0.1
0% (0.79)	unknown	0	-0.4	0	0.1
95% (< 0.000	unknown	0	-0.5	0.7	0.4
0% (0.45)	unknown	0	0.2	0	-0.1
95% (< 0.000	unknown	0	-0.1	0.4	0.4
0% (0.71)	unknown	0	0.1	0.2	0.4
95% (0.0026	unknown	0	0.5	0.5	0.4
95% (0.0009	unknown	0	0.4	-0.2	0
75% (0.052)	unknown	0	-0.3	0	0.1
95% (< 0.000	unknown	0	0.9	-0.3	-0.1
95% (< 0.000	unknown	0	0.6	-1.4	-1.3
95% (< 0.000	unknown	0	-0.2	0.8	0.4
95% (< 0.000	unknown	0	0.7	-0.5	-0.9
95% (0.045)	unknown	0	0.7	0.3	0.6
95% (< 0.000	unknown	0	1.1	0.1	0
95% (0.0008	unknown	0	-0.4	0	-0.3
95% (< 0.000	unknown	0	0.2	0.6	0.5
95% (0.0088	unknown	0	0.3	0.5	0.3
95% (< 0.000	unknown	0	0.1	-1	-1
0% (0.19)	unknown	0	1	1.4	1.5
95% (< 0.000	unknown	0	0.2	-0.6	-0.9
0% (0.49)	unknown	0	0.5	0.1	0.2
0% (0.91)	unknown	0	-0.1	-0.2	0
95% (0.0085	unknown	0	-0.3	-1.1	-0.9
0% (0.47)	unknown	0	0.6	-0.1	-0.1
95% (0.0005	unknown	0	1.3	-1	-0.8
0% (0.17)	unknown	0	0	0.5	0.4
95% (< 0.000	unknown	0	0.4	-0.8	-0.8
95% (0.0019	unknown	0	0.3	0	-0.1
95% (< 0.000	unknown	0	-0.5	0.4	0.3
95% (< 0.000	unknown	0	0.5	-0.6	-0.5
0% (0.061)	unknown	0	0.7	0	0.1
0% (0.23)	unknown	0	0.6	0.7	0.5
95% (0.0004	unknown	0	-0.1	0.8	0.7
95% (0.0011	unknown	0	0.8	0	0.2
0% (0.13)	unknown	0	-0.4	0.5	0.4
95% (0.0026	unknown	0	0.3	-0.3	-0.1
95% (0.0001	unknown	0	0.3	-0.8	-0.8
75% (0.026)	unknown	0	-0.2	0.1	-0.3
95% (0.045)	unknown	0	-0.1	0.9	0.7
0% (0.40)	unknown	0	1.6	0.9	0.8

95% (0.0056)	unknown	0	0.3	0.5	0.4
95% (0.0035)	unknown	0	0	0.1	0.4
0% (0.70)	unknown	0	0.4	-0.6	-1
0% (0.052)	unknown	0	0.4	0.2	0.1
95% (< 0.000	unknown	0	-0.3	0.7	0.7
0% (0.26)	unknown	0	0.2	0.4	0
95% (0.0052)	unknown	0	0.5	0.3	0.3
95% (0.0007	unknown	0	0.3	-0.7	-0.7
75% (0.093)	unknown	0	-0.2	0.3	-0.3
0% (0.25)	unknown	0	0.2	0.4	0.8
95% (< 0.000	unknown	0	0.9	0.3	0.4
95% (0.0005	unknown	0	0.5	-0.2	-0.4
0% (0.058)	unknown	0	0.4	0.3	0.3
0% (0.35)	unknown	0	0.2	-0.1	-0.2
95% (0.014)	unknown	0	0.7	0.7	0.5
0% (0.13)	unknown	0	0.3	-0.2	-0.2
95% (< 0.000	unknown	-0.1	1.1	-0.1	-0.2
95% (0.0001	unknown	0	0.6	-0.5	-0.5
95% (< 0.000	unknown	0	-0.1	0.6	0.5
75% (0.25)	unknown	0	1	0.3	-0.1
0% (0.44)	unknown	0	0.4	0.3	0.3
0% (0.19)	unknown	0	0.3	0.2	0.4
0% (0.47)	unknown	0	0.1	0.5	0.3
95% (< 0.000	unknown	0	-0.4	0.4	0.2
0% (0.20)	unknown	0	0.2	-0.2	-0.2
95% (0.0001	unknown	0	0.2	0.4	0.7
0% (0.056)	unknown	0	0.4	0.6	0.6
0% (0.12)	unknown	0	0.3	-0.1	0.5
95% (< 0.000	unknown	0	0.2	0.5	0.5
0% (0.25)	unknown	0	0.2	-0.2	-0.1
95% (< 0.000	unknown	0	0.6	-0.3	-0.6
95% (0.013)	unknown	0	0.7	-0.5	-0.8
95% (0.029)	unknown	0	-0.1	0.6	0.6
95% (< 0.000	unknown	0	0.4	-0.4	-0.4
0% (0.69)	unknown	0	0.1	0.3	0.6
0% (0.30)	unknown	0	0.8	0.6	0.4
95% (0.0098)	unknown	0	0	0.2	0.1
95% (< 0.000	unknown	0	0.2	-1.1	-0.9
95% (< 0.000	unknown	0	0.3	-0.1	0.1
95% (0.0080)	unknown	0	0.3	-0.5	0.1
0% (0.48)	unknown	0	0.5	0.9	0.5
95% (0.016)	unknown	0	-0.5	-0.5	-0.4
95% (0.034)	unknown	0	-0.4	0.6	0.6
95% (0.0082)	unknown	0	0.1	-0.5	-0.5

0% (0.47)	unknown	0	0.4	-0.2	-0.1
0% (0.81)	unknown	0	0.3	0.1	0.2
95% (0.0023)	unknown	0	0.1	-0.2	-0.1
95% (0.0003	unknown	0	0.5	0.1	-0.3
0% (0.19)	unknown	-0.1	0.8	0	-0.1
95% (0.020)	unknown	0	-0.1	0.2	0.4
95% (< 0.000	unknown	0	-0.2	0.2	0
95% (0.046)	unknown	0	0.7	-0.1	-0.1
0% (0.46)	unknown	0	0.4	0.2	0.1
0% (0.58)	unknown	0	0.2	0	-0.1
95% (0.0003	unknown	0	0.1	0.6	0.9
95% (0.039)	unknown	0	-0.6	-0.2	-0.5
0% (0.72)	unknown	0	0.4	0.1	0.1
95% (< 0.000	unknown	0	0.5	-0.1	-0.4
95% (0.018)	unknown	0	0.2	0.4	0.5
95% (0.042)	unknown	0	0.4	0.6	0.3
0% (0.18)	unknown	0	0.8	-0.8	-1.2
95% (< 0.000	unknown	0	0.6	-0.5	-0.7
0% (0.46)	unknown	0	0.5	0.3	0.4
95% (0.0007	unknown	0	0.2	0.5	0.5
75% (0.066)	unknown	0	0.7	0.3	-0.3
0% (0.89)	unknown	0	0.1	-0.2	-0.3
95% (0.0069)	unknown	0	0.6	-1.4	-1
75% (0.29)	unknown	0.1	0.9	0.6	0.7
95% (0.045)	unknown	0	0.1	0.8	0.4
95% (0.031)	unknown	0	0.6	-0.2	-0.3
95% (0.019)	unknown	0	0.6	-0.7	-0.7
95% (0.020)	unknown	0	0.2	-0.9	-1.4
75% (0.0022)	unknown	0.1	0.7	-0.2	-0.1
75% (0.0012)	unknown	-0.1	0.2	0.3	0.3
75% (0.0071)	unknown	-0.1	0.2	0.3	0.4
0% (0.30)	unknown	0	0.9	0.4	0.5
75% (0.061)	unknown	0	0.2	0.8	0.9
75% (0.068)	unknown	0	-0.2	0.1	0.3
95% (0.0005	unknown	0	-0.3	0.3	0.6
0% (0.86)	unknown	0	0.2	0.3	0.2
0% (0.079)	unknown	0	0.7	0.2	0.2
95% (< 0.000	unknown	0	1	-0.3	-0.3
0% (0.22)	unknown	0	0	0.3	0.3
75% (0.087)	unknown	0	0	-0.4	-0.3
95% (< 0.000	unknown	0	-0.3	0.4	0.4
0% (0.36)	unknown	0	0.3	0.1	-0.2
95% (0.0047)	unknown	0	0.5	-1.2	-0.8
0% (0.79)	unknown	0	0.1	0.1	0.2

75% (0.059)	unknown	0	-0.1	0	0.2
75% (0.055)	unknown	0	0.4	0.1	0
95% (0.018)	unknown	0	-0.1	0.4	0.4
0% (0.97)	unknown	0	0.1	-0.1	0
0% (0.13)	unknown	0	0	0.4	0.4
0% (0.30)	unknown	0	0.6	0.3	0.1
0% (0.60)	unknown	0	0.2	0.3	0.5
95% (0.037)	unknown	0	0	-0.1	-0.3
0% (0.85)	unknown	0	0.1	0	-0.1
0% (0.18)	unknown	0	-0.2	-0.8	-1.2
0% (0.48)	unknown	0	-0.1	0.2	0.2
0% (0.30)	unknown	0	0.6	0	0.2
95% (< 0.000	unknown	0	0.2	-0.1	-0.1
95% (0.046)	unknown	0	0.7	0.3	0.4
95% (< 0.000	unknown	0	0.4	-0.7	-0.7
0% (0.92)	unknown	0	-0.1	-0.2	-0.1
95% (0.013)	unknown	0	0.6	-0.4	-0.3
0% (0.064)	unknown	0	0.8	0.1	-0.2
0% (0.25)	unknown	0	0.6	0.4	0.5
95% (0.046)	unknown	0	0.7	0	-0.2
0% (0.19)	unknown	0	0.4	0.6	0.8
0% (0.25)	unknown	0	0.1	-0.3	-0.3
0% (0.28)	unknown	0	0.1	-0.4	-0.1
95% (0.0016)	unknown	0	0.7	-0.9	-1.3
0% (0.42)	unknown	0	0	0.3	-0.2
0% (0.24)	unknown	0	0	0.5	0.5
75% (0.079)	unknown	0	0.4	0	-0.5
75% (0.097)	unknown	0	-0.1	-0.6	-0.1
0% (0.33)	unknown	0	-0.1	0.3	0.2
0% (0.54)	unknown	0	0.4	0	0.3
0% (0.13)	unknown	0	0.7	0.2	0.5
0% (0.085)	unknown	0	0	-0.9	-0.9
95% (0.012)	unknown	0	-0.1	0.4	0.1
0% (0.094)	unknown	0	0.4	0.1	-0.3
0% (0.42)	unknown	0	0.7	-0.4	0.1
0% (0.76)	unknown	0	0.8	0.8	0.5
0% (0.061)	unknown	-0.2	0.9	2.3	1.7
0% (0.70)	unknown	0	0.3	-0.2	-0.1
0% (0.16)	unknown	0	0.7	0	0.5
0% (0.72)	unknown	0	0.2	0.1	0
0% (0.31)	unknown	0	-0.4	0.2	0.5
95% (0.021)	unknown	0	0.3	0.1	0.1
0% (0.83)	unknown	0	0.5	0.2	0.4
0% (0.30)	unknown	0	-0.2	0	0

0% (0.24)	unknown	0	0.3	0.6	-0.1
0% (0.56)	unknown	0	1.3	-0.2	No Values
75% (0.043)	unknown	0	0.4	-0.9	-0.4
0% (0.20)	unknown	0	-0.2	0.4	0.2
0% (0.25)	unknown	0	0.2	-0.3	-0.1
0% (0.18)	unknown	0	0.4	0.3	0.2
0% (0.84)	unknown	0	-0.4	0.2	0
0% (0.20)	unknown	0	0.1	-0.3	-0.5
0% (0.40)	unknown	0	0.7	-0.9	-1.2
75% (0.081)	unknown	0	0.6	-0.6	-1.1

results showing the proteins identified by MASCOT and X! Tandem and peptides matching each

A m:37.0/s:14.6, Bad (50%) m:11.6/s:4.32 m:30.3/s:2.00 m:NA m:5.12/s:4.29 [all charge states]
A m:38.0/s:14.6, Bad (50%) m:11.6/s:4.56 m:30.1/s:2.10 m:NA m:5.22/s:4.44 [all charge states]

rbamidomethyl), +304 on Y (iTRAQ8plex)

314/s:0.0809 m:0.617/s:0.0898, Bad (50%) m:27.4/s:4.17 m:0.0671/s:0.508 m:0.0714/s:0.0514 m
312/s:0.0844 m:0.611/s:0.0901, Bad (50%) m:26.8/s:4.20 m:-0.104/s:0.515 m:0.0613/s:0.0482 m

.0282,0.932,0.0390,0.000700]; [0.000600,0.0377,0.933,0.0288,0.000]; [0.000900,0.0471,0.933,0

protein.

ı:0.431/s:0.118 [all charge states]
:0.415/s:0.113 [all charge states]

.0188,0.000]; [0.00140,0.0566,0.933,0.00870,0.000]; [0.000,0.000,0.000,0.000,0.000]; [0.00270,

,0.0744,0.921,0.00180,0.000]

Table S3. Reactome pathway. Human cholangiocyte proteins associated with Reactome pathwa

Category	Term	Count	%	PValue
REACTOME_PATHWA\	REACT_6167:Influenza Infectior	50	15.15	3.03E-28
REACTOME_PATHWA\	REACT_71:Gene Expression	67	20.30	2.00E-24
REACTOME_PATHWA\	REACT_1762:3' -UTR-mediated	38	11.52	8.20E-23
REACTOME_PATHWA\	REACT_17015:Metabolism of pı	50	15.15	2.94E-21
REACTOME_PATHWA\	REACT_125:Processing of Cappe	17	5.15	8.60E-05
REACTOME_PATHWA\	REACT_6185:HIV Infection	22	6.67	2.51E-04
REACTOME_PATHWA\	REACT_578:Apoptosis	17	5.15	5.68E-04
REACTOME_PATHWA\	REACT_13635:Regulation of act	8	2.42	0.00552566
REACTOME_PATHWA\	REACT_1698:Metablism of nucl	10	3.03	0.01359661
REACTOME_PATHWA\	REACT_9035:APC/C:Cdh1-mediı	8	2.42	0.03090836
REACTOME_PATHWA\	REACT_11045:Signaling by Wnt	8	2.42	0.03090836
REACTOME_PATHWA\	REACT_474:Metabolism of carb	10	3.03	0.04352214
REACTOME_PATHWA\	REACT_6850:Cdc20:Phospho-AI	8	2.42	0.04485484
REACTOME_PATHWA\	REACT_383:DNA Replication	10	3.03	0.05151479

ys after incubation with *Opisthorchis viverrini* exosomes.

Proteins	List Total	Pop Hits	Pop Total	old Enrichmer
P36578, P62750, P62277, Q07020, P2763	171	157	3398	6.32845383
P36578, P62750, P47897, Q07020, P6227	171	350	3398	3.80394319
P36578, P46777, P62750, P46779, P6227	171	108	3398	6.99176955
P36578, P62750, P62277, Q07020, P607(	171	217	3398	4.57865093
P84103, O75937, P22626, Q07955, P079:	171	110	3398	3.07102605
Q13200, O43242, P25789, P25786, O755	171	184	3398	2.37592169
Q13200, O43242, P25789, P25786, Q063	171	129	3398	2.61870438
P62987, O43242, Q13200, P25789, P612(	171	44	3398	3.61297182
P05141, P23921, P22234, P00491, P2210	171	77	3398	2.58069416
P62987, O43242, Q13200, P25789, P612(	171	61	3398	2.60607804
P62987, O43242, Q13200, P25789, P612(	171	61	3398	2.60607804
P04406, P00558, P00338, P06733, P0407	171	94	3398	2.11397288
P62987, O43242, Q13200, P25789, P612(	171	66	3398	2.40864788
P62987, O43242, P33991, Q13200, P257(	171	97	3398	2.04859227

Bonferroni	Benjamini	FDR
1.58E-26	1.58E-26	2.95E-25
1.04E-22	5.19E-23	1.94E-21
4.26E-21	1.42E-21	7.97E-20
1.53E-19	3.83E-20	2.86E-18
0.0044614	8.94E-04	0.08350818
0.01299322	0.00217736	0.24405723
0.02909015	0.0042085	0.55006245
0.25033666	0.03537551	5.2410823
0.50927638	0.07604983	12.4540283
0.80457868	0.15062946	26.2901322
0.80457868	0.15062946	26.2901322
0.90112283	0.18970139	35.1000501
0.90803813	0.18033954	35.9733001
0.93608698	0.19067631	40.1812903

Table S4. Phagosome pathway. Human cholangiocyte proteins involved in the Phagosome patl

#Query_ID	KEGG_description	ko_description
sp|P60709|ACTB_HUMAN	actin beta/gamma 1	Phagosome
sp|P27797|CALR_HUMAN	calreticulin	Phagosome
sp|P01024|CO3_HUMAN	complement component 3	Phagosome
sp|P13473|LAMP2_HUMAN	lysosomal-associated membrane protein 1/2	Phagosome
sp|P02786|TFR1_HUMAN	transferrin receptor	Phagosome
sp|P07437|TBB5_HUMAN	tubulin beta	Phagosome
sp|O75396|SC22B_HUMAN	vesicle transport protein SEC22	Phagosome

hway after incubation with *Opisthorchis viverrini* exosomes.

#Query_ID	Control	0.5 h	3 h	16 h
ACTB_HUMAN	0	-0.6	0.6	0.5
CALR_HUMAN	-0.1	0.4	-1.1	-1.2
CO3_HUMAN	0	0.1	0.9	0.2
LAMP2_HUMAN	-0.1	0	-1.1	-1.1
TFR1_HUMAN	-0.1	-0.5	0.7	0.5
TBB5_HUMAN	0.1	-0.6	0.4	0.4
SC22B_HUMAN	0	-0.8	0.6	0.6

Table S5. Proteins related to wound healing and cancer pathways that were differentia

Pathway	Uniprot-Accessio	Access name	Protein name	Control
Adherens junction	O60716	CTND1_HUM	Catenin delta-1	0.1
Adherens junction	P60709	ACTB_HUMA	Actin, cytoplasmic	0
Bladder cancer	P42771	CD2A1_HUM	Cyclin-dependent	0
Cell adhesion	Q13740	CD166_HUM	CD166 antigen	0
Chemical carcinogene	P09211	GSTP1_HUM	Glutathione S-trar	0
Endometrial cancer	P62993	GRB2_HUMA	Growth factor rece	0
Focal adhesion	P19105	ML12A_HUM	Myosin regulatory	0
Focal adhesion	P29400	CO4A5_HUM	Collagen alpha-5(	0
Focal adhesion	P12109	CO6A1_HUM	Collagen alpha-1(	0
Focal adhesion	P62993	GRB2_HUMA	Growth factor rece	0
Focal adhesion	Q13177	PAK2_HUMA	Serine/threonine-p	0
Focal adhesion	P60709	ACTB_HUMA	Actin, cytoplasmic	0
Focal adhesion	Q15942	ZYX_HUMAN	Zyxin	0
Focal adhesion	Q03135	CAV1_HUMA	Caveolin-1	0
Gap junction	P07437	TBB5_HUMA	Tubulin beta chair	-0.1
Gap junction	P62993	GRB2_HUMA	Growth factor rece	0
MicroRNAs in cancer	P42771	CD2A1_HUM	Cyclin-dependent	0
MicroRNAs in cancer	P62993	GRB2_HUMA	Growth factor rece	0
MicroRNAs in cancer	P61978	HNRPK_HUM	Heterogeneous nu	0
MicroRNAs in cancer	P16949	STMN1_HUM	Stathmin	0
MicroRNAs in cancer	P29966	MARCS_HUM	Myristoylated alan	0
MicroRNAs in cancer	Q16658	FSCN1_HUM	Fascin	0
MicroRNAs in cancer	P09493	TPM1_HUMA	Tropomyosin alph	0
MicroRNAs in cancer	P08670	VIME_HUMA	Vimentin	0
Non-small cell lung ca	P42771	CD2A1_HUM	Cyclin-dependent	0
Non-small cell lung ca	P62993	GRB2_HUMA	Growth factor rece	0
Pancreatic cancer	P42771	CD2A1_HUM	Cyclin-dependent	0
Pathways in cancer	P42771	CD2A1_HUM	Cyclin-dependent	0
Pathways in cancer	P29400	CO4A5_HUM	Collagen alpha-5(	0
Pathways in cancer	P62993	GRB2_HUMA	Growth factor rece	0
Pathways in cancer	P09211	GSTP1_HUM	Glutathione S-trar	0
Pathways in cancer	P08238	HS90B_HUM	Heat shock protei	-0.1
Pathways in cancer	P06753	TPM3_HUMA	Tropomyosin alph	0
Pathways in cancer	P12270	TPR_HUMAN	Nucleoprotein TPI	0
Prostate cancer	P62993	GRB2_HUMA	Growth factor rece	0
Prostate cancer	P09211	GSTP1_HUM	Glutathione S-trar	0
Prostate cancer	P08238	HS90B_HUM	Heat shock protei	-0.1
Proteoglycans in canc	P23588	IF4B_HUMAN	Eukaryotic transla	0
Proteoglycans in canc	P60709	ACTB_HUMA	Actin, cytoplasmic	0
Proteoglycans in canc	Q03135	CAV1_HUMA	Caveolin-1	0
renal cell carcinoma	P62993	GRB2_HUMA	Growth factor rece	0

renal cell carcinoma	Q13177	PAK2_HUMA	Serine/threonine-p	0
Small cell lung cancer	P29400	CO4A5_HUM	Collagen alpha-5(	0
Thyroid cancer	P06753	TPM3_HUMA	Tropomyosin alph	0
Thyroid cancer	P12270	TPR_HUMAN	Nucleoprotein TPI	0
Tight junction	P19105	ML12A_HUM	Myosin regulatory	0
Tight junction	Q9H4G0	E41L1_HUM	Band 4.1-like prot	0.1
Tight junction	P35579	MYH9_HUMA	Myosin-9	0
Tight junction	P60709	ACTB_HUMA	Actin, cytoplasmic	0
Tight junction	Q9UDY2	ZO2_HUMAN	Tight junction prot	0
Trans. misreg. in canc	Q01844	EWS_HUMAI	RNA-binding prote	0
Trans. misreg. in canc	P35637	FUS_HUMAN	RNA-binding prote	0
Trans. misreg. in canc	Q92804	RBP56_HUM	TATA-binding pro	0
Trans. misreg. in canc	Q16695	H31T_HUMA	Histone H3.1t	0
Viral carcinogenesis	P42771	CD2A1_HUM	Cyclin-dependent	0
Viral carcinogenesis	Q16531	DDB1_HUMA	DNA damage-binc	0
Viral carcinogenesis	P62993	GRB2_HUMA	Growth factor rece	0
Viral carcinogenesis	P06396	GELS_HUMA	Gelsolin	0
Viral carcinogenesis	P61978	HNRPK_HUM	Heterogeneous nu	0
Viral carcinogenesis	P14618	KPYM_HUMA	Pyruvate kinase P	0
Viral carcinogenesis	P43487	RANG_HUMA	Ran-specific GTP	0
Viral carcinogenesis	P01024	CO3_HUMAN	Complement C3	0
Viral carcinogenesis	P62258	1433E_HUMA	14-3-3 protein eps	0
Viral carcinogenesis	Q99879	H2B1M_HUM	Histone H2B type	0.2
Viral carcinogenesis	P62805	H4_HUMAN	Histone H4	0.1

lly regulated in human cholangiocytes after co-culture with exosomes from *Opisthorchis vi*

0.5h	3h	16h
-0.1	0.3	0.6
-0.6	0.6	0.5
1.2	-0.6	-0.4
-0.5	-1.1	-1.2
-0.9	0.1	0.2
0.6	-0.6	-0.7
0.5	-1.3	-1.2
-0.1	0.6	0.6
0.7	0	-0.2
0.6	-0.6	-0.7
0.9	0.5	0.6
-0.6	0.6	0.5
0.9	0.2	0.2
-0.6	0.6	0.8
-0.6	0.3	0.4
0.6	-0.6	-0.7
1.2	-0.6	-0.4
0.6	-0.6	-0.7
0.8	0.1	0
0.6	-1.7	-1.8
0	-1.3	-1.2
0.6	0.3	0.4
0.2	-2.2	-2.3
0.3	0.5	0.7
1.2	-0.6	-0.4
0.6	-0.6	-0.7
1.2	-0.6	-0.4
1.2	-0.6	-0.4
-0.1	0.6	0.6
0.6	-0.6	-0.7
-0.9	0.1	0.2
-0.5	0.6	0.4
0.6	-1.6	-1.6
0.6	-0.2	0.1
0.6	-0.6	-0.7
-0.9	0.1	0.2
-0.5	0.6	0.4
0.7	-0.6	-0.6
-0.6	0.6	0.5
-0.6	0.6	0.8
0.6	-0.6	-0.7

0.9	0.5	0.6
-0.1	0.6	0.6
0.6	-1.6	-1.6
0.6	-0.2	0.1
0.5	-1.3	-1.2
0.8	0.3	0.4
0.5	0.3	0.6
-0.6	0.6	0.5
0.1	0.5	0.6
0.5	-1	-0.9
0.6	-0.5	-0.5
0.8	-1.2	-0.9
-0.6	0.8	0.8
1.2	-0.6	-0.4
-0.4	0.7	0.4
0.6	-0.6	-0.7
0.7	0.4	0.4
0.8	0.1	0
-0.3	0.7	0.8
0.5	-0.7	-1.2
0.1	0.9	0.2
0.2	-0.5	-0.6
-0.1	0.6	0.5
-0.8	0.6	0.5

***verrini* .** Proteins significantly up- or downregulated in cholangiocytes after incubation with exoso

›mes were subjected to functional enrichment analysis using the Kyoto Encyclopedia of Genes anc

l Genomes (KEGG). A $\log_2$=0.6 corresponding to a 1.5-fold change in proteins with *P* -value <0.(

)5 was considered to be significant.

Click here to download Video: Supplementary_video.mov